THE *LOW-DENSITY LIPOPROTEIN RECEPTOR* KNOCK-OUT MOUSE: A MODEL FOR THE STUDY OF ENERGY BALANCE

by

YING FAI TIFFANY NGAI

B.Sc., The University of British Columbia, 2007

A THESIS SUBMITTED IN PARTIAL FULFILLMENT OF
THE REQUIREMENTS FOR THE DEGREE OF

MASTER OF SCIENCE

in

THE FACULTY OF GRADUATE STUDIES

(Medical Genetics)

THE UNIVERSITY OF BRITISH COLUMBIA

(Vancouver)

April 2010

Abstract

The discovery of leptin and other humoral signals which regulate food intake and energy expenditure has greatly contributed to our understanding of molecular pathways controlling energy homeostasis. Leptin produced by adipocytes, insulin produced by the pancreas, and ghrelin produced by the stomach all contribute to the body's energy balance. One question remaining is whether the lipid transport system also plays a role.

Our hypothesis is that lipid clearance is important in the maintenance of energy homeostasis. The low-density lipoprotein receptor (Ldlr) is a key molecule involved with lipid clearance. The experiments presented in this thesis used the *Ldlr-/-* mouse to study the Ldlr's role in energy balance. One aim of this thesis was to provide a detailed analysis of the energy balance phenotype of the *Ldlr-/-* mouse. Another aim of this thesis was to use the *Ldlr-/-* mouse to study the potential interaction between Ldlr and the leptin signaling pathway.

Adult *Ldlr-/-* mice and *Ldlr+/+* controls on a C57BL/6J background were fed either a chow or a high-fat, high-sucrose Western-type diet (WTD) for eight weeks. Physiological studies of food intake, energy expenditure, activity, heat production, insulin sensitivity, and leptin responsiveness were performed. As well, the effect of these diet interventions on circulating leptin and on leptin gene expression was examined.

On the chow diet, *Ldlr-/-* mice had lower energy expenditure and higher activity levels relative to controls. On the WTD, *Ldlr-/-* mice gained less weight relative to *Ldlr+/+* mice, specifically gaining less fat mass. Increased thermogenesis in *Ldlr-/-* mice fed the WTD was detected. Additionally, leptin responsiveness was blunted in chow-fed *Ldlr-/-* mice, suggesting a novel role for the Ldlr pathway that extends to leptin's regulation of energy balance.

In addition to its known role in lipid transport, these results from the *Ldlr-/-* mouse demonstrate the importance of the Ldlr in regulating energy homeostasis and suggest a direct physiological link between dyslipidemia and energy balance.

Table of Contents

List of Tables

List of Figures

List of Abbreviations and Symbols

α-MSH	=	α-Melanocyte-stimulating hormone
Agrp	=	Agouti-related protein
Apoa-IV	=	Apolipoprotein a-IV
ApoB-100	=	Apolipoprotein b-100
Apoe	=	Apolipoprotein e
BBB	=	Blood brain barrier
BMI	=	Body mass index
Cart	=	Cocaine- and amphetamine-regulated transcript
CCK	=	Cholecystokinin
CNS	=	Central nervous system
db/db	=	*Diabetic* leptin receptor-deficient genotype
DEXA	=	Dual energy X-ray absorptiometry
EE	=	Energy expenditure
EGF	=	Epidermal growth factor
FH	=	Familial hypercholesterolemia
HMG CoA	=	3-Hydroxy-3-methylglutaryl coenzyme A
ICV	=	Intracerebroventricular
IDL	=	Intermediate density lipoprotein
IL-6	=	Interleukin-6
IPGTT	=	Intraperitoneal glucose tolerance test
IPITT	=	Intraperitoneal insulin tolerance test
LDL	=	Low density lipoprotein
Ldlr	=	Low density lipoprotein receptor
LH	=	Lateral hypothalamus
LPL	=	Lipoprotein lipase
Lrp1	=	LDL receptor-related protein
Mch	=	Melanin concentrating hormone
Mc4r	=	Melanocortin 4 receptor
MDCT	=	Multi-detector computed tomography
Npy	=	Neuropeptide y
ob/ob	=	*Obese* leptin-deficient genotype
Pomc	=	Pro-opio melanocortin
PVH	=	Paraventricular hypothalamus
QMR	=	Quantitative magnetic resonance
qRT-PCR	=	Quantitative reverse transcriptase polymerase chain reaction
REE	=	Resting energy expenditure
RER	=	Respiratory exchange ratio
SREBP	=	Sterol regulatory element binding protein
TEF	=	Thermic effect of food
TNF-α	=	Tumor necrosis factor-α
Ucp1	=	Uncoupling protein 1
VLDL	=	Very low density lipoprotein
WHO	=	World health organization
WTD	=	Western type diet

Acknowledgements

There are many people who have helped immensely in the formation of this thesis. First and foremost, I would like to thank Dr. William Gibson for his consistent encouragement and mentorship over my years as a graduate student. He has been an excellent teacher in many aspects and I have greatly appreciated the opportunity to work with him. I would also like to sincerely thank my supervisory committee members, Drs. Louis Lefebvre and Neal Boerkoel, whose advice, insight, and support have been invaluable over the years. Additionally, many thanks are required for my lab mates, Sandra Babich and Melissa Glier, who have been incredibly helpful in providing ideas and assisting in animal and molecular biology techniques. Melissa was also extremely helpful and played a key role in the experiments pertaining to thermogenesis. I would also like to thank Whitney Quong for her role in the experiments presented in this thesis. She has been a wonderful student and a pleasure to work with. In addition, I would like to recognize Pallavi Walia and Ellen Ni from Dr. JP Chanoine's Laboratory for their kindness and support. Post-doctoral fellow Dr. Maria Glavas from Dr. Timothy Kieffer's Laboratory was also crucial in the planning of experiments on leptin responsiveness presented in this thesis. I would also like to thank Janette King and Roger Dyer from Dr. Sheila Innis's Laboratory for their assistance in the direct calorimetry studies. The experiments in this thesis were made possible with funding support from the Natural Sciences and Engineering Council of Canada and by the Canucks for Kids Fund. Lastly, I would very much like to thank my family: my mother, Brandon, Benson, and Michelle, and JP. I am incredibly grateful to have their continued support.

CHAPTER 1: Introduction

1.1 The *Ldlr-/-* Mouse to Study Energy Balance

Obesity is rapidly becoming an issue of serious concern worldwide[1,2]. Research in recent decades has uncovered multiple and complex pathways controlling food intake and energy expenditure (EE) which have contributed to our understanding of energy balance. Of particular importance is the hormone leptin, which is produced by adipocytes and is central in the regulation of body weight. The overall purpose of this thesis was to investigate the role that the Ldlr pathway holds in the maintenance of energy homeostasis. To achieve this, a transgenic mouse knockout model lacking the low-density lipoprotein receptor (*Ldlr)* was utilized.

My specific aims were to determine:

1) Are differences in body composition, food intake, EE, activity levels, and heat production present between *Ldlr-/-* mice and wildtype controls?

2) Does Ldlr gene ablation lead to changes in leptin physiology and signaling?

In this introduction I will provide the relevant background information pertaining to obesity in humans and the molecular pathways which regulate energy balance. I will then review our current knowledge of the lipid transport system and research suggesting its involvement with energy homeostasis. Lastly, I will discuss the Ldlr and provide a rationale to support my hypothesis for the Ldlr's significance in energy balance.

1.2 Obesity: Implications for Human Health

1.2.1 Obesity Defined

The World Health Organization (WHO) defines obesity as an "abnormal or excessive fat accumulation that presents a risk to health"[3]. Excessive body fat increases risk for various diseases[4-6]. Thus, research regarding obesity and its development has significant implications for human health.

Body mass index (BMI) is often used for assessing obesity in humans, particularly for its reproducibility and ease of acquisition[7]. BMI is calculated by dividing the weight of an individual in kilograms by the height in meters squared (kg/m^2). In adults, a BMI>25 is considered overweight, whereas a BMI>30 is considered obese[7]. Differences in the rates of obesity-associated comorbidities between ethnicities also suggest that ethnic-specific BMI cut-offs may more accurately predict risk for adverse consequences of obesity[8]. Other anthropometric methods such as waist-to-hip ratio and waist circumference are currently being assessed for sensitivity and efficacy in measuring obesity[9,10]. While anthropometric measures of body weight are easily attainable, body composition analysis using dual energy X-ray absorptiometry (DEXA) and quantification of abdominal adiposity using multi-detector computed tomography (MDCT) provide more information regarding the phenotype of obese patients[11,12]. To date, however, BMI is still the most commonly accepted method to diagnose obesity[3].

1.2.2 Epidemiology of Obesity

Over recent decades, obesity has become increasingly prominent in Canada as well as globally[3,13]. In 2005, the WHO estimated that 1.6 billion adults were overweight

and at least 400 million adults were obese worldwide[3]. By the year 2015, the WHO predicts that approximately 2.3 billion adults will be overweight and over 700 million obese. In Canada, it was estimated in 2004 that 5.5 million adults had a BMI greater than 30, qualifying these individuals as obese. From 1978 to 2004, the prevalence of obesity in Canada rose dramatically from 13.8% to 23.1%[14].

Pediatric obesity is also a major issue of concern[15]. In 2007, the WHO estimated 22 million children under the age of 5 years were overweight throughout the world; over 75% of these children live in low-to-middle income countries[3]. From 1978 to 2004, the rate of childhood obesity in Canada tripled from 3% to 9%[14].

This dramatic increase in obesity worldwide is creating a financial burden for many healthcare programs[16]. Thus, it is important and justified to study the fundamental differences between the physiological state considered normal weight and that considered obese. With the advance of medical research concerning obesity, better management and treatment regimens may be designed to combat this growing global problem.

1.2.3 Pathophysiology of Obesity

The increase in prevalence of obesity in many countries over recent years has contributed to an increase in cardiovascular disease[6], certain forms of cancer[4], and type 2 diabetes[5]. In fact, evidence clearly supports the strong correlation between type 2 diabetes and obesity[17]. Obesity combined with hypercholesterolemia and hypertriglyceridemia is often seen in patients who develop type 2 diabetes[18]. Specifically, central visceral adiposity predisposes more strongly to type 2 diabetes and cardiovascular disease than does subcutaneous adiposity[19]. This is why measures that specifically address the

individual's regional fat distribution, such as waist-to-hip ratio or MDCT-based volumetric quantification of abdominal adiposity, may be better indicators of metabolic health than measures of overall adiposity[20]. Understanding the physiology and pathology of obesity will allow the development of therapies to treat it and improve the lives of the many people who are affected by it.

1.3 Regulators of Energy Balance

1.3.1 Adipose Expansion in Obesity

Obesity is characterized by a substantial increase in fat tissue. Adipocytes have a unique architecture, whereby a large lipid droplet accumulates and stores triglycerides in a manner not harmful to the cell[21,22]. Due to this large lipid droplet, most other organelles in the cell appear displaced, making the function of adipocyte as a lipid storage cell readily ascertainable[21,22]. Over recent years, however, research has shifted the view of adipose tissue from an inert energy storage depot to a dynamic organ that secretes autocrine, paracrine and endocrine factors which regulate many aspects of physiology[23]. Adipose tissue is a critical regulator of energy balance through modulation of both food intake and EE[24]. While the details of how obesity directly increases the risk for various diseases remain unknown, researchers have investigated the changes in physiology which occur as adiposity increases. These changes include alterations in levels of circulating adipocyte-secreted factors termed "adipokines"[25], which affect functioning of various nonadipose organs as well as whole-organism biology[23].

1.3.2 The Discovery of Leptin

Leptin is a hormone secreted by adipocytes and acts as a key indicator of the body's energy stores[26]. The study of leptin has provided a clearer understanding of the pathways which regulate energy balance and to date leptin remains the best studied adipokine[27]. The genetically *obese* (*ob/ob)* mouse mutant was first isolated at the Jackson Laboratory in 1950[28]. *ob/ob* mice are hyperphagic, develop spontaneous obesity, and have deficits in fertility[29] and in thermoregulation[30]. The mutated leptin gene causing the *obese* phenotype was later mapped by positional cloning and found to be a circulating factor that is secreted by adipocytes[31]. Leptin expression has also been detected at low levels in various other tissues, including skeletal muscle, pancreas, and brain[32]. When exogenous leptin was administered to leptin-deficient *ob/ob* mice, their food intake decreased and EE increased, resulting in substantial and impressive weight loss[33,34]. Mutations in leptin have also been described in obese humans. The remarkable success of leptin therapy for these patients with congenital leptin-deficiency has been well-documented, with both weight loss and improved metabolic status observed post treatment[35-37].

In "common" obesity that is not caused by leptin deficiency, serum leptin levels show a positive correlation with fat mass[38-40]. Leptin is generally elevated in obese individuals suggesting resistance to leptin's weight-lowering effects develops concurrently with obesity. Leptin gene expression in adipose tissue is also positively correlated with adiposity[38,41]. Interestingly, hyperleptinemia that occurs with obesity results from increased leptin secretion by subcutaneous adipose tissue more so than by visceral adipose tissue[42]. This difference in response to weight gain observed between

subcutaneous and visceral adipose tissue may contribute to the differences in metabolic risk associated with expansion of these two fat depots.

1.3.3 The Leptin Receptor

Leptin exerts its anorectic effects through the leptin receptor. Leptin receptor deficient (*db/db*) mice have an obese phenotype largely identical to that of *ob/ob* mice. However, *db/db* mice are extremely leptin resistant, due to lack of the crucial leptin receptor. The leptin receptor is most highly expressed the mediobasal hypothalamus, predominantly in the ventromedial nucleus, dorsomedial nucleus, and the arcuate nucleus[43,44]. Activation of the leptin receptor results in transduction of leptin's signal to downstream neural pathways, triggering decreased food intake and increased EE in *ob/ob* mice. Transgenic mice with a neuronal-specific deletion of the leptin receptor showed obesity and a metabolic profile similar to *db/db* mice, suggesting that most of leptin's actions on energy balance are centrally mediated [45].

While the cause of leptin resistance in common obesity is currently unknown, research has suggested decreased transport of leptin across the blood brain barrier (BBB) as a potential mechanism[46]. To enter the brain interstitial fluid, leptin must be actively transported across the BBB endothelial cells by leptin receptors, which act as leptin transporters[46]. Researchers have shown that in obese humans leptin in the cerebrospinal fluid does not correlate with circulating serum plasma levels[47], supporting the hypothesis of decreased transport and delivery of leptin to the brain. Decreased intracellular signal transduction at the post-receptor level may also contribute to leptin resistance[48].

1.3.4 Leptin in the Hypothalamus

Early brain stimulating and brain lesioning studies suggested specific centers in the hypothalamus were responsible for mediating food intake[49]. Further studies at the molecular level have shown that these regions are regulated by leptin[46]. Specifically, the arcuate nucleus is a major region in the hypothalamus responsible for the integration and transduction of the leptin signal to downstream neural pathways[46,50].

In the arcuate nucleus there are two distinct leptin-responsive neuronal populations that express the leptin receptor, illustrated in **Figure 1.1**. These populations act as first order neurons to leptin's signal. One subpopulation coexpresses the orexigenic molecules *neuropeptide Y* (*Npy*) and *agouti-related protein* (*Agrp*), which act to decrease EE and promote food intake[51]. Activation of the leptin receptor in Npy/Agrp neurons causes decreased expression and decreased release of Npy and Agrp, increased EE, and decreased food intake. The second subpopulation of neurons coexpress the anorexigenic molecules *pro-opio melanocortin* (*Pomc*) and *cocaine- and amphetamine- regulated transcript* (*Cart*)[52,53]. *Pomc* encodes for the precursor transcript to α–melanocyte-stimulating hormone (α-MSH). Both α-MSH and Cart are neuropeptides that increase EE and decrease food intake[46]. Activation of the leptin receptor in Pomc/Cart neurons increases expression and release of these anorexigenic molecules. The neuropeptides produced by first order leptin neurons then act as effector molecules, activating or inhibiting second order neurons downstream[46,50].

Brain centers which contain second order leptin neurons include the paraventricular hypothalamus (PVH) and lateral hypothalamus (LH)[46]. Early studies showed that stimulating the PVH inhibited food intake, whereas stimulating the LH

decreased food intake[46]. In contrast, PVH lesions resulted in hyperphagia and obesity, whereas LH lesions resulted in hypophagia and weight loss[46]. Under normal conditions, activation of second order leptin neurons promotes transcriptional changes of neuropeptides that regulate energy balance. These include molecules such as melanin concentrating hormone (Mch) and orexins A and B[54]. **Table 1.1** lists neuropeptides that have been implicated in energy balance.

One well-characterized example of how leptin exerts it effects on energy balance involves the melanocortin pathway. The receptor for α-MSH is the melanocortin 4 receptor (Mc4r), which is expressed in the PVH[54]. When leptin activates α-MSH production in the arcuate nucleus, α-MSH activates Mc4rs located at the PVH, triggering decreased food intake[55]. Furthermore, Agrp is a Mc4r antagonist that is repressed in the presence of leptin, minimizing Mc4r inhibition[55]. Mutations in Mc4r have been isolated in both mouse models and in human patients; in both cases, severe obesity is associated with Mc4r deficiency[56-58].

1.3.5 Other Adipokines

Since leptin's discovery, other adipocyte-derived factors have also been isolated and studied. Another well-defined adipokine is adiponectin[59]. Adiponectin is a 30kDa protein known to circulate in several multimeric forms. The high molecular-weight form of adiponectin has been suggested to be the most physiologically relevant and active form[59]. Adiponectin also exists in circulation at very high levels, comprising approximately 0.01% of total plasma protein[23]. In contrast to leptin, serum adiponectin levels correlate inversely with adiposity levels[60]. Adiponectin loss-of-function models

have shown varying effects of adiponectin deficiency on body weight and metabolic function[61,62]. Adiponectin has been demonstrated to have anti-inflammatory properties[25]. As well, when adiponectin is administered to obese diabetic mice, improvements in insulin sensitivity and fatty acid oxidation have been documented[59].

Emerging evidence suggests that obesity is a state of inflammation[25] and that adipocytes play a role in mediating inflammatory responses. Cytokines secreted from adipose tissue play an important role during the pathogenesis of obesity. Specifically, tumor necrosis factor-α (TNF-α) secreted from adipose tissue has important effects on glucose homeostasis. TNF-α induces insulin resistance[63] and TNF-α serum levels are elevated in obese and insulin resistant individuals[64], although most of the TNF-α secreted by adipocyte tissue derives from resident macrophages which have infiltrated the adipose depot[25]. Interleukin-6 (IL-6) is another cytokine produced by adipocytes, with effects similar to TNF-α[25]. Lastly, resistin is another adipokine whose function is thus far not well-characterized. Like TNF-α, resistin is highly expressed in human macrophages[65]. Studies from rodents suggest that resistin may have hyperglycaemic action[23]. However, it is controversial whether resistin may have these effects in humans[23].

1.3.6 Other Hormones Involved in Energy Balance

In addition to adipocyte derived factors, various other hormones are also involved with body weight regulation[50]. Insulin administered directly to the brain reduces food intake, much like leptin does[46]. Insulin levels circulating in brain interstitial fluid correlate with insulin levels circulating in serum[50], and neurons of the arcuate nucleus express the insulin receptor and respond to insulin administered to the central nervous

system (CNS). Activation of the insulin receptor at these arcuate neurons elicits responses similar to activation of the leptin receptor[50]. Thus, insulin (produced by pancreatic β-cells) acts as an anorectic hormone much like leptin (produced by adipocytes)[46]. In addition, neurons in the arcuate nucleus also express the ghrelin receptor[50]. Ghrelin is a hormone produced by the stomach that reaches peak levels just prior to meal initiation. When ghrelin activates its receptor, food intake is stimulated[50]. Another hormone mediating energy balance is cholecystokinin (Cck), which is secreted by intestinal endocrine cells and activates receptors on the afferent vagus nerve to terminate feeding[50]. Thus, the brain integrates adipocyte-derived, pancreas-derived and gut-derived signals with signals from inflammatory cells and other tissues to regulate energy balance. **Figure 1.2** summarizes these regulators.

The discovery of multiple and complex pathways for food intake and energy expenditure have contributed much to our understanding of energy homeostasis. However, questions remain as to whether other physiological systems also contribute to these energy homeostasis pathways. In this thesis, I will explore specifically the role that the lipid transport system may have.

1.4 Lipid Transport System and Lipoprotein Receptors

1.4.1 Lipid Metabolism

Circulating hydrophobic lipids are transported in biochemical particles called lipoproteins. Lipoproteins consist of a hydrophilic phospholipid monolayer surrounding a hydrophobic lipid core[66]. Lipoproteins are classified by their density and relative triglyceride to cholesterol content. High-density lipoproteins (HDLs) and low-density

lipoproteins (LDLs) have the highest cholesterol and lowest triglyceride content, whereas very-low-density lipoproteins (VLDLs) have the lowest cholesterol and highest triglyceride content[67].

As dietary triglycerides are absorbed from the intestine, they are packaged into chylomicrons. Chylomicrons are hydrolyzed by lipoprotein lipase (LPL) to produce cholesterol-rich chylomicron remnants, which are then removed from circulation by the liver[68]. The liver also releases endogenous triglycerides packaged in VLDLs. VLDLs are also hydrolyzed by LPL, eventually becoming cholesterol-rich LDLs, which are then cleared from circulation by the liver[68]. Cholesterol contained in LDL particles has been well studied for its contribution to the development of atherosclerosis[69]. As excess cholesterol collects in circulation, cholesterol is deposited in the arterial wall, leading to formation and expansion of atherosclerotic plaques[70]. Atherosclerosis is a complex disease affected by both genetic and environmental factors[71] and is important in the development of cardiovascular disease. *Sclerosis* describes the thickening of arterial walls due to formation of plaques, and the prefix *athero-* denotes that these plaques are made up of fatty materials, particularly cholesterol[72].

Lipoproteins are unable to cross the BBB[73]. Thus, lipoproteins within the brain and cerebrospinal fluid are thought to remain separate from those in the systemic lipoprotein system. The distinct lipoprotein pool of the CNS is produced by glial cells[73].

1.4.2 Structure of Lipoprotein Receptors

Apolipoproteins are found embedded in the outer phospholipid monolayer of lipoproteins[66] and function as ligands for receptor-mediated endocytosis and delivery of

lipids to target cells[74]. The receptors for apolipoproteins belong to the low-density lipoprotein receptor (LDLR) gene family are expressed ubiquitously, but those in the liver play a significant role in lipid clearance and lipoprotein metabolism[75]. Deficient lipoprotein clearance by the liver results in dyslipidemia. Seven mammalian LDLR gene family members have been identified[76]. **Table 1.2** (adapted from Hertz, 2001[77]) and **Figure 1.3** (from Beffert et al., 2004[76]) displays the properties of the LDLR gene family members. All lipoprotein receptors share common structural domains characteristic of this class of proteins, including a ligand binding domain, epidermal growth factor (EGF) homology domains, a transmembrane domain, and a cytoplasmic tail containing at least one NPxY motif[76]. Each LDLR gene family member displays slightly altered affinities for the different apolipoprotein classes[68]. Thus, each lipoprotein receptor has a slightly different role in the clearance of the various classes of lipoproteins.

1.4.3 Lipoprotein Receptors and Cholesterol Synthesis

In addition to the uptake of lipoproteins, the role of lipoprotein receptors in regulating intracellular cholesterol synthesis has been well defined. While cholesterol is important for many cellular processes, excess cholesterol within cells is toxic[70]. Genes involved with cholesterol synthesis are transcriptionally regulated to maintain cellular cholesterol levels in a tightly controlled range. Cholesterol biosynthesis is regulated by a feedback system, which integrates information from intracellular cholesterol levels with the availability of cholesterol in the circulation. This pathway is regulated by sterol regulatory element binding proteins (SREBPs), a family of membrane-bound transcription factors associated with the endoplasmic reticulum[70]. SREBPs regulate many

genes involved with cholesterol synthesis and cellular uptake[78]. In particular, SREBPs control transcription of 3-hydroxy-3-methylglutaryl coenzyme A reductase (HMG CoA reductase), the rate-determining enzyme in the cholesterol synthesis pathway[78]. Statins are a popular class of drugs which inhibit HMG CoA reductase[74]. As HMG CoA reductase activity is reduced by statins, intracellular cholesterol synthesis decreases in the liver, resulting in increased production of lipoprotein receptors and clearance of cholesterol-rich lipoproteins from the bloodstream[74]. Overall, this results in a decrease in atherosclerotic plaque formation[74]. The effectiveness of statins for decreasing cardiovascular events has been well documented[79]. Thus, understanding the role of lipoprotein receptors and genes involved with cholesterol synthesis has yielded important treatment modalities for diseases involving dyslipidemia.

1.5 Role of Lipid Transport System in Energy Balance

Because obesity and hypertriglyceridemia often occur concurrently[18], researchers have examined the molecules central to lipid metabolism for a role in regulating energy balance. Apolipoprotein a-IV (Apoa-IV), which is expressed in the liver, intestine, and hypothalamus, controls food intake and body weight through interaction with the hypothalamic melanocortin system[80,81]. Central infusion of another apolipoprotein, Apolipoprotein e (Apoe), caused reduced food intake in a dose dependent manner. Expression of *Apoe* transcripts decreases upon fasting and normalizes upon refeeding, and is also altered in states of diet-induced obesity and in *ob/ob* mice[82]. Intracerebroventricular (ICV) leptin administration blocks the effect of fasting on *Apoe*

transcript levels[83]. **Figure 1.4** shows the interpretation of these results by researchers presented in a model of how Apoe is involved with leptin signaling.

Apoe-/- mice gain less weight than wild-type mice when given a high-fat diet[84,85]. Improved glucose tolerance in *Apoe*-/- mice relative to *Apoe*+/+ mice was also reported after high-fat diet feeding[85]. This suggests that gene ablation of *Apoe* partially ameliorates the effects of high-fat diets on metabolic profile. Both the Ldlr and the LDL receptor-related protein-1 (Lrp1) are receptors for Apoe[77].

Transgenic mice lacking *Lrp1* have an early embryonic lethal phenotype[86]. However, mice lacking *Lrp1* specifically in adipose tissue are viable. These mice were found to have decreased body weight relative to wildtype mice when fed either a high-fat diet or a chow diet[87]. Adipose-tissue specific knock-down of mouse *Lrp1* also improved glucose tolerance and increased EE. Increased muscle thermogenesis was thought to be the reason for increased EE[87]. However, *Lrp1* adipocyte-specific knockout mice had substantial impairment in regulating body temperature[87]. From this evidence, the authors of this study suggested that *Lrp1* in adipose tissue is an important regulator of energy homeostasis.

1.6 The Low-density Lipoprotein Receptor

1.6.1 Discovery of LDLR and Significance in Disease

The LDLR was discovered by Drs. Joseph L. Goldstein and Michael S. Brown. The study of the LDLR resulted in the emergence of "receptor-mediated endocytosis" as a new fundamental concept in cellular biology. The research by Drs. Goldstein and Brown on the regulation of cholesterol metabolism earned them the Nobel Prize in

Medicine in 1985. Mutations in LDLR cause the autosomal dominant human disease familial hypercholesterolemia (FH). Patients heterozygous for a non-functioning *LDLR* allele have a two-fold increase in LDL plasma levels and generally develop heart attacks before age 60 years[74]. Approximately one in one million individuals are homozygous for mutations in LDLR. FH homozygotes have between six- to eight- fold elevations in plasma LDL levels and generally develop heart attacks before age 20 years[74]. The *LDLR* gene is expressed ubiquitously, but highly in the liver and in the brain[88,89]. The LDLR is key for the clearance of lipids from circulation[90,91] and has an affinity for LDL particles containing ApoB-100, and for VLDL particles and chylomicron remnants containing ApoE[74] (refer to **Table 1.2**).

1.6.2 The *Ldlr-/-* Mouse

The *Ldlr-/-* mouse was generated in 1991 by Ishibashi and colleagues[92]. Thus far, the *Ldlr-/-* mouse model has helped to elucidate basic processes of lipid metabolism and atherosclerosis. Hyperlipidemia and hypertriglyceridemia are major contributors to atherosclerosis in humans[72], though mice are generally resistant to atherosclerosis[71]. Dietary challenges of levels of cholesterol as high as 1.25% (wt/wt) in mice resulted in only moderate levels of atherosclerosis and did not recapitulate the scenario in humans[71,93]. However, the generation of the *Ldlr-/-* mouse produced an excellent research model to study the development of atherosclerotic plaques. In *Ldlr-/-* mice fed a standard rodent chow diet (<0.04% wt/wt cholesterol), total plasma cholesterol levels were elevated twofold[92]. This elevation was due specifically to an increase in intermediate density lipoproteins (IDL) and LDLs, while HDLs levels remained unchanged[92].

Research has shown that HDL cholesterol is protective against atherosclerotic plaque formation[94]. Thus the increase in serum cholesterol in *Ldlr-/-* mice was solely due to an increase in atherosclerosis promoting IDLs and LDLs. When *Ldlr-/-* mice were fed moderate levels of dietary cholesterol (0.2% wt/wt cholesterol), a threefold increase in IDL and LDL serum cholesterol levels and atherosclerotic plaque formation were observed in *Ldlr-/-* mice, which did not occur in *Ldlr+/+* mice[92]. Since their publication, *Ldlr-/-* mice have become a model to test the effectiveness of therapeutics or nutritional regimes to decrease atherosclerosis[71,95,96].

The role of the *Ldlr* in energy balance has yet to be thoroughly assessed. Previous data has suggested that molecules involved in the apolipoprotein-lipoprotein system may be involved with maintaining energy balance[80-83,87]. However, the role of the *Ldlr* in the context of energy homeostasis pathways has yet to be explored. The *Ldlr-/-* mouse is an excellent opportunity to study the function that this major fat receptor may play in maintaining energy homeostasis. Besides understanding the direct role the Ldlr plays in energy balance, studies in the *Ldlr-/-* mouse can also serve as research model to understand the effect of impaired lipid transport or dyslipidemia on energy balance.

1.7 Review of the *Ldlr-/-* Mouse and Energy Balance

1.7.1 Energy Balance in the *Ldlr-/-* Mouse

Experiments in this thesis focus on *Ldlr-/-* mice on a C57BL/6J strain background. In this section, I will provide a brief review of how the *Ldlr-/-* mouse has been utilized to study energy balance, first with a review of the experiments and the phenotype of the o*b/ob;Ldlr-/-* double knockout mouse. Thereafter, I will review the

literature previously reported regarding body weight and energy balance phenotypes of the *Ldlr-/-* mouse.

1.7.2 Leptin Deficient *Ldlr-/-* Mice

The basis for generating the *ob/ob;Ldlr-/-* double knockout mouse was to study how obesity can further enhance defects of lipid transport[97-100]. Despite the fact that leptin deficient *ob/ob* mice and leptin-receptor deficient *db/db* mice develop severe obesity and dyslipidemia, *ob/ob* and *db/db* mice do not develop atherosclerotic lesions[101,102]. This is due to an increase in serum atheroprotective HDLs, as opposed to atherogenic LDLs[94]. In contrast, *ob/ob;Ldlr-/-* double knockout mice develop severe hypercholesterolemia, hypertriglyceridemia, and atherosclerosis that was similar to the phenotype found in *Ldlr-/-* mice[97]. VLDL clearance was further impaired in *ob/ob;Ldlr-/-* mice compared to *Ldlr-/-* mice[97]. In examining energy balance in *ob/ob;Ldlr-/-* double knockout mice, the authors of these studies found no detectable differences in body weight or adipose depot weights compared with the severely obese *ob/ob* mice[98,103]. Thus, it appears that in leptin-deficient *Ldlr-/-* mice, the obesity observed can be attributed to loss of leptin, with the further loss of the *Ldlr* being insufficient to further alter the *obese* phenotype. Though the Ldlr may be involved with energy homeostasis, the Ldlr may function at a level downstream of leptin's effects on energy balance and may not be detectable in *ob/ob;Ldlr-/-* double knockout mice.

1.7.3 Weight Gain in the *Ldlr-/-* Mouse

Selected studies have investigated the energy balance phenotype in *Ldlr-/-* mice. While *Ldlr-/-* mice have been reported to exhibit diet-induced weight gain and glucose intolerance with high-fat diet feeding, many of these reports have used *Ldlr-/-* mice exclusively without direct comparison to *Ldlr+/+* mice[97,104-107]. In this thesis, I wish to address how the Ldlr may contribute to energy balance through comparing *Ldlr-/-* mice with *Ldlr+/+* mice. I will first review the reports that have compared their energy balance phenotypes directly.

Schreyer *et al.*[108] examined the weight gain of *Ldlr-/-* mice relative to *Ldlr+/+* controls when both genotypes were fed a high-energy diabetogenic diet (5.45 kcal/g: 27% kcal from carbohydrate and 56% kcal from fat) and found that *Ldlr-/-* mice gained more weight relative to wildtype controls after 16 weeks of feeding[108]. No differences were observed between *Ldlr+/+* mice and *Ldlr-/-* mice in calories consumed or in dietary fat absorption during the period measured[108]. *Ldlr-/-* mice alone developed severe hypertriglyceridemia, hyperleptinemia, and atherosclerosis relative to *Ldlr+/+* mice[108]. However, despite the severe obese and dislipidemic state of *Ldlr-/-* mice on the diabetogenic diet, fasting glucose and insulin levels were only moderately elevated in *Ldlr-/-* mice after 16 weeks on the diabetogenic diet[108].

During the collection of data for this thesis, a paper was published coincidentally examining the *Ldlr-/-* mice using the same diet as in my experiments. Karagiannides *et al.*[85] examined weight gain in *Ldlr-/-* mice and *Ldlr+/+* mice fed a "Western-type diet" (WTD) (4.5Cal/g, 42.7% kcal from carbohydrate and 42% kcal from fat) for 15 weeks[85]. The WTD is less energy dense than the diabetogenic diet used in the experiments by

Schreyer *et al.*[108]. Interestingly, this study found that *Ldlr-/-* mice gained less weight relative to wild-type mice on the WTD[85], the opposite phenotype as described for *Ldlr-/-* mice on the diabetogenic diet[108]. In terms of glucose tolerance and insulin sensitivity, *Ldlr-/-* mice on the WTD were found to have a slightly improved metabolic profile than wild-type mice[85]. In this study, *Apoe-/-* mice were found to gain less weight on the WTD than *Ldlr-/-* mice and wild-type mice, whereas *Apoe3* knock-in mice gained more weight than wild-type mice on the WTD. Because *Ldlr* is a major receptor for *Apoe*, and *Ldlr-/-* mice demonstrated an intermediate phenotype between wild-type mice and *Apoe-/-* animals, the authors of this study hypothesized that the *Ldlr* mediates some of the effects of *Apoe* on energy balance[85]. The activity of other receptors which also have an affinity for *Apoe* (see **Table 1.2**) likely account for the observed differences between the *Apoe-/-* and *Ldlr-/-* mouse models[85].

1.7.4 Conclusions from Reports of Weight Gain in *Ldlr*-/- Mice

The observed differences in weight gain between *Ldlr-/-* mice fed each of these high-fat diets suggest that *Ldlr* gene knockout alters susceptibility to diet-induced obesity, but in a manner that depends on the energy density and macronutrient content of the diet. Regardless of inconsistencies among reports, current evidence from studies with the *Ldlr-/-* mouse suggests that signaling through Ldlr may modulate aspects of energy balance. However, in-depth studies of obese and diabetic phenotypes in *Ldlr-/-* mice are required to elucidate this relationship more fully. Studies have shown that an absolute increase in energy consumption is not a requirement for weight gain on high-fat diets[109]. Animals fed high-fat diets may consume less energy than animals fed low-fat diets and

still gain more weight, an effect attributable to a concomitant decrease in EE provoked by energy dense high-fat diets. Since increased caloric consumption has not been reported in *Ldlr-/-* mice relative to wild-type mice, it is possible that different types of high-fat diets affect the EE of *Ldlr-/-* mice differently than *Ldlr+/+* mice.

1.7.5 Other Energy Balance Phenotypes of the *Ldlr-/-* Mouse

Physical activity is an important contributor to total EE in animals[110]. A study by Edler *et al.*[111] examined the behavioural and developmental phenotype of *Ldlr-/-*[111]. The authors of this study rationalized that because *Ldlr* is expressed in the brain, *Ldlr* deficiency might affect behaviour. While *Ldlr-/-* mice did not show deficits in spatial memory or major developmental defects, activity levels were increased in *Ldlr-/-* mice[111]. This suggests that *Ldlr* may be involved in central regulation of activity, a significant source of EE in animals.

In addition to the differences in body weight gain reported in *Ldlr-/-* mice, impaired glucose tolerance in *Ldlr-/-* mice relative to *Ldlr+/+* mice has been reported with high-fat diet feeding[108,112]. Adiposity is known to have a profound impact on insulin sensitivity[113]. Thus, I hypothesized that if *Ldlr-/-* mice have altered weight gain in response to energy dense diets, insulin sensitivity would also be affected by knockout of the *Ldlr* gene.

1.8 Rationale for Hypothesis

Thus far, research suggests a role of lipoprotein transport molecules in control of appetite and leptin signaling. My hypothesis is that the Ldlr is an important regulator of energy balance. The Ldlr is a strong candidate for mediating the lipid transport system's

effects on energy balance because: 1) the Ldlr has a significant role in the clearance of lipoproteins from circulation and 2) the Ldlr has a high affinity for Apoe, which has anorectic effects when administered to rodents. The *Ldlr-/-* mice used in my experiments were from a congenic inbred strain. Such strains provide an excellent means to study the effects that removal of a single gene can have on physiology, as the contribution of genetic variability at other loci is minimized. While the *Ldlr-/-* mouse has been tested extensively as a model for atherosclerosis, the energy balance phenotype of this mouse model has not been thoroughly examined. Particularly, characteristics important to energy balance such as food intake and EE have not been thoroughly studied.

In this thesis, I examined the phenotype of *Ldlr-/-* mice on a standard rodent chow diet and on a WTD. Using the methods described in Chapter II, I surveyed energy balance in *Ldlr-/-* mice. Initially, *Ldlr-/-* mice were characterized while consuming a "standard" laboratory chow diet to identify baseline differences between *Ldlr-/-* mice and *Ldlr+/+* mice in the absence of a high-fat diet challenge. I next analyzed *Ldlr-/-* mice on a WTD to elucidate how *Ldlr-/-* mice respond when challenged with an energy dense diet. Data on weight gain, body composition, EE, and glucose homeostasis was collected. These results are presented in Chapter III. In addition, I examined circulating leptin levels and leptin responsiveness, results which are presented in Chapter IV.

Table 1.1. Neuropeptides implicated in the control of energy homeostasis.

Molecule	Regulation by leptin
OREXIGENIC	
NPY*	↓
Agrp*	↓
MCH	↓
Hypocretin 1 and 2/orexin A and B	↓
Galanin	?
Noradrenaline	?
ANOREXIGENIC	
α-MSH*	↑
CRH*	↑
TRH*	↑
Cart	↑
IL-1β*	↑
Urocortin*	?
Glucagon-like peptide 1	?
Oxytocin	?
Neurotensin	?
Serotonin	?

Orexigenic molecules promote increased energy intake, anorexigenic molecules promote the opposite effect. An asterisk designates documented, coordinated effects on both food intake and energy expenditure that promotes a change in energy stores. Arrows indicate direction of effect exerted by leptin. This table is from Schwartz *et al.*, 2000., used with permission from the Nature Publishing Group.

Table 1.2. Properties of the seven LDL receptor family members.

Receptor	Ligands	Functions	Mutational Phenotypes
LDL receptor	ApoB, ApoE	Lipoprotein/cholesterol uptake	Familial hypercholesterolemia, atherosclerosis, heart disease
LRP	ApoE, α2-macroglobulin, plasminogen activators, protease/inhibitor complexes, lipase, amyloid precursor protein	Lipoprotein and protease uptake, synaptic transmission, modulation of amyloid precursor protein processing?	Conventional knockout is early embryonic lethal; liver specific knockout viable, lipoprotein clearance defect
Megalin	ApoB, ApoE, proteases and inhibitors, carrier proteins for lipophilic vitamins, parathyroid hormones	Embryonic cholesterol homeostasis?, Ca^{2+}-homeostasis, required for forebrain development,	Holoprosencephaly, vitamin D deficiency
VLDL receptor	ApoE, Reelin	Cortical lamination, neuronal migration, predominant Reelin receptor in the cerebellum	Rostral cerebellar foliation defects
ApoER2	ApoE, Reelin	Cortical lamination, neuronal migration, predominant Reelin receptor in the neocortex	Severe cortical and hippocampal lamination defects, *vldlr/aper2* double mutants are phenotypically indistinguishable from *reeler* mice
LRP1B	Unknown, ApoE binding likely	Frequently deleted in tumors, role in tissue remodeling and metastasis?	Unknown
MEGF7	Unknown, ApoE binding likely	Expression in the brain suggests possible roles during development and maintenance of the CNS	Unknown

Table adapted from Herz, 2001

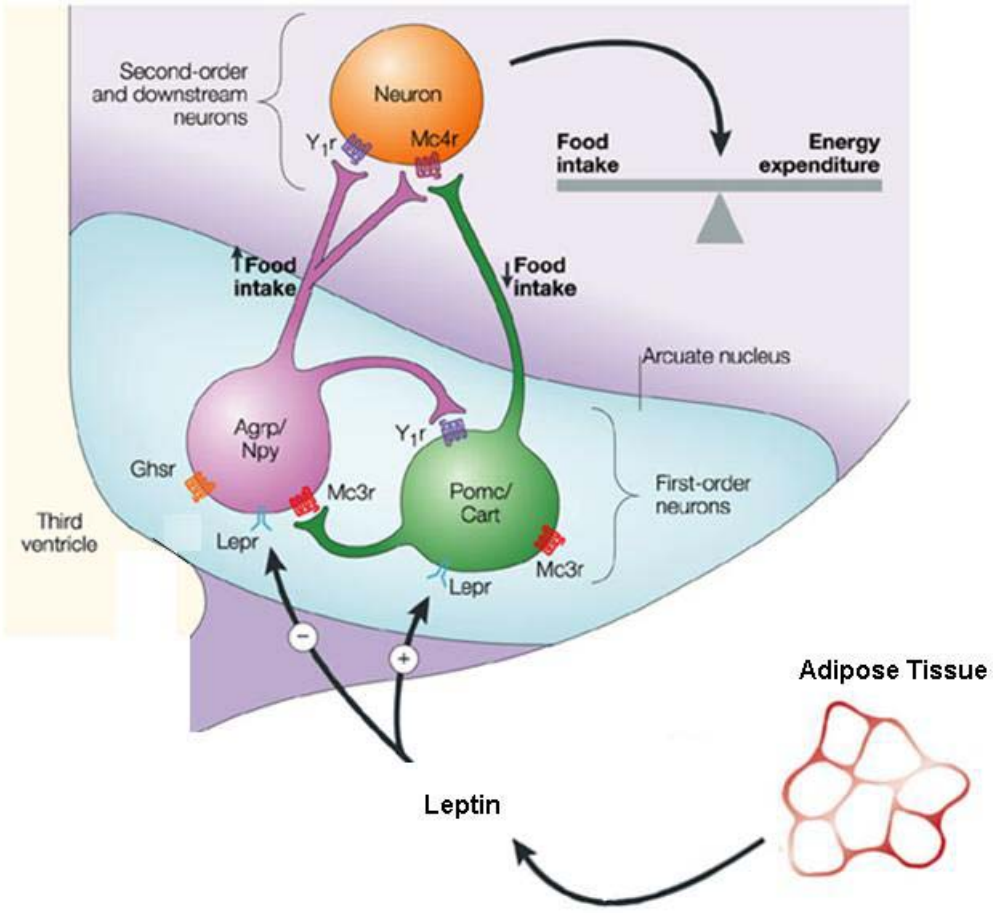

Figure 1.1. Control of energy homeostasis by arcuate nucleus neurons. Two sets of neurons in the arcuate nucleus — Agrp/Npy and Pomc/Cart neurons — are known to be regulated by circulating hormones. Agrp (agouti-related protein) and Npy (neuropeptide Y) are neuropeptides that stimulate food intake and decrease energy expenditure, whereas alpha-melanocyte stimulating hormone (a post-translational derivative of proopiomelanocortin, Pomc) and Cart (cocaine- and amphetamine-regulated transcript) are neuropeptides that inhibit food intake and increase energy expenditure. Leptin is a hormone that circulates in proportion to body adipose stores; it inhibits Agrp/Npy neurons and stimulate adjacent Pomc/Cart neurons. This figure is adapted from Barsh & Schwartz, 2002., used with Nature Publishing Group's permission.

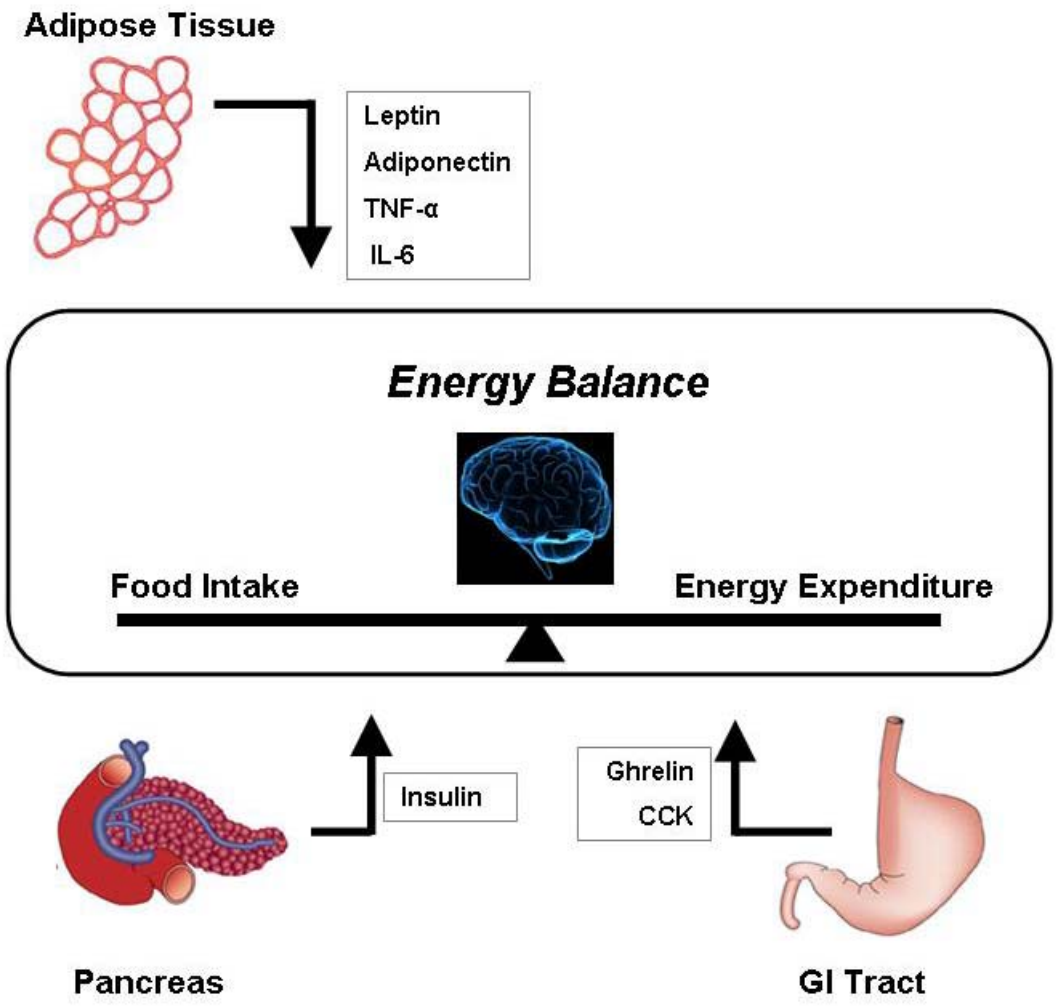

Figure 1.2. Humoral factors affecting energy balance. Adipose tissue, pancreas, and stomach produce humoral factors which affect the overall energy balance phenotype of animals. Adipose tissue produces leptin, adiponectin, TNF-α, and IL-6. The pancreas produces insulin. The gastrointestinal tract produces ghrelin and CCk. These images are adapted from Barsh & Schwartz, 2002., used with Nature Publishing Group's permission.

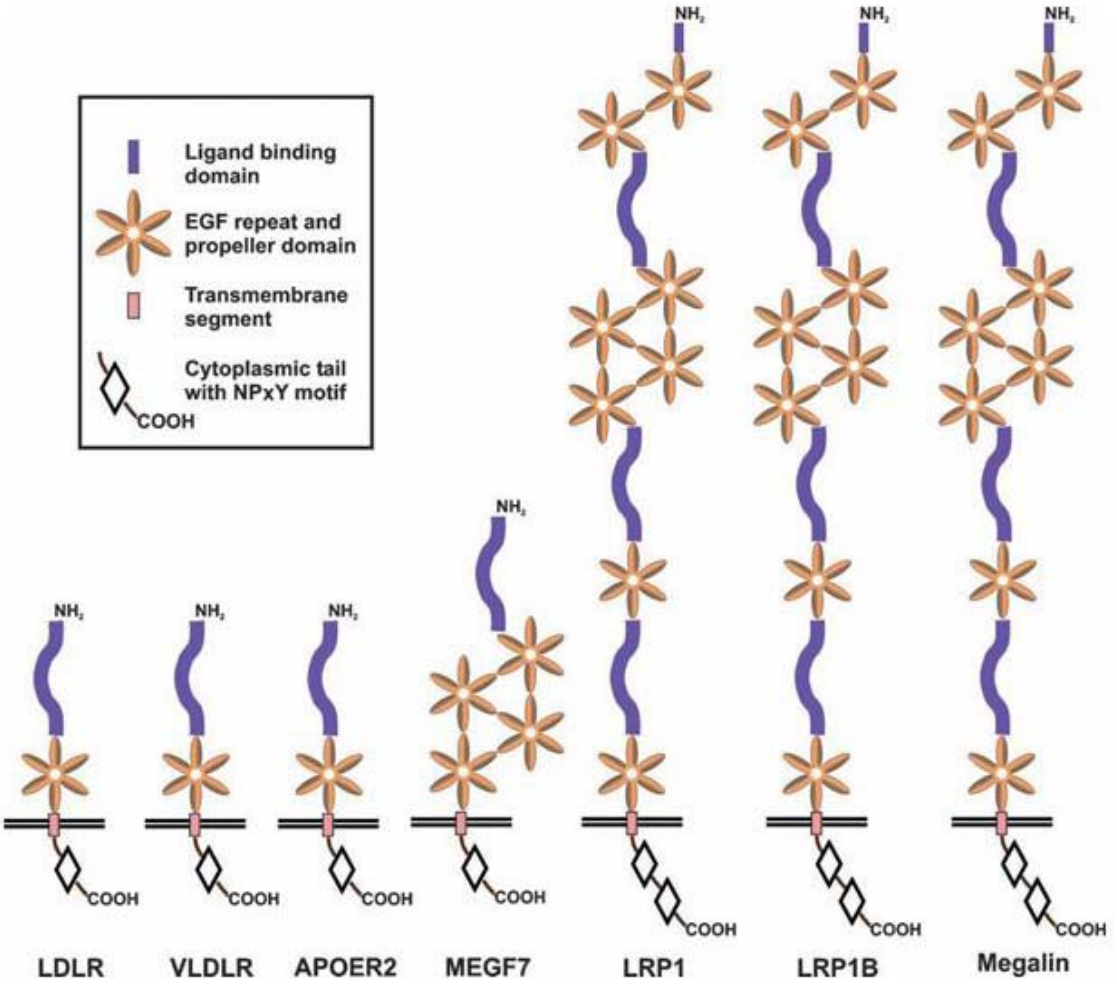

Figure 1.3. Schematic representation of the seven mammalian LDL receptor (LDLR) family members. Each LDLR member contains one or more ligand binding domains, epidermal growth factor (EGF)-precursor like propeller domains, a single transmembrane segment, and a cytoplasmic tail containing one or more NPxY motifs. The latter serves as both endocytosis signals and docking sites for adaptor proteins that couple the receptors to intracellular signaling pathways. This figure is from Beffert *et al.*, 2004.

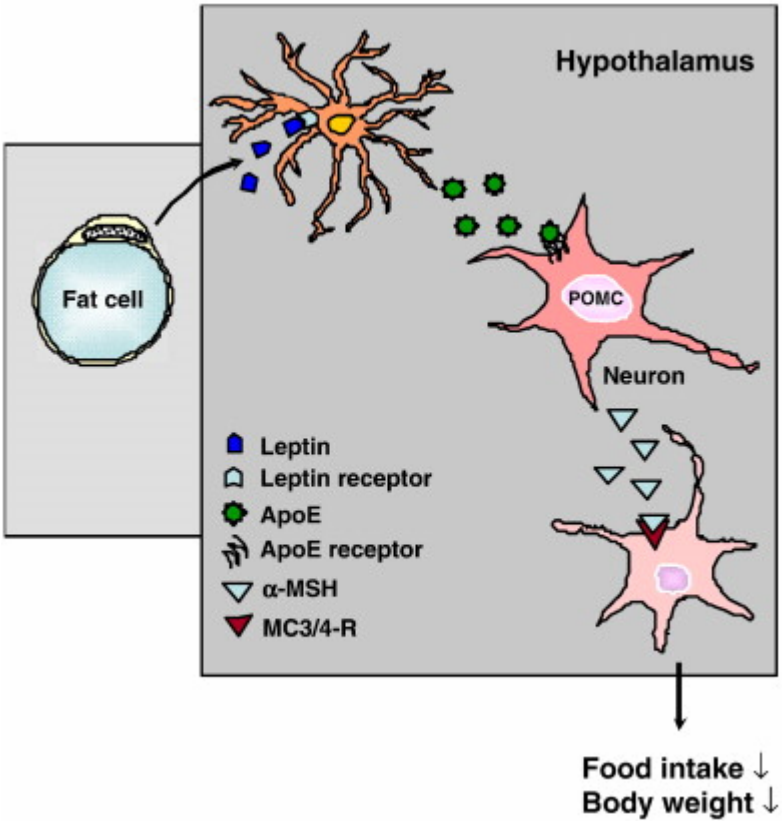

Figure 1.4. **Model for the interaction of Apoe with leptin and Pomc in the control of food intake and body weight.** This figure is a model hypothesized by Shen *et al.*, 2009 and is used with permission. Apoe gene expression in the hypothalamus is stimulated by leptin. The secreted Apoe is hypothesized to bind its receptors located on Pomc neurons and stimulate Pomc gene expression, resulting in more α-MSH cleaved and released. The secreted α-MSH presumably binds to MC3/4 receptors and consequently reduces the food intake and body weight.

CHAPTER 2: Materials and Methods

2.1 Introduction to the Study of Energy Balance

2.1.1 Energy Balance

To study the interaction between lipid metabolism and energy homeostasis, the *Ldlr-/-* mouse strain was used as an animal model for dyslipidemia. The overall aim of these experiments was to investigate the effect of deletion of the mouse *Ldlr* gene on energy balance. Both physiological measurements and molecular biological techniques were employed to compare *Ldlr-/-* mice to wildtype *Ldlr+/+* mice. From these results, the impact on energy homeostasis due to the loss of an important receptor for lipoprotein clearance can be elucidated. Total energy usage, energy intake, and energy stored were analyzed to obtain a global understanding of the energy balance phenotype in *Ldlr-/-* mice.

The energy balance status of an animal can be expressed mathematically by the simple equation:

Energy Intake = Energy Expenditure + Energy Stored

Based on this equation derived from the First Law of Thermodynamics[23], the energy which is accumulated by the animal in adipose stores is a result of excess energy intake relative to energy use[23]. However, because organisms have evolved to compensate for perturbations to homeostasis, the above variables are not independent in biological systems. For instance, should ingested calories decrease, most animal systems respond with a compensatory decrease in EE. Thus, energy balance is not static, but depends on

continuous feedback systems that respond to the body's energetic status, needs, and demands[23].

2.1.2 Energy Expenditure

The total energy expended by an animal is largely accounted for by its resting metabolic rate (RMR)[110]. RMR refers to the energy required to maintain basal level of functioning when the animal is well-rested, fasting, and in a thermoneutral environment[110]. The RMR represents the most minimal amount of energy that is used to preserve the cells comprising an individual. In addition to RMR, total energy expended by an animal is affected by the activity level of the animal and by adaptive thermogenesis[23]. The process of adaptive thermogenesis involves physiological adjustments to maintain body temperature in cold environments, as well as the thermic effect of food (TEF). TEF describes the phenomenon of increased heat production observed in animals after consumption of a meal[110]. The methods described below used an open-circuit indirect calorimetry system to determine total EE in mice.

2.1.3 Energy Intake

The total energy consumed was also examined in mice. While the absolute number of calories consumed is important, total energy intake, EE, and energy balance are also strongly affected by macronutrient composition of diets[114]. Therefore, the effect of variation in macronutrient diet composition was tested on *Ldlr-/-* mice, in order to study whether impaired lipid transport might alter the usual responses elicited by a high-fat, high-carbohydrate diet. In addition, to address absorption of calories from diet

consumed, caloric content of fecal matter was examined to ensure that ingested calories correlated with calories absorbed in *Ldlr-/-* mice relative to wildtype controls.

2.1.4 Energy Stored

Animals store energy in order to prepare for times of energy deprivation[23]. Energy storage results from a higher level of energy intake than energy expenditure. The amount of energy stored by an organism is sensitive to cumulative effects. Therefore, even a small increase in energy consumed over energy used can have major consequences on energy balance if this discrepancy is chronic[23]. Obesity manifests in cases where excessive energy stored in fat depots becomes serious enough to pose a risk for health. To examine total energy stored in mice, scale weight measurements as well as body composition data were collected from *Ldlr+/+* mice and *Ldlr-/-* mice. Body composition was determined using quantitative magnetic resonance (QMR) technology, a technique which provides quantitative information on the total lean muscle mass and the total body fat mass stored in individual animals[115].

2.1.5 Further Indicators of Energy Balance

The association between obesity and type 2 diabetes is widely recognized and obesity is known to contribute to insulin resistance and hyperinsulinemia[113]. Glucose clearance and insulin sensitivity are crucial indicators of metabolic functioning. Thus, in addition to measures of energy balance, physiological data on glucose homeostasis were obtained from *Ldlr-/-* mice. Response to leptin administration in *Ldlr-/-* mice was also evaluated. Leptin is an important hormone regulating glucose homeostasis and energy

balance, and leptin responsiveness may serve as an indicator of leptin pathway functioning in *Ldlr-/-* animals. Furthermore, serum protein levels and gene expression levels of molecules important in the regulation of energy balance were studied.

2.2 Experimental Animals and Diets

Ldlr+/+ mice and *Ldlr-/-* mice on a C57BL/6 background (Jackson Laboratories, Stock Nos. 000664 and 002207) were housed under a standard 12-hour light/dark cycle. Male mice were used in experiments to avoid possible confounding effects of estrous cycling. Separate cohorts of mice were analyzed at 10 weeks age and at 18 weeks age from each genotype. All mice were weaned onto a standard rodent chow diet (5P76, Research Diets, New Brunswick, NJ: 3.46 kcal/g of diet, 14%kcal from fat, 26.0% kcal from protein, and 60.0% kcal from carbohydrates). For cohorts of mice analyzed at 18 weeks age, mice were either maintained on the chow diet or switched at 10 weeks age to a Western-Type diet (TD.88137 Harlan Teklad, Madison, WI: 4.5 kcal/g of diet, 42.0% kcal from fat, 15.2% kcal from protein, 42.7% kcal from carbohydrate). During periods of diet exposure, mice were housed in groups of three to five animals per cage, and weight gain was documented weekly. Animals were transitioned from group-housing to single housing at least three days before placement in metabolic cages, so that they would be pre-acclimatized prior to metabolic studies (see below). Mice were sacrificed via rapid cervical dislocation and organs were dissected out, weighed, and snap-frozen in liquid nitrogen. All procedures were performed according to guidelines and with the approval of the University of British Columbia Animal Care Committee.

2.3 Characterization in Metabolic Chambers

2.3.1 Metabolic Chambers

Ldlr+/+ mice and *Ldlr-/-* mice were placed in metabolic cages designed to mimic the home-cage environment (LabMaster, TSE Systems, Germany), and were provided with nestlet bedding material. It was necessary to house animals singly to obtain accurate measurements of respiratory exchange ratio (RER), EE, activity levels, and food intake on individual mice. Metabolic cages were located at the Child and Family Research Institute Animal Facility. In total, eight metabolic cages were housed in a temperature control unit, with the capacity to regulate temperatures between 0ºC and 40ºC. Ambient room temperature was maintained between 24ºC – 25ºC. Animals were allowed at least one dark phase to acclimatize to the metabolic cage conditions; continuous monitoring graphs in this thesis display this initial acclimatization period. All calculated values for RER, EE, resting energy expenditure (REE), activity, and food intake only use measurements obtained post-acclimatization.

2.3.2 Indirect Calorimetry

O_2 consumption and CO_2 production were measured via an open-circuit indirect calorimetry system, with sensors sampling air from each cage once every fifteen minutes. RER, an indicator of fuel metabolism, was calculated from the ratio of VCO_2 (ml/hr) produced to VO_2 (ml/hr) consumed[116]. EE per gram of lean body mass (kcal/kg/hr) was calculated from the equation: VO_2 * [3.815 + 1.232 * RER] * 0.001 / lean body mass (kg)[116]. (Lean body mass was quantified by QMR – see below). REE was estimated from the average of the five lowest EE recordings for each animal during the light phase[117].

2.3.3 Activity Levels

Infrared beams along the x, y, and z axis of metabolic cages collected data on activity levels. Activity was assayed by automatic recording of infrared beam breakage by animals traveling within their cages. Repeated breakage of the same beam was defined as fine movement. Consecutive breaking of adjacent beams was defined as locomotor activity. Absolute number of beam breaks was recorded automatically.

2.3.4 Food and Water Intake

Food intake and water intake were monitored through weight sensors directly associated with food baskets and water holders. The weights of the food and water holders in each metabolic cage were recorded automatically every fifteen minutes. Food and water intake were inferred from the recorded change in weight. The bottoms of the cages were examined daily to document unconsumed food or water that had been removed from the baskets.

2.3.5 Thermogenesis and Cold Challenge

Body temperature was monitored continuously by temperature transmitters (Mini-Mitter, Bend, OR) implanted under the skin in the interscapular region in *Ldlr*+/+ and *Ldlr*-/- mice. For the implantation surgery, animals were anesthetized using gaseous isofluorane. Body temperature transmitters were inserted into the subcutaneous tissue through a 0.5 cm incision, which was closed via sutures. Animals were given at least two days to recover after the surgery before body temperature was recorded. With the body temperature transmitters implanted, mice were also subjected to a cold-challenge

experiment. Mice were placed in the temperature control unit, set to maintain temperature at 4°C. Thermogenic adaptation to this temperature was observed over a four hour period.

2.4 Body Composition

Total body composition was measured in live conscious animals using QMR technology, which distinguishes differential proton states between lipids, lean tissues, and free water (EchoMRI-100 Echo Medical Systems, Houston, TX)[115]. Conscious animals were placed individually in the QMR system for approximately one minute while the machine collected body composition data. Lean mass and fat mass were quantified, and residual mass was calculated by subtracting the lean and fat mass QMR readings from the total scale weight of the animal.

2.5 Serum Protein Concentrations

Blood was collected either through the saphenous vein after a four-hour fast or through a cardiac puncture and allowed to clot at room temperature for 15 minutes. Serum was extracted after centrifugation at 3000 rpm for 10 min and stored at –20ºC. Samples were tested for leptin and insulin levels using enzyme linked immunosorbent assays (ELISA, ALPCO Salem, NH) within one month of collection. The insulin ELISA (Cat# 90080) and leptin ELISA (Cat# 90030) were used according to manufacturer's protocol.

2.6 Energy Content of Mouse Fecal Matter

Direct calorimetric analysis of *Ldlr*+/+ and *Ldlr*-/- mouse fecal matter was conducted using the 1241 Oxygen Bomb Calorimeter (Parr Instrument Company, Moline, IL). Mouse fecal matter was frozen upon collection. Before calorimetric analysis samples were dried at room temperature for at least three days. Standardization of the bomb calorimeter was conducted using one gram benzoic acid pellets (Fisher Scientific, Waltham, MA). Butanol was used as an accelerant for the reaction. Approximately 300 mg of fecal sample and 200ul of butanol were used in each combustion reaction. The sample was placed in the bomb in association with the fuse wire. The bomb was then immersed in exactly one liter of water. Baseline water temperature was recorded for six minutes prior to ignition and deemed stable. Post-ignition, the temperature of the water was recorded for 10 min. Samples were examined following each reaction to ensure complete combustion had occurred. The interior of the bomb was then washed with distilled water. The washings were titrated with 0.0709N sodium carbonate solution using methyl red as an indicator. Titrating the washings of the interior surface of the bomb allowed for quantification of nitric acid formed during combustion. The energy of the sample was calculated using the following equation:

$$H_g = \frac{tW - e_1 - e_2 - H_{but}}{m}$$

H_g = gross heat of combustion (calories per gram)

t = net temperature rise recorded

W = energy equivalent of the calorimeter, as determined through standardization through benzoic acid pellets.

$\mathbf{e_1}$ = correction in calories for heat of nitric acid formation

$\mathbf{e_2}$ = correction in calories for heat of combustion of fused wire

$\mathbf{H_{but}}$ = heat from combustion of 200ul of butanol.

m = dry fecal mass (g)

2.7 Glucose Homeostasis

Intraperitoneal glucose tolerance tests (IPGTTs) and insulin tolerance tests (IPITTs) were conducted in *Ldlr-/-* mice to examine glucose homeostasis. Group-housed *Ldlr+/+* and *Ldlr-/-* mice were fasted for four hours prior to IPGTTs and IPITTs[118]. For both tests, blood glucose was measured at baseline and at 15 min, 30 min, 60 min, 90 min, and 120 min post injection using a standard glucometer (Breeze Glucometer Bayer, Toronto, Ontario). For all glucose measurements, animals were restrained and a blood droplet was isolated from the saphenous vein and analyzed with the glucometer. For IPGTTs, 50% dextrose solution (anhydrous dextrose, Fisher Scientific, Waltham, MA) was injected at a dose of 1.5g/kg of body weight. For IPITTs, insulin (Novolin ge Toronto, Novo Nordisk Canada Inc., Mississauga, ON) was injected at a dose of 0.75U/kg of body weight.

2.8 Quantifying Physiological Response to Leptin Administration

To allow animals to become accustomed to temporary restraint, mice were routinely handled for one month prior to the start of these physiological studies. All injections were administered one hour before the dark phase. Animals were sham injected

for four days prior to treatment injections. Thereafter, animals were injected with either 2μg/g of mouse recombinant leptin (Peprotech, Rocky Hill, NJ) or an equal volume of saline vehicle each day for two days. Mice were then allowed four days to recover to baseline conditions, during which time sham injections continued. Subsequently, mice received two consecutive days of the crossover treatment. Mice were weighed daily and housed in metabolic cages (see above) during treatment days. Each saline-treated animal acted as its own control for analysis of this crossover experiment.

2.9 Quantitative Reverse-Transcriptase Polymerase Chain Reaction

RNA isolation was performed using the RNeasy Mini-kit (Qiagen, Germantown, MD) following manufacturer's instructions. A Nanodrop2000c Spectrophotometer (Thermo Fisher Scientific, Waltham, MA) was used to check RNA purity (A260/A280 ratio between 1.9 – 2.1) and concentration. Quality of the RNA was also confirmed via agarose gel electrophoresis and visual confirmation of intact 18S and 28S rRNA bands. cDNA was synthesized using the RT-Transcribe Kit (Invitrogen, Carlsbad, CA), and was again checked using the Nanodrop2000c for concentration and purity (A260/A280 ratio between 1.7 – 1.9). All quantitative reverse-transcriptase polymerase chain reaction (qRT-PCR) primers are listed in **Table 2.1**. Proper efficiency of all primers (Invitrogen, Carlsbad, CA) was examined by generating a standard curve using serial dilutions of cDNA sample. qRT-PCR was performed using the ABI3500 Fast Machine (Applied Biosystems, Carlsbad, CA). qRT-PCR was set up using the Express SYBR GreenER master mix (Invitrogen, Carlsbad, CA). All primer reactions required an annealing temperature of 62ºC. The presence of non-specific PCR products was ruled out using

melt-curve analysis for every reaction. Expression of genes relative to β-actin was determined using the ΔΔCt method[119].

2.10 Statistics

t-tests were used for standard comparison of two groups. One-way ANOVAs and two-way ANOVAs were conducted with Bonferroni post-tests to account for multiple testing. Repeated-measures ANOVA statistics were used for leptin responsive experiments, IPGTTs, IPISTs, and data generated in the metabolic cages. Calculated p-values less than 0.05 were chosen to be considered significant.

Table 2.1. Primers for qRT-PCR.

Gene	Forward Primer	Reverse Primer	Product Size
β-actin	ACGGCCAGGTCATCACTATTG	CAAGAAGGAAGGCTGGAAAAGA	70
Leptin	GAGACCCCTGTGTCGGTTC	CTGCGTGTGTGAAATGTCATTG	139
Ucp1	AGGCTTCCAGTACCATTAGGT	CTGAGTGAGGCAAAGCTGATTT	133
Npy	CGCCACGATGCTAGGTAACA	GCCAGAATGCCCAAACACA	84
Pomc	ATGCCGAGATTCTGCTACAGT	TCCAGCGAGAGGTCGAGTTT	170
Ldlr	GTTGACGGCTCCCATGAGTG	GTCCTTGCAGTCTGCCTCG	156
Apoe	AACAGACCCAGCAAATACGCC	CTCATTGATTCTCCTGGGCC	154

All primers displayed 5'→ 3'.

CHAPTER 3: Energy Balance in the *Ldlr-/-* Mouse

3.1 Energy Balance of *Ldlr*-/- Mice on Chow

3.1.1 *Ldlr-/-* Mice at 10 Weeks Age

Mice with genotypes of either *Ldlr*+/+ or *Ldlr*-/- were originally ordered from Jackson Laboratories and were maintained in breeding colonies at the CFRI Animal Research Facility, as described in Chapter II. A cohort of male *Ldlr*+/+ and *Ldlr*-/- mice were analyzed in metabolic cages at 10 weeks of age, after bone maturation and sexual maturity had been reached[120]. At this age, no differences in body weight or body composition were detected between knockout mice and wild-type mice (**Figure 3.1A**). However, continuous monitoring of food intake in the metabolic cages revealed that *Ldlr*-/- mice consumed 9% fewer calories of the standard chow diet than *Ldlr*+/+ mice (**Figure 3.1B**) (*Ldlr*+/+: 3.90g/mouse/day, *Ldlr*-/-: 3.57g/mouse/day, p=0.02). Additionally, despite no differences in body weight REE and dark phase EE was slightly reduced in *Ldlr*-/- mice (**Figure 3.2A & B**). RER and activity levels, both fine and locomotor, were not different between the *Ldlr*-/- mice and *Ldlr*+/+ mice at this age (**Figure 3.2C, D, & E**). Fasting blood glucose levels and glucose tolerance in *Ldlr*-/- mice were also not different from *Ldlr*+/+ mice at 10 weeks of age (**Figure 3.3**).

3.1.1 *Ldlr-/-* Mice on a Chow Diet at 18 Weeks Age

In a different cohort of *Ldlr*+/+ or *Ldlr*-/- mice, animals were maintained in group-housed conditions on the chow diet until 18 weeks of age. At 18 weeks, the mice were analyzed in the QMR machine and in the metabolic cages. *Ldlr*-/- mice did not

weigh differently from *Ldlr*+/+ mice and total lean mass and total fat mass were also not significantly different at this age (**Figure 3.4A**). Dissected epididymal fat pads weighed less in *Ldlr*-/- mice, but inguinal fat pad weights did not differ between knockout and wildtype animals (**Figure 3.4B**). Interestingly, average interscapular brown fat pads of *Ldlr*-/- mice weighed more than those of *Ldlr*+/+ mice (**Figure 3.4C**). In addition, decreased food intake in *Ldlr*-/- mice, which was observed at 10 weeks of age, was further decreased to 40% fewer calories than *Ldlr*+/+ mice at 18 weeks of age (**Figure 3.4D**, *Ldlr*+/+: 3.80g/mouse/day, *Ldlr*-/-: 2.28g/mouse/day). Indirect calorimetric analysis showed that REE was decreased in *Ldlr*-/- mice (**Figure 3.5A**). Continuous monitoring of oxygen use and carbon dioxide production showed that *Ldlr*-/- mice had decreased EE in the light and dark phase relative to *Ldlr*+/+ mice (**Figure 3.5B**). RER was decreased in *Ldlr*-/- mice in the dark phase (**Figure 3.5C**). As well, *Ldlr*-/- mice had increased fine movement and locomotor activity in the day time (**Figure 3.5D & E**).

In a separate cohort of *Ldlr*+/+ and *Ldlr*-/- mice fed a chow diet, fasting glucose levels were measured at 24 weeks of age. Fasting glucose levels were not different in *Ldlr*-/- mice than in *Ldlr*+/+ mice (**Figure 3.6A**). In addition, IPGTTs performed in group-housed animals showed no differences in glucose clearance between *Ldlr*+/+ mice and *Ldlr*-/- mice on the chow diet (**Figure 3.6B**).

3.2 *Ldlr*-/- Mice Gain Less Weight on WTD

3.2.1 Acute Response to WTD Feeding

Next, the response of *Ldlr*-/- mice fed a WTD was examined. A group of *Ldlr*+/+ mice and *Ldlr*-/- mice that were weaned onto the chow diet at approximately three weeks

of age were switched WTD starting at 10 weeks of age. Acute responses to the WTD were monitored using metabolic cages. The 10-week old mice were placed in the metabolic cages and allowed four days to acclimatize before the standard rodent chow diet was removed and replaced with the WTD. In the first day following the switch, both genotypes consumed more calories per day compared to the prior chow-feeding day (**Figure 3.7A & B**). Analysis of each individual day following the switch to WTD feeding revealed that the initial increase in caloric intake occurs in the first day of WTD feeding. Caloric intake on WTD gradually declines to previous levels (on chow) by day 4 after the switch to WTD feeding (**Figure 3.7B**). While the initial caloric consumption on a chow diet was significantly lower in *Ldlr-/-* mice relative to *Ldlr+/+* mice, after WTD feeding began the caloric consumption became equal between the genotypes. *Ldlr-/-* mice were consuming the same number of calories as did *Ldlr+/+* mice within the first 4 days of WTD feeding (**Figure 3.7C** – data from **Figure 3.7B** re-graphed for comparison).

Data from the metabolic cages during the initial switch to WTD also showed that indirect calorimetry parameters were significantly altered by acute exposure to WTD in both *Ldlr+/+* and *Ldlr-/-* mice: Light phase EE was increased in both genotypes following WTD exposure, suggesting partial compensation by homeostatic responses to energy dense diets (**Figure 3.8A**). Dark phase EE was also affected with acute diet switch in *Ldlr+/+* and *Ldlr-/-* mice (**Figure 3.8A**). Average light phase RER was increased in both *Ldlr+/+* and *Ldlr-/-* mice in second day of WTD feeding, but was lowered to pre-WTD RER by the third day of WTD (**Figure 3.8B**). Very acute decreases in dark phase locomotor and fine movement activity levels were also observed in both genotypes immediately following diet switch (**Figure 3.9A & B**).

3.2.2 Response to Chronic WTD Feeding

Ldlr-/- mice weighed significantly less than controls after just five weeks exposure to the WTD (**Figure 3.10A**). After eight weeks on the WTD, *Ldlr-/-* mice weighed significantly less; this difference in body mass was attributable to a specific failure to gain fat mass, with lean mass and residual mass not differing between the two genotypes (**Figure 3.10B**). Dissection of visceral and inguinal fat pads showed that both white adipose depots were significantly reduced on the WTD in *Ldlr-/-* mice (**Figure 3.10C**). However, interscapular brown adipose tissue weights did not differ between *Ldlr-/-* mice and *Ldlr+/+* mice after exposure to the eight weeks of WTD feeding (**Figure 3.10D**). To test whether the failure of *Ldlr-/-* mice to gain weight on WTD was due to malabsorption of nutrients, direct calorimetry to determine energy content of fecal matter in *Ldlr+/+* mice and *Ldlr-/-* mice was performed with the assistance of W. Quong. The energy content of fecal matter did not differ between the two genotypes (**Figure 3.10E**). After chronic WTD exposure, food intake of *Ldlr-/-* mice was identical to controls. After eight weeks, *Ldlr+/+* and *Ldlr-/-* mice had similar total energy intakes on the WTD (**Figure 3.10F**). REE and total EE were reduced in *Ldlr-/-* mice fed the WTD (**Figure 3.11A & B**). However, a difference in response to the WTD was detected between the genotypes. 18-week old *Ldlr+/+* mice fed the WTD for eight weeks had an average dark phase EE of 26.18 kcal/hr/kg (**Figure 3.11B**), while *Ldlr+/+* mice fed chow had an average dark phase EE of 22.80 kcal/hr/kg (**Figure 3.5B**). This signifies a 14.8% increase in EE caused by WTD feeding which was not significantly different ($p>0.05$ with Bonferroni post-test). *Ldlr-/-* mice fed the WTD for eight weeks had an average dark phase EE of 22.33 kcal/hr/kg (**Figure 3.11B**), while *Ldlr-/-* mice fed chow had an

average dark phase EE of 16.52 kcal/hr/kg (**Figure 3.5B**). This signifies a 35.2% increase in EE caused by WTD feeding in *Ldlr-/-* mice, a difference that was statistically significant ($p<0.01$ with Bonferroni post-test). No differences in RER or activity levels were seen between *Ldlr-/-* mice and wildtype mice after WTD feeding (**Figure 3.11C, D, & E**).

Because I detected differences in body weight and white adipose tissue mass without significant differences in food intake or energy expenditure between knockout and wildtype animals, thermogenesis was examined in *Ldlr-/-* mice. In a new group of mice fed the WTD for 2-6 weeks, body temperature transmitters were implanted subcutaneously in the interscapular region. Thereafter, the mice were placed singly housed in the metabolic cages to monitor body temperature. This monitoring showed that *Ldlr-/-* mice had a higher average body temperature than did *Ldlr+/+* mice during the dark phase (**Figure 3.12A**). After three days of monitoring body temperature, mice were exposed to a 4°C cold challenge experiment for four hours. During exposure to 4°C, no differences in ability to regulate body temperature were observed between *Ldlr-/-* mice and *Ldlr+/+* mice (**Figure 3.12B**). With differences in brown adipose tissue (**Figure 3.4C**) and differences in thermogenesis (**Figure 3.12A**) observed between *Ldlr+/+* and *Ldlr-/-* mice, the functioning of brown adipose tissue thermoregulation in *Ldlr-/-* was studied next. Uncoupling protein 1 (*Ucp1*) is a mitochondrial inner-membrane protein expressed in brown adipose tissue and is important for thermogenesis in brown fat[121]. *Ucp1* functions to decouple the proton transport chain from the ATP synthesis[121]; thus, energy is dissipated in the form of heat as opposed to ATP generation. To examine whether brown-adipose tissue thermogenesis was different in *Ldlr-/-* mice, brown adipose

expression of *Ucp1* was examined using qRT-PCR. Expression levels of *Ucp1* in brown adipose tissue were not different between *Ldlr-/-* mice and *Ldlr+/+* mice (**Figure 3.12C**).

I also examined glucose homeostasis after WTD feeding in 24 week old mice. *Ldlr-/-* mice had significantly lower fasting glucose levels relative to wildtype mice after 14 weeks WTD exposure (**Figure 3.13A**). IPGTTs showed that *Ldlr-/-* mice cleared exogenous glucose from circulation more readily than *Ldlr+/+* mice (**Figure 3.13B**). Fasting insulin levels in *Ldlr-/-* mice were significantly higher than in wildtype mice, suggesting improved insulin secretion may be the mechanism for improved glucose tolerance (**Figure 3.13C**). However, IPITTs showed no differences in global insulin sensitivity (**Figure 3.13D**).

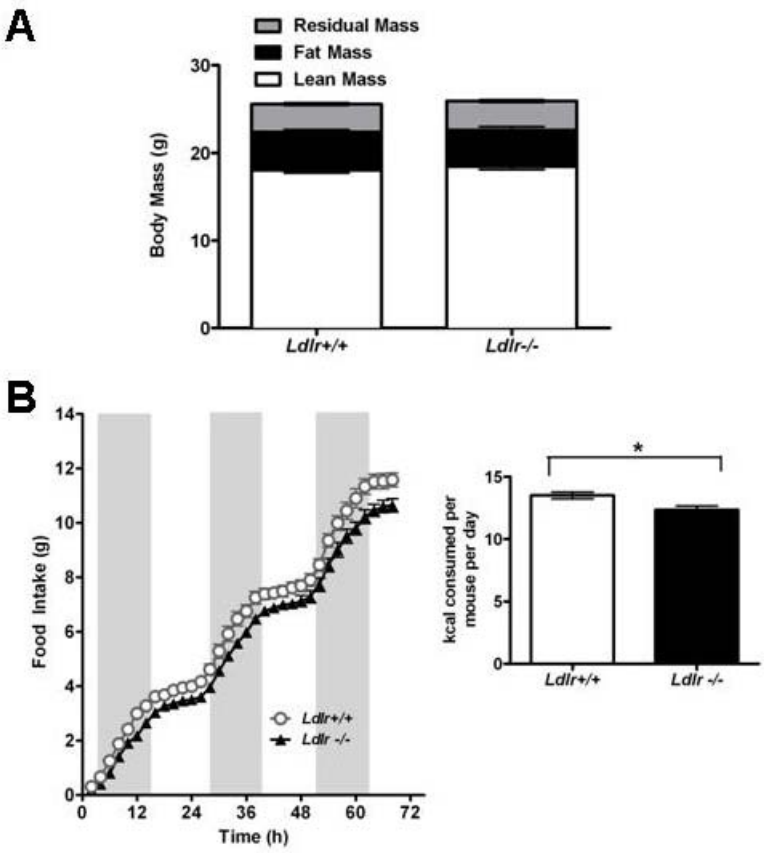

Figure 3.1: **Body weight and food intake in 10-week old *Ldlr-/-* mice on chow.** **A.** Body weight and body composition of 10-week old mice did not differ between wildtype and *Ldlr*-/- mice. **B.** Continuous monitoring of food intake showed that *Ldlr*-/- mice consumed slightly fewer calories (9%) relative to *Ldlr*+/+ mice. Grey bars represent the dark phase. n=6 for *Ldlr*+/+ mice, n=7 for *Ldlr-/-* mice. *$p<0.05$. Data represent mean ± SEM.

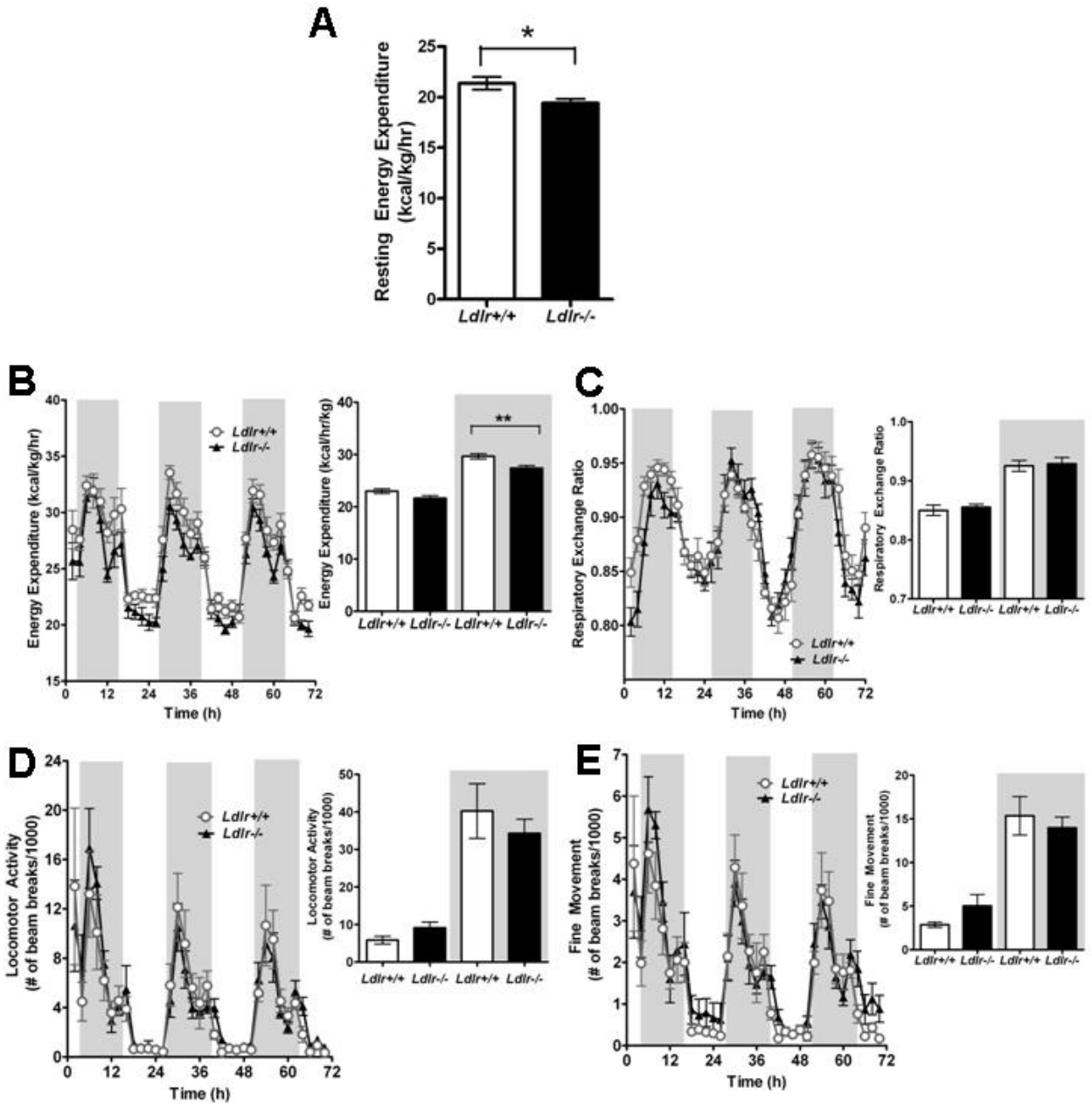

Figure 3.2: Energy expenditure in 10-week old Ldlr-/- mice on chow. *Ldlr-/-* mice had lower resting energy expenditure **(A)** and energy expenditure **(B)** than wildtype mice. Respiratory exchange ratio **(C)**, locomotor activity **(D)**, and fine movement **(E)** was not different between genotypes. Grey bars represent the dark phase. n=6 for *Ldlr*+/+ mice, n=7 for *Ldlr*-/- mice. *p<0.05, **p<0.01. Data represent mean ± SEM.

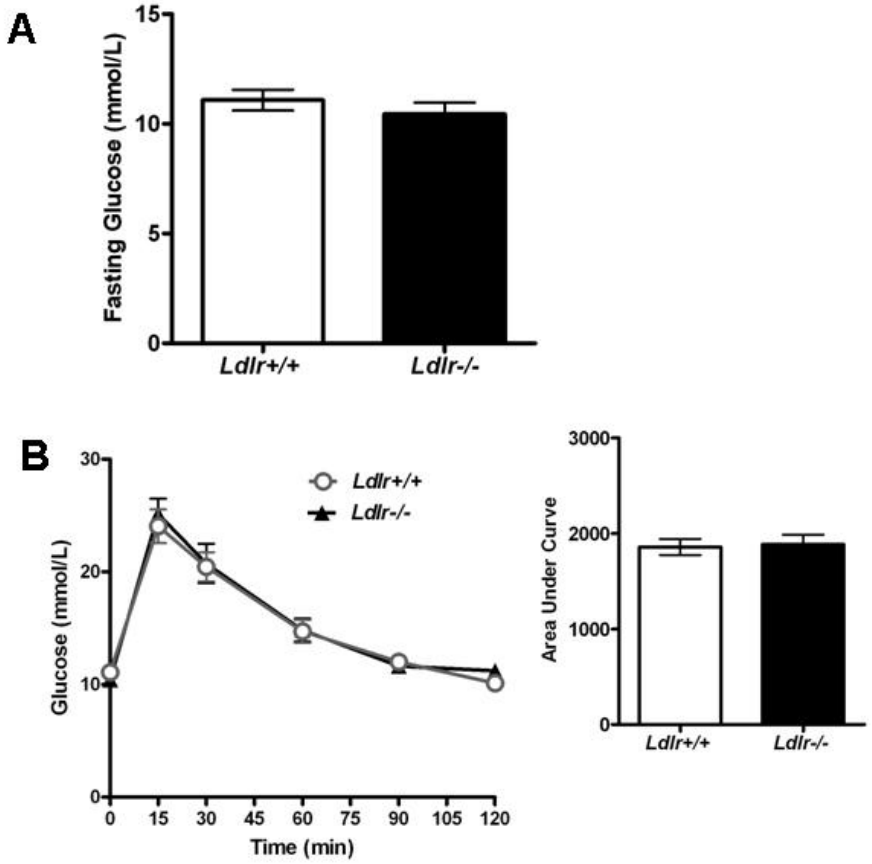

Figure 3.3: **Glucose homeostasis of 10-week old *Ldlr*-/- mice on a standard chow diet.** **A.** Fasting serum glucose levels were not different between *Ldlr*-/- mice and wildtype mice at 10-weeks of age. **B.** IPGTTs showed no differences in glucose clearance at 10 weeks of age between the two genotypes. n=5 for *Ldlr*+/+ mice, n=7 for *Ldlr*-/- mice. Data represent mean ± SEM.

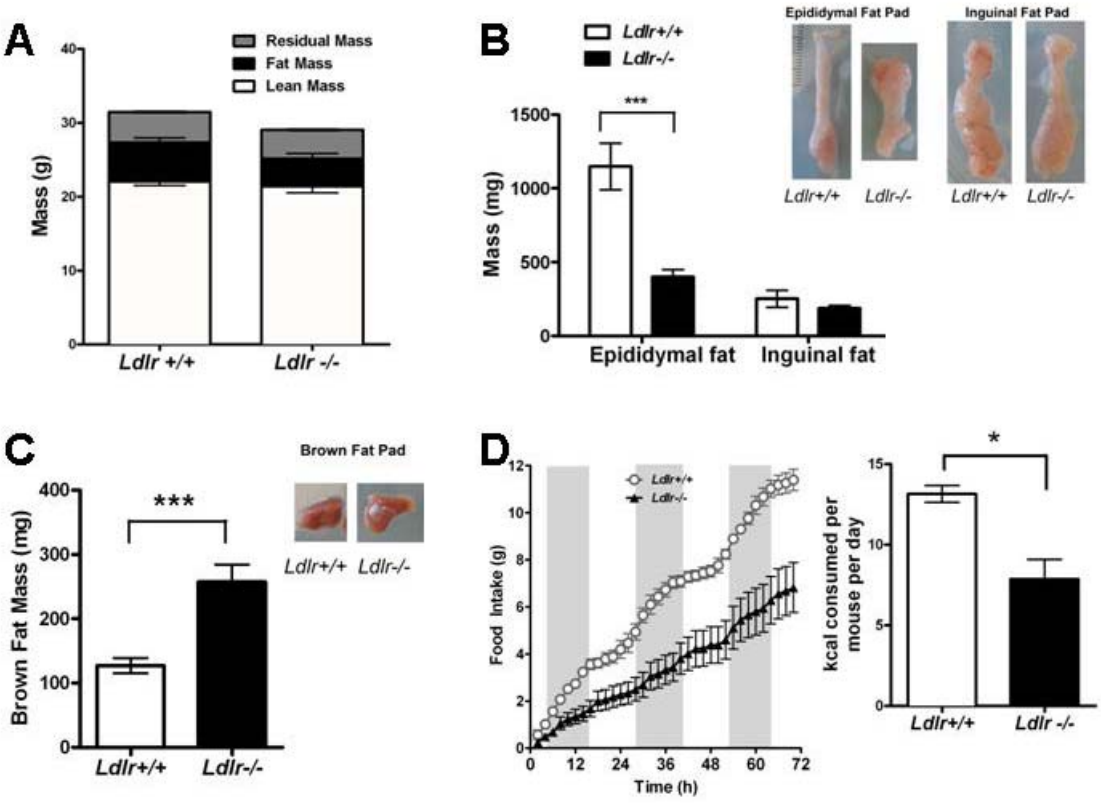

Figure 3.4: Body composition and food intake in 18-week old *Ldlr*-/- mice on chow. **A.** Body weight and body composition of 18-week old mice did not differ between *Ldlr*+/+ and *Ldlr*-/- mice. **B.** Weights of the epididymal visceral fat pad and inguinal subcutaneous fat pad dissected from mice. **C.** Weights of the interscapular brown fat pad dissected from mice, showing increased brown fat mass in *Ldlr*-/- mice. **D.** Continuous food intake monitoring demonstrated that *Ldlr*-/- mice consumed significantly less calories relative to *Ldlr*+/+ mice. Grey bars represent the dark phase. n=4 for *Ldlr*+/+ mice, n=6 for *Ldlr*-/- mice. Data represent mean ± SEM. *p<0.05, ***p<0.001.

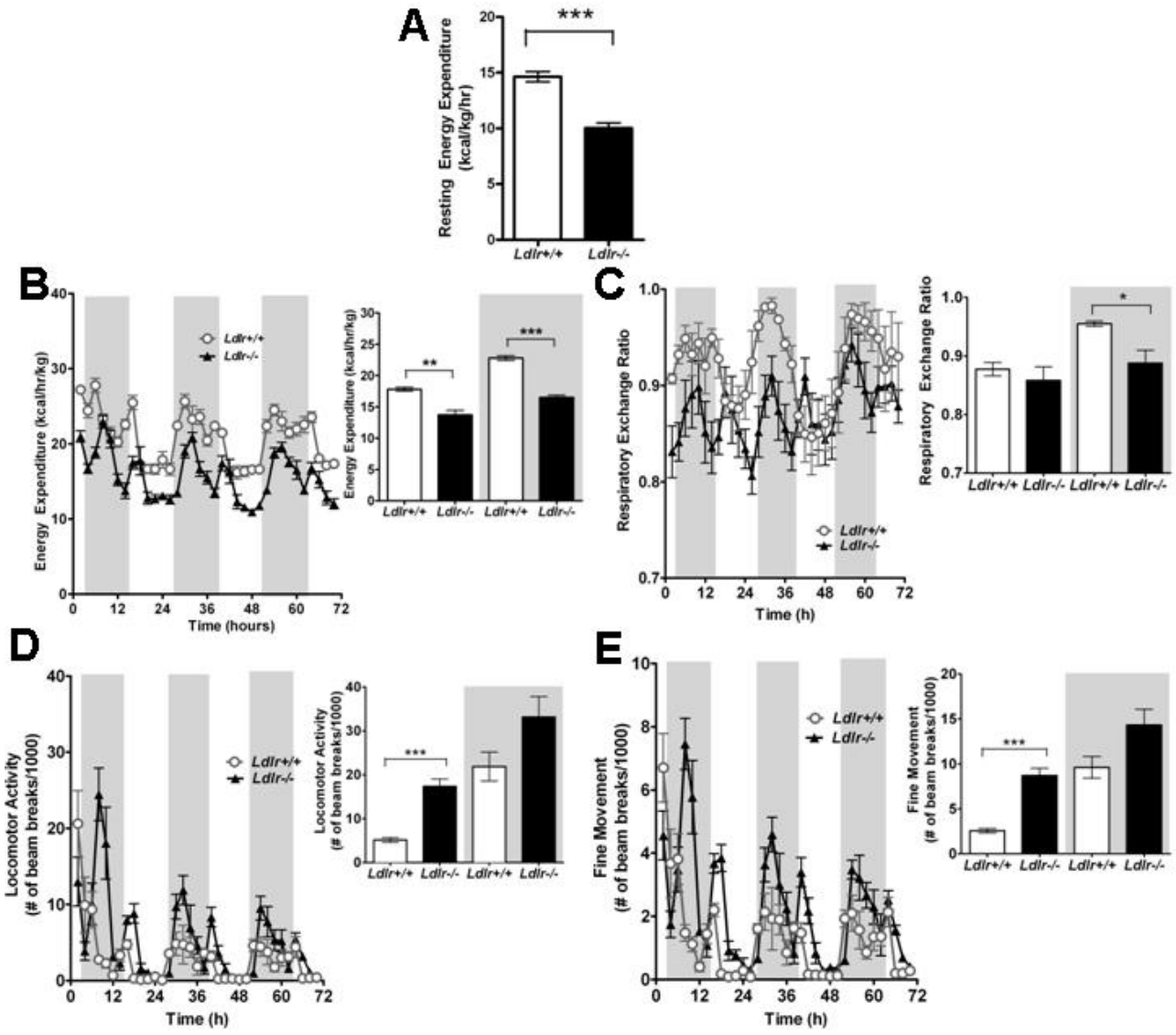

Figure 3.5: Energy expenditure in 18-week old *Ldlr*-/- mice fed chow. The energy balance phenotype of *Ldlr*+/+ mice and *Ldlr*-/- mice at 18 weeks of age was analyzed. Grey bars represent the dark phase. *Ldlr*-/- mice showed decreased resting energy expenditure **(A)**, decreased energy expenditure **(B)**, and decreased RER **(C**). Locomotor activity **(D)** and fine movement **(E)** were also increased in *Ldlr*-/- mice at this age. n=4 for *Ldlr*+/+ mice, n=6 for *Ldlr*-/- mice. *p<0.05, **p<0.01, ***p<0.001. Data represent mean ± SEM.

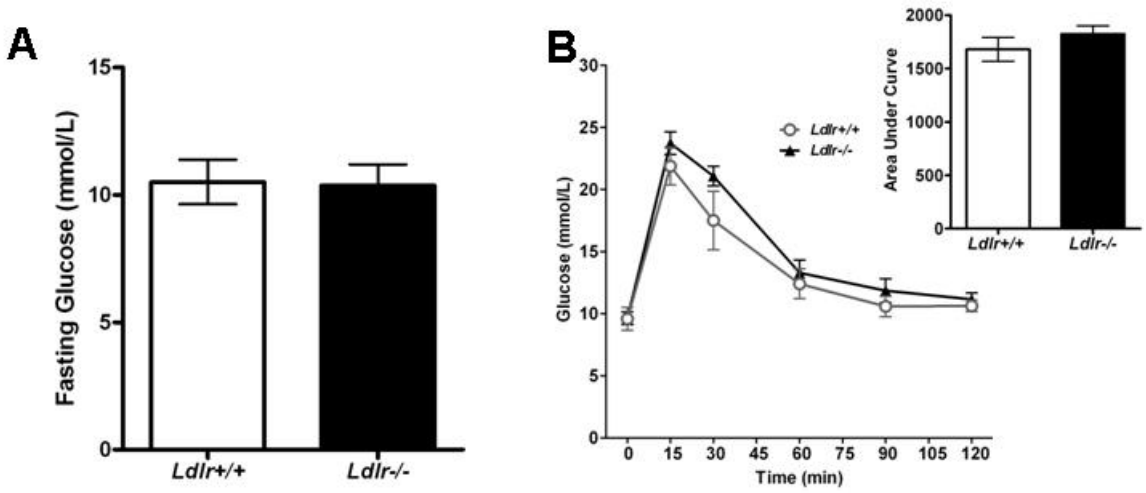

Figure 3.6: Glucose homeostasis of 24-week old *Ldlr*-/- mice on chow. A. Fasting serum glucose levels were not different between *Ldlr*-/- mice and wildtype mice at 24 weeks of age. **B.** IPGTTs showed no differences in glucose clearance at 24 weeks of age between the two genotypes. n=5 for *Ldlr*+/+ mice, n=7 for *Ldlr*-/- mice. Data represent mean ± SEM.

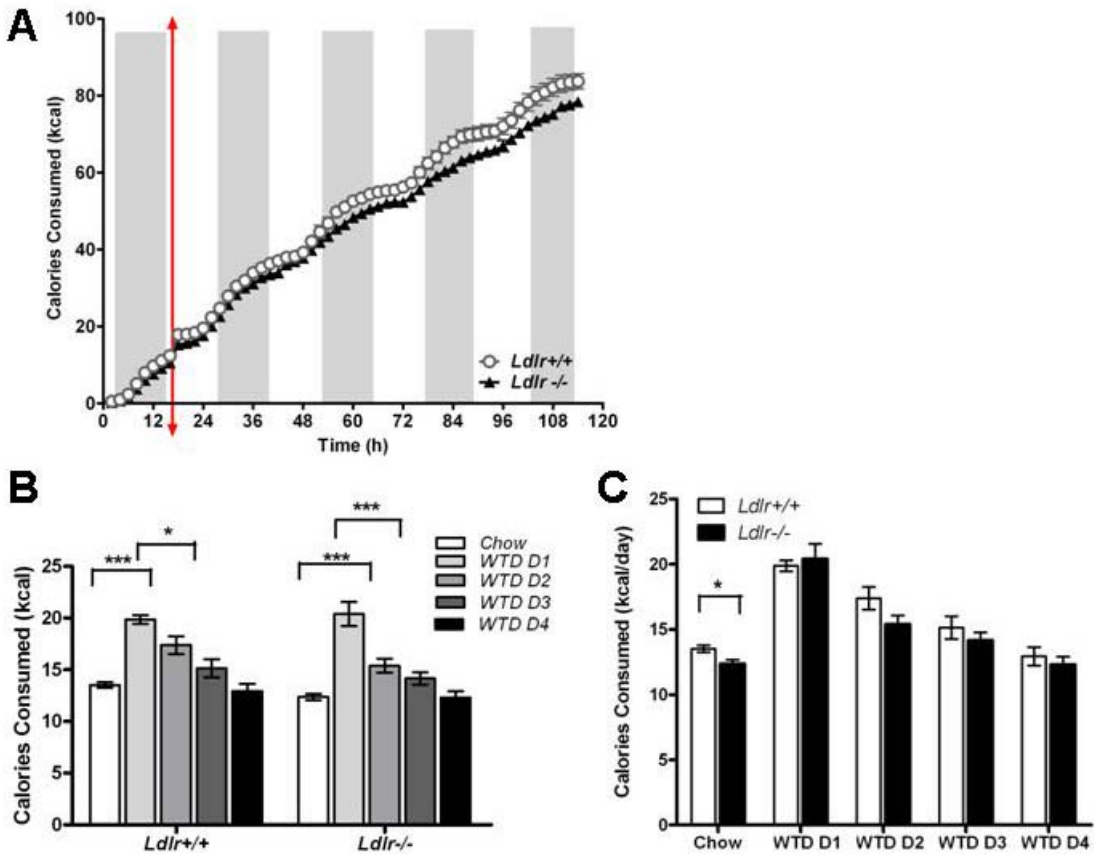

Figure 3.7: Food intake of *Ldlr*-/- mice acutely exposed to WTD at 10-weeks. **A.** Continuous food intake monitoring of *Ldlr*+/+ and *Ldlr*-/- mice when chow diet was switched to WTD (arrowed line). Grey bars represent the dark phase. **B.** Comparison of caloric consumption in *Ldlr*+/+ mice and *Ldlr*-/- mice over the first four days of WTD feeding. **C.** Comparison of caloric consumption between *Ldlr*+/+ mice and *Ldlr*-/- mice during the first four days of WTD feeding. n=4 for *Ldlr*+/+ mice, n=6 for *Ldlr*-/- mice. *p<0.05, ***p<0.001. Data represent mean ± SEM.

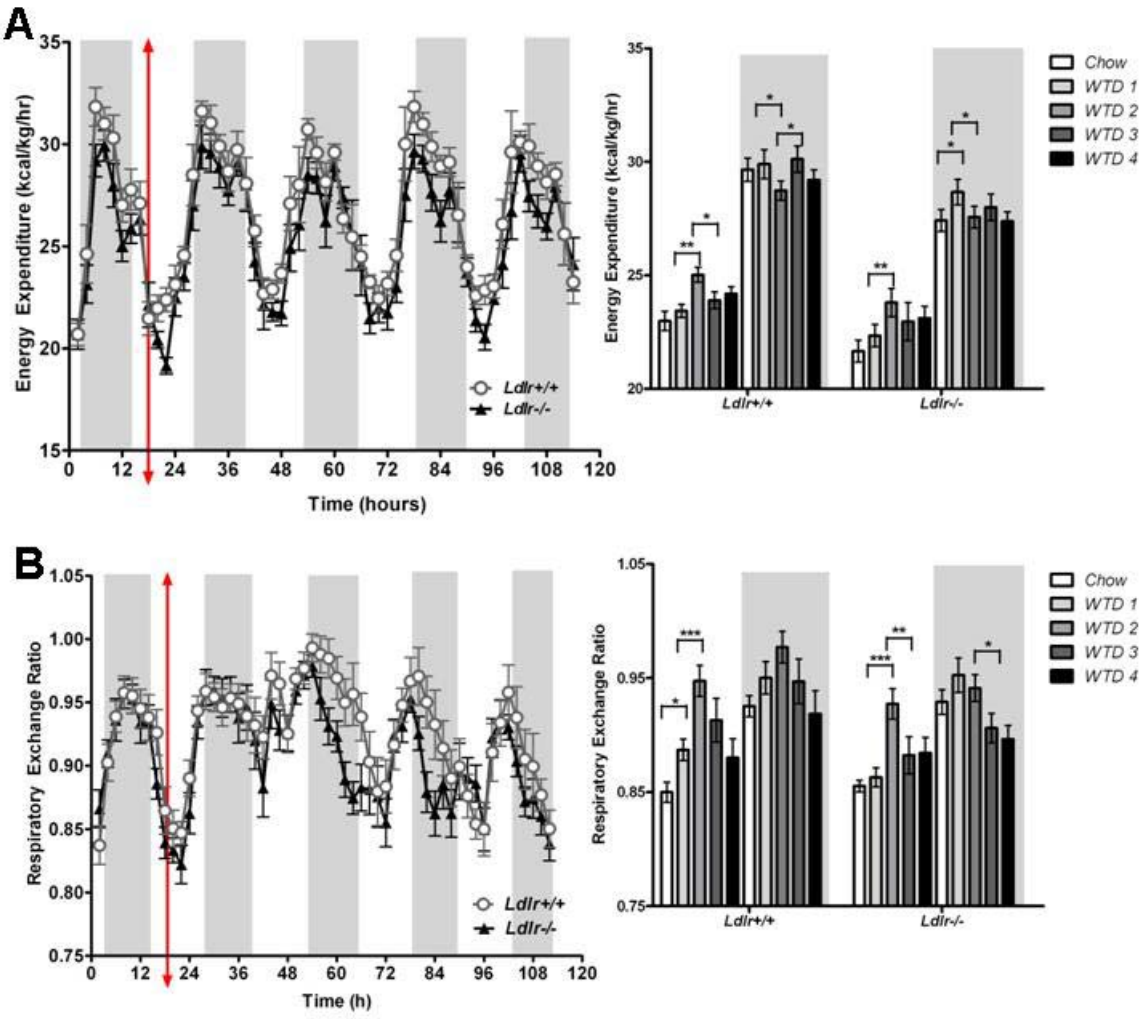

Figure 3.8: Energy expenditure in *Ldlr*-/- mice acutely exposed to WTD at 10-weeks. Continuous monitoring of energy expenditure and RER was conducted when *Ldlr*+/+ and *Ldlr*-/- mice were switched from a chow diet to WTD (arrowed line). Grey bars represent the dark phase. **A.** Energy expenditure of both *Ldlr*+/+ mice and *Ldlr*-/- mice was acutely affected with WTD diet feeding. **B.** Respiratory exchange ratio of both *Ldlr*+/+ and *Ldlr*-/- mice was also acutely affected with switching to WTD feeding. n=4 for *Ldlr*+/+ mice, n=6 for *Ldlr*-/- mice. *p<0.05, **p<0.01, ***p<0.001. Data represent mean ± SEM.

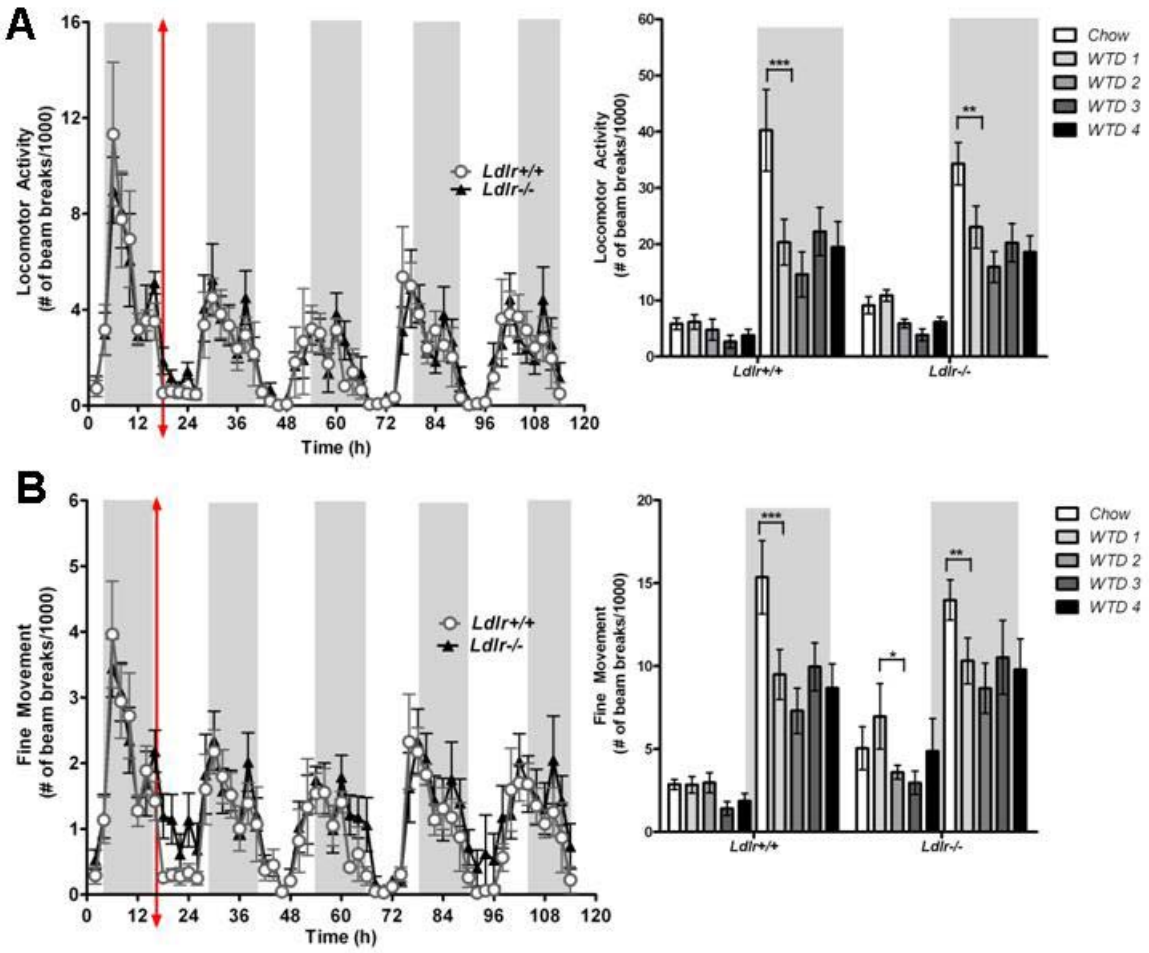

Figure 3.9: Activity levels in *Ldlr*-/- mice acutely exposed to WTD at 10-weeks. Continuous monitoring of activity levels was conducted when *Ldlr*+/+ and *Ldlr*-/- mice were switched from a chow diet to WTD (arrowed line). Grey bars represent the dark phase. **A.** Dark phase locomotor activity was acutely lowered after switch to WTD feeding in *Ldlr*+/+ and *Ldlr*-/- mice. **B.** Fine movement was also lowered following the initial switch from chow to WTD in *Ldlr*+/+ and *Ldlr*-/- mice. n=4 for *Ldlr*+/+ mice, n=6 for *Ldlr*-/- mice. *p<0.05, **p<0.01, ***p<0.001. Data represent mean ± SEM.

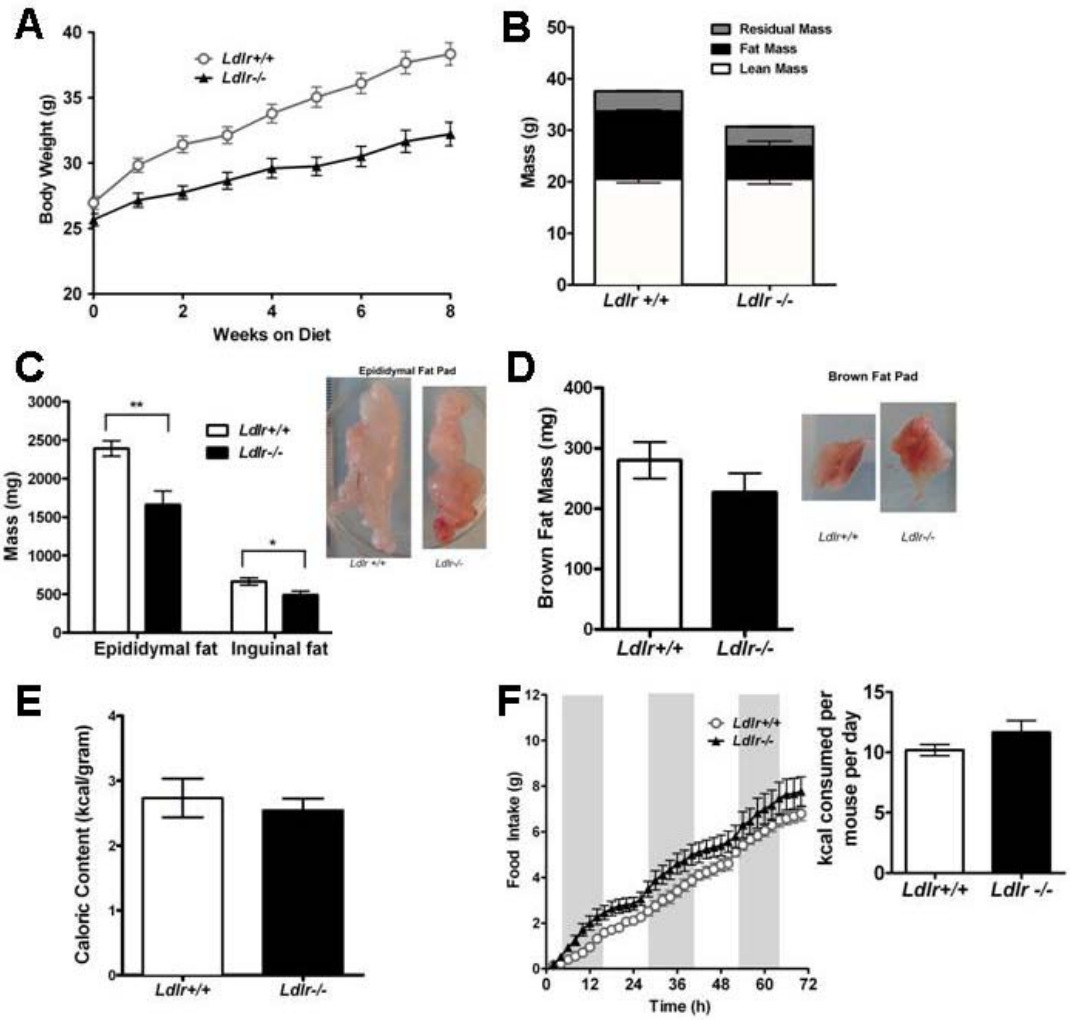

Figure 3.10: Body composition and food intake in *Ldlr-/-* mice fed a WTD. **A.** *Ldlr*-/- mice gained significantly less weight on WTD than *Ldlr*+/+ mice did. (n=16-20.) **B.** Body weight and body composition after 8 weeks on the WTD shows that *Ldlr*-/- mice specifically failed to gain fat mass relative to wildtype mice. **C.** Weights of the epididymal visceral fat pad and inguinal subcutaneous fat pad, dissected from mice. *Ldlr*-/- mice had decreased epididymal and inguinal fat pad masses relative to *Ldlr*+/+ mice. **D.** Weight of interscapular brown fat pad dissected from mice. No significant difference was observed between *Ldlr*-/- mice and *Ldlr*+/+ mice. **E.** No difference in caloric content of mouse fecal matter was observed. **F.** Continuous monitoring of food intake showed that *Ldlr*-/- mice were consuming more calories per gram of mouse on the WTD than *Ldlr*+/+ mice. Grey bars represent the dark phase. n=8 for *Ldlr*+/+ mice, n=6 for Ldlr-/- mice. *p<0.05, **p<0.01. Data represent mean ± SEM.

Data in Figure 3.10E was obtained with the assistance of W. Quong

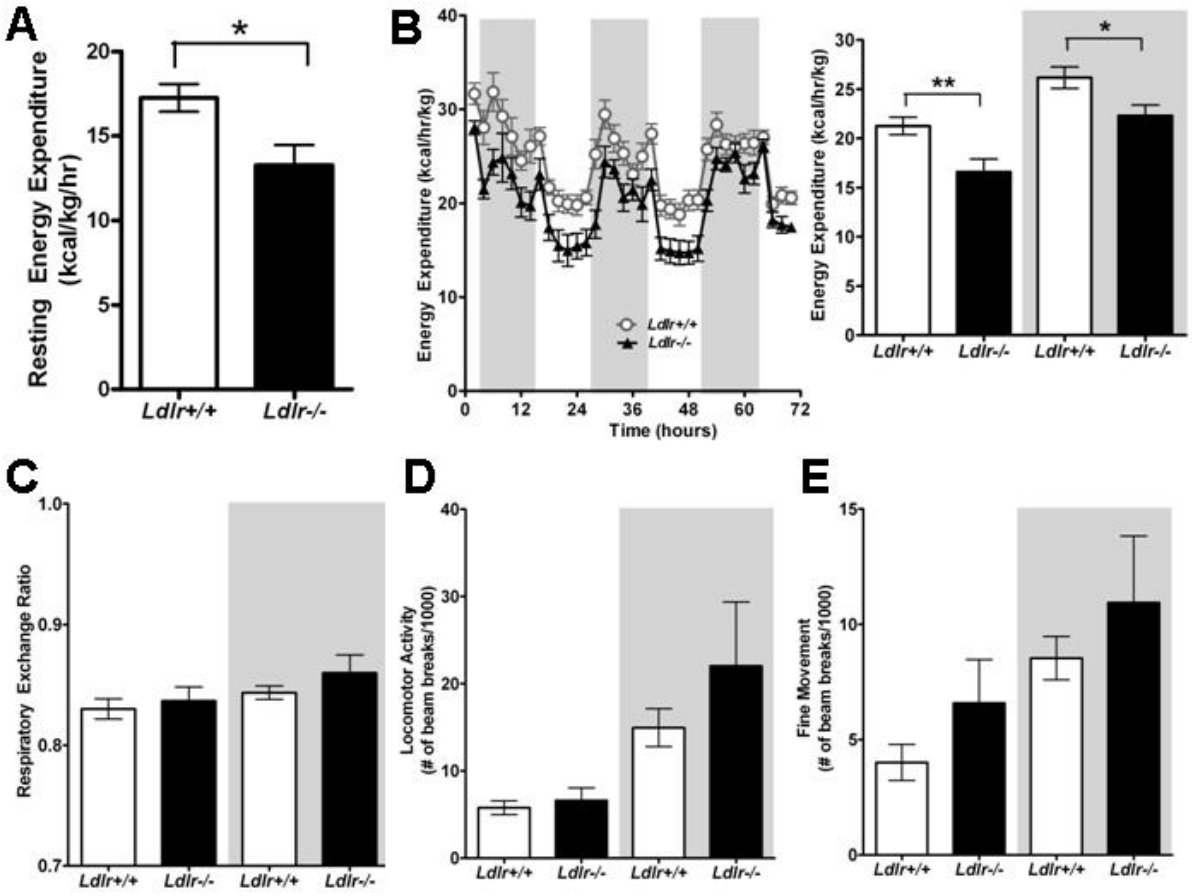

Figure 3.11: Energy expenditure in *Ldlr*-/- mice on WTD. The energy balance phenotype of *Ldlr*+/+ mice and *Ldlr*-/- mice after eight weeks of WTD feeding was examined. Grey bars represent the dark phase. Resting energy expenditure **(A)** and energy expenditure **(B)** were decreased in *Ldlr*-/- mice. No differences were detected in RER **(C),** locomotor activity **(D)**, or fine movement **(E)** between *Ldlr*-/- mice and wildtype mice after eight weeks exposure to the WTD. n=8 for *Ldlr*+/+ mice, n=6 for *Ldlr*-/- mice. *p<0.05, **p<0.01. Data represent mean ± SEM.

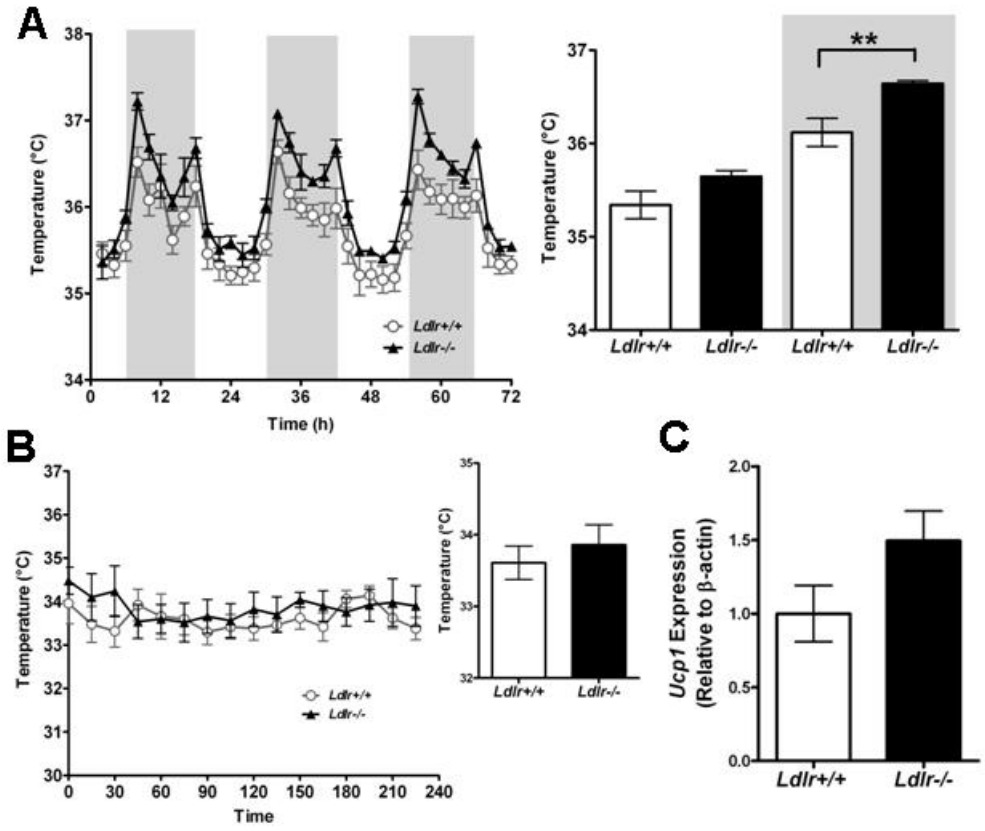

Figure 3.12: Thermoregulation in *Ldlr*-/- mice on WTD. A. Continuous monitoring of body temperature showed that after 2-6 weeks of WTD feeding, *Ldlr*-/- mice had higher body temperature during the dark phase relative to *Ldlr*+/+ mice. Grey bars represent the dark phase. n=5 per genotype. **B.** 4-hr cold challenge experiment showed no significant deficits in regulation of body temperature during exposure to 4°C in *Ldlr*-/- mice. n=5 per genotype. **C.** qRT-PCR analysis showed no differences in *Ucp1* expression in BAT. n=6 for *Ldlr*+/+, n=5 for *Ldlr*-/- mice. **p<0.01. Data represent mean ± SEM.

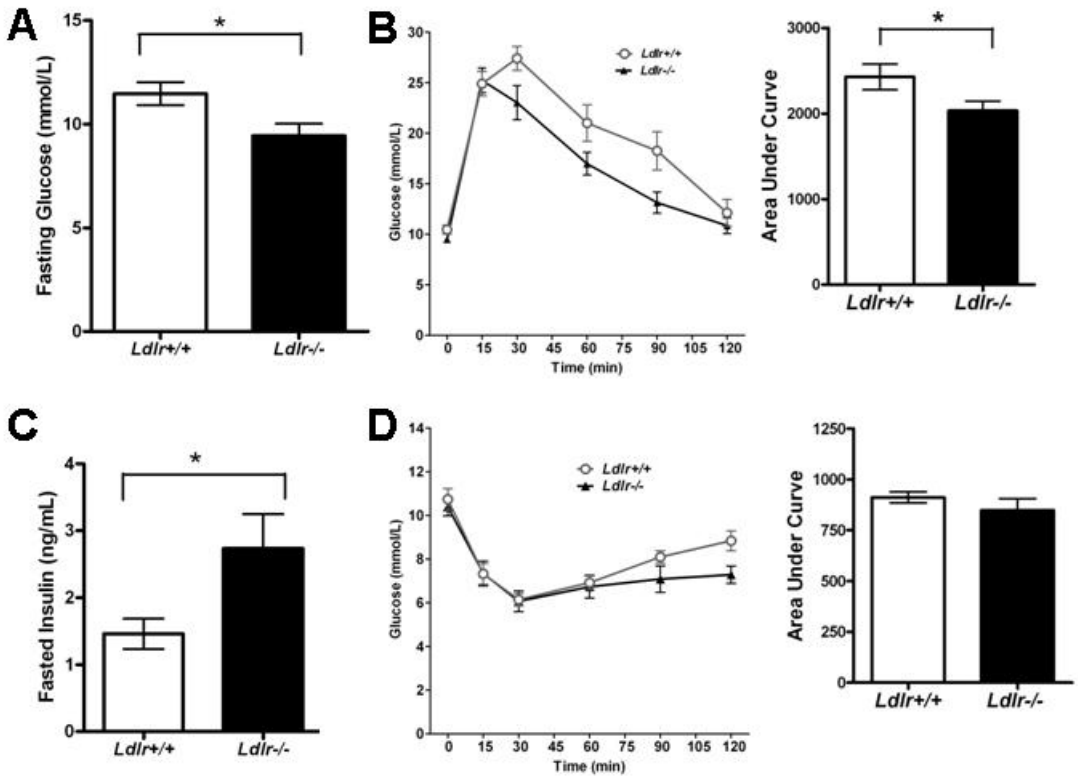

Figure 3.13: Glucose homeostasis of *Ldlr*-/- mice on WTD A. *Ldlr-/-* mice had lower fasting blood glucose levels relative to wildtype mice after 14-weeks exposure to the WTD. **B.** IPGTTs and area under the curve analysis showed that *Ldlr-/-* mice had slightly better glucose clearance than *Ldlr*+/+ mice. **C.** Fasting insulin levels were also elevated in *Ldlr*-/- mice. **D.** IPITTs and area under the curve analysis showed no significant differences in insulin sensitivity at this timepont between *Ldlr-/-* mice and *Ldlr*+/+ mice. n=10 for *Ldlr*+/+ mice and n=10 for *Ldlr-/-* mice. *$p<0.05$. Data represent mean ± SEM.

CHAPTER 4: Leptin Signaling in *Ldlr-/-* Mice

4.1 Endogenous Leptin in *Ldlr-/-* Mice

4.1.1 Serum Leptin Levels

As described in Chapter 3, *Ldlr-/-* mice did not gain as much fat mass when fed the WTD as *Ldlr+/+* mice. To investigate the possibility of differences in endocrine activity of *Ldlr-/-* white adipose tissue depots on WTD, I studied serum leptin levels in *Ldlr-/-* mice and in *Ldlr+/+* controls. After twelve weeks of WTD feeding, *Ldlr+/+* mice had increased leptin levels relative to chow fed mice, which correlated with their increased fat mass (**Figure 4.1A**). However, *Ldlr-/-* mice also had increased serum leptin levels after twelve weeks of WTD feeding, despite their failure to gain significant amounts of adipose mass on the WTD (**Figure 4.1A**). When serum leptin levels were corrected per gram of fat mass, as detected by QMR, *Ldlr-/-* mice on the WTD appeared to be secreting more leptin per gram of fat tissue relative to chow fed mice, whereas wildtype mice do not secrete more leptin per gram of fat tissue on the WTD (**Figure 4.1B**). Serum leptin levels were also plotted as a dependent variable of fat mass to examine the correlation of fat mass and leptin levels in the different groups by visual means (**Figure 4.1C**).

4.1.2 Leptin Gene Expression in Adipocytes

qRT-PCR of leptin gene expression in white adipose tissue of *Ldlr+/+* mice was performed with the assistance of W. Quong. These experiments showed that leptin gene expression was up-regulated with WTD feeding, both in the epididymal visceral fat pad

(**Figure 4.2A**) and in the inguinal subcutaneous fat pad (**Figure 4.2B**). However, analysis of *Ldlr-/-* mice showed that WTD feeding did not provoke an increase in leptin gene expression in the epididymal visceral fat pad (**Figure 4.2A**) or in the inguinal subcutaneous fat pad (**Figure 4.2B**) relative to levels in chow-fed animals.

4.2 Leptin Responsiveness and Functioning in *Ldlr-/-* Mice

4.2.1 Leptin Administration

I next sought to examine how gene ablation of *Ldlr* would affect leptin responsiveness by examining acute response to intrapertioneal (IP) leptin administration in *Ldlr+/+* and *Ldlr-/-* mice fed a chow diet. Prior to these experiments, I performed a pilot study to determine the effectiveness of IP leptin administration at a dose of 2μg/g for increasing serum leptin levels in wildtype and *Ldlr-/-* mice. Leptin was injected in a different group of mice, and serum was collected at 15 min, 30 min, 1 hr, 2 hr, and 3 hr post-injection and analyzed for leptin concentration by ELISA. Serum leptin levels were confirmed to be elevated to over 160ng/ml (40x physiological levels, **Figure 4.3A**) in mice of both genotypes half an hour after leptin administration. No differences in serum leptin levels were detected between *Ldlr+/+* and *Ldlr-/-* mice two hours after the IP leptin injection (**Figure 4.3B**). As expected, leptin administration significantly decreased body weight in *Ldlr+/+* mice (**Figure 4.4A**). However, the same dose of injected leptin did not elicit this effect in *Ldlr-/-* mice (**Figure 4.4A**). Two days of leptin administration also significantly decreased food intake in *Ldlr+/+* mice. However, like body weight, decreased food intake was not observed in *Ldlr-/-* mice when treated with leptin when compared to treatment with saline (**Figure 4.4B**). In addition, leptin also significantly

decreased respiratory exchange ratio (**Figure 4.5A, B & C**) and energy expenditure (**Figure 4.5D, E & F**) in wildtype mice, but not in *Ldlr-/-* animals. Leptin administration had no effect on locomotor activity or fine movement levels in wildtype mice or in *Ldlr-/-* mice (**Figure 4.6**).

4.2.2 Hypothalamic Gene Expression

Since leptin signaling appeared to be altered in *Ldlr-/-* animals, gene expression of neuropeptides downstream of leptin were examined. Specifically, orexigenic *Npy* and anorexigenic *Pomc* expression was studied. Initially, hypothalamic blocks were collected from wildtype animals which were freely fed or 48-hour fasted. Gene expression analysis showed that, as predicted, *Npy* expression increased after a 48-hour fast **(Figure 4.7A)** and *Pomc* expression decreased significantly after a 48-hour fast **(Figure 4.7B)**, validating the qRT-PCR assay. However, examination of *Npy* and *Pomc* expression in *Ldlr-/-* mice showed no alterations in *Npy* **(Figure 4.7C)** and *Pomc* **(Figure 4.7D)** expression, either in chow-fed or WTD-fed animals.

Previous studies have shown that a 48-hour fast can induce changes in hypothalamic gene expression of neuropeptides regulating energy balance. I have demonstrated that *Npy* expression increased and *Pomc* expression decreased after a 48-hour fast. I chose to examine expression of *Ldlr* and *Apoe* in the hypothalamus in freely-fed or 48-hour fasted wildtype mice, to study whether changes in gene expression of these two molecules involved with lipid transport are mediated by energy status. With assistance from W. Quong, qRT-PCR showed that *Ldlr* and *Apoe* expression in the hypothalamus was not responsive to 48-hour fasting in wildtype mice **(Figure 4.7E & F)**.

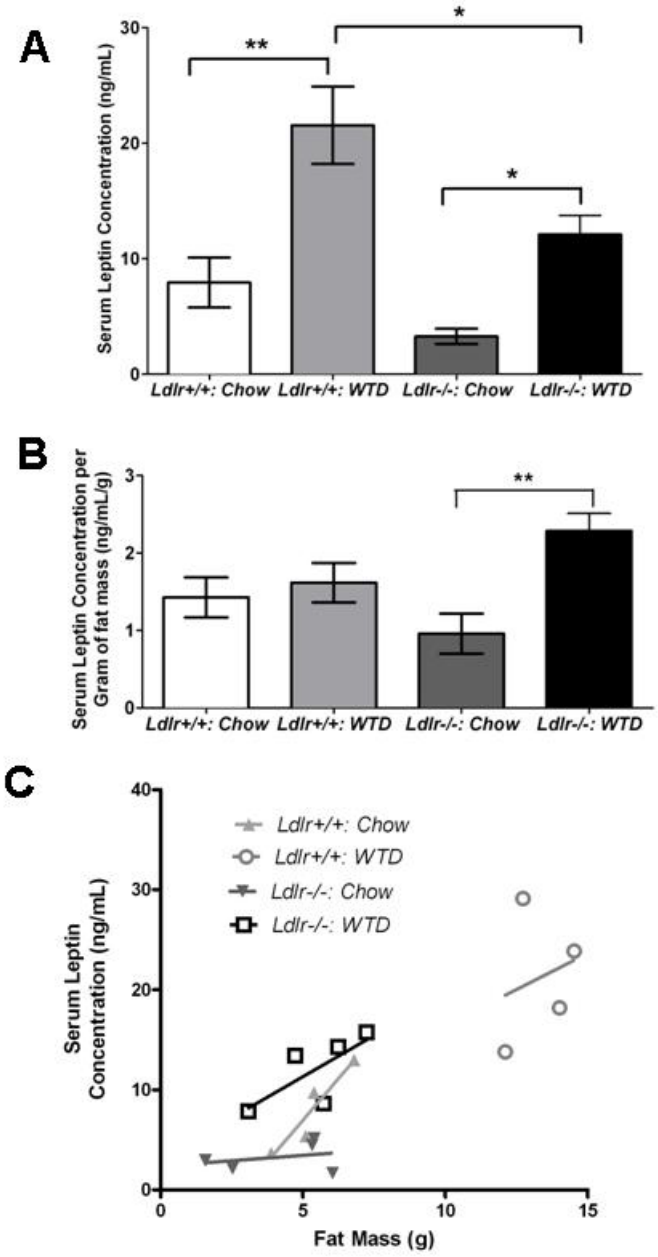

Figure 4.1: Endogenous leptin levels in *Ldlr*-/- mice. A. Serum leptin levels were higher in both genotypes after exposure to WTD. **B.** Serum leptin levels corrected per gram of fat mass showed that *Ldlr*-/- mice on the WTD had higher circulating levels of leptin than would be expected from their adiposity. **C.** Serum leptin levels plotted relative to fat mass per individual mouse. Serum leptin levels: n=4-5/group. *p<0.05, **p<0.01. Data represent mean ± SEM.

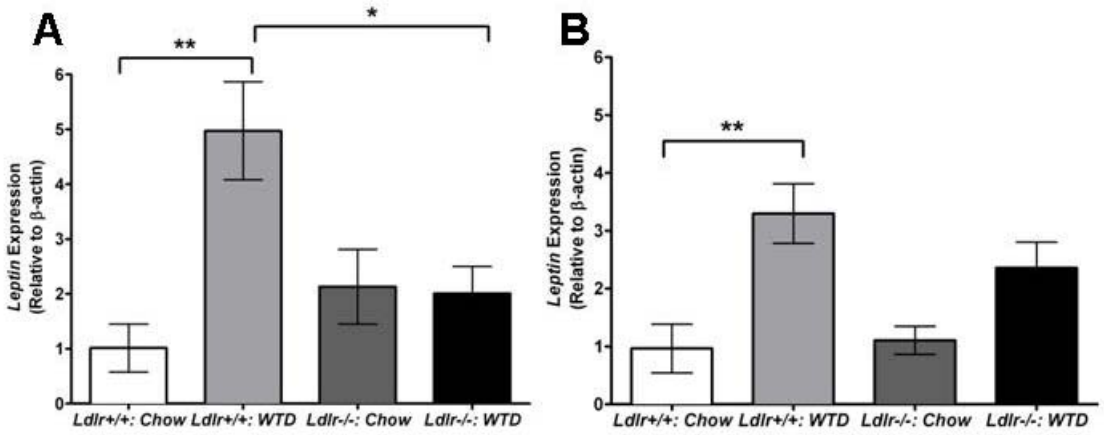

Figure 4.2: **Leptin transcripts in *Ldlr*-/- mice.** Leptin gene expression in the inguinal fat pad **(A)** and in the epididymal fat pad **(B)** were higher in wildtype mice on the WTD, but not in *Ldlr*-/- mice on the WTD. QRT-PCR data: n=6-8 per group. *$p<0.05$, **$p<0.01$. Data represent mean ± SEM.

Data in Figure 4.2A & B was obtained with the assistance of W. Quong.

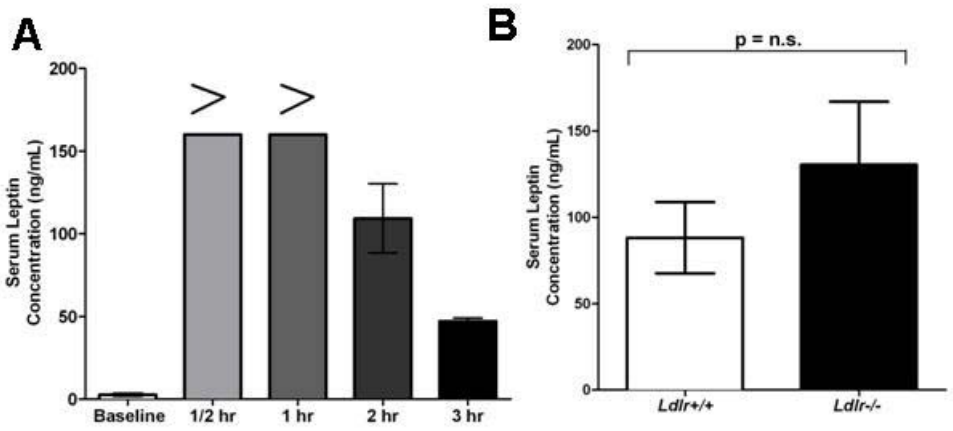

Figure 4.3: **Serum leptin levels following IP leptin administration. A.** Serum leptin level were increased half an hour following IP leptin administration, and this elevation persisted to three hours post-injection (n=2-4). **B.** Two hours following IP leptin administration, serum leptin levels were not significantly different between *Ldlr*+/+ mice and *Ldlr*-/- mice. n=4 per genotype. n.s. = not significant. Data represent mean ± SEM.

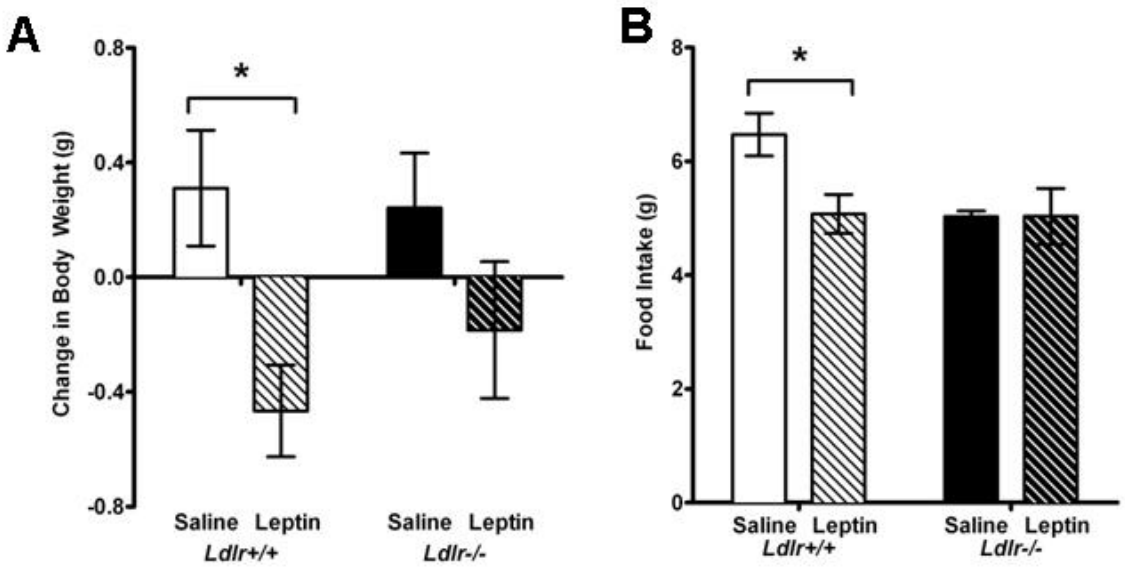

Figure 4.4: Effects of leptin on body weight and food intake in *Ldlr*-/- mice. 26-week old male mice received intraperitoneal injections of leptin for two consecutive days. **A.** *Ldlr*+/+ mice had significantly reduced body weight after two days of leptin injections, but *Ldlr*-/- mice did not have decreased body weight following leptin injections. **B.** *Ldlr*+/+ mice had decreased food intake after leptin administration, whereas food intake of *Ldlr*-/- mice was unchanged. n=8 for *Ldlr*+/+ mice, n=7 for *Ldlr*-/- mice. Data represent mean ± SEM. *$p<0.05$.

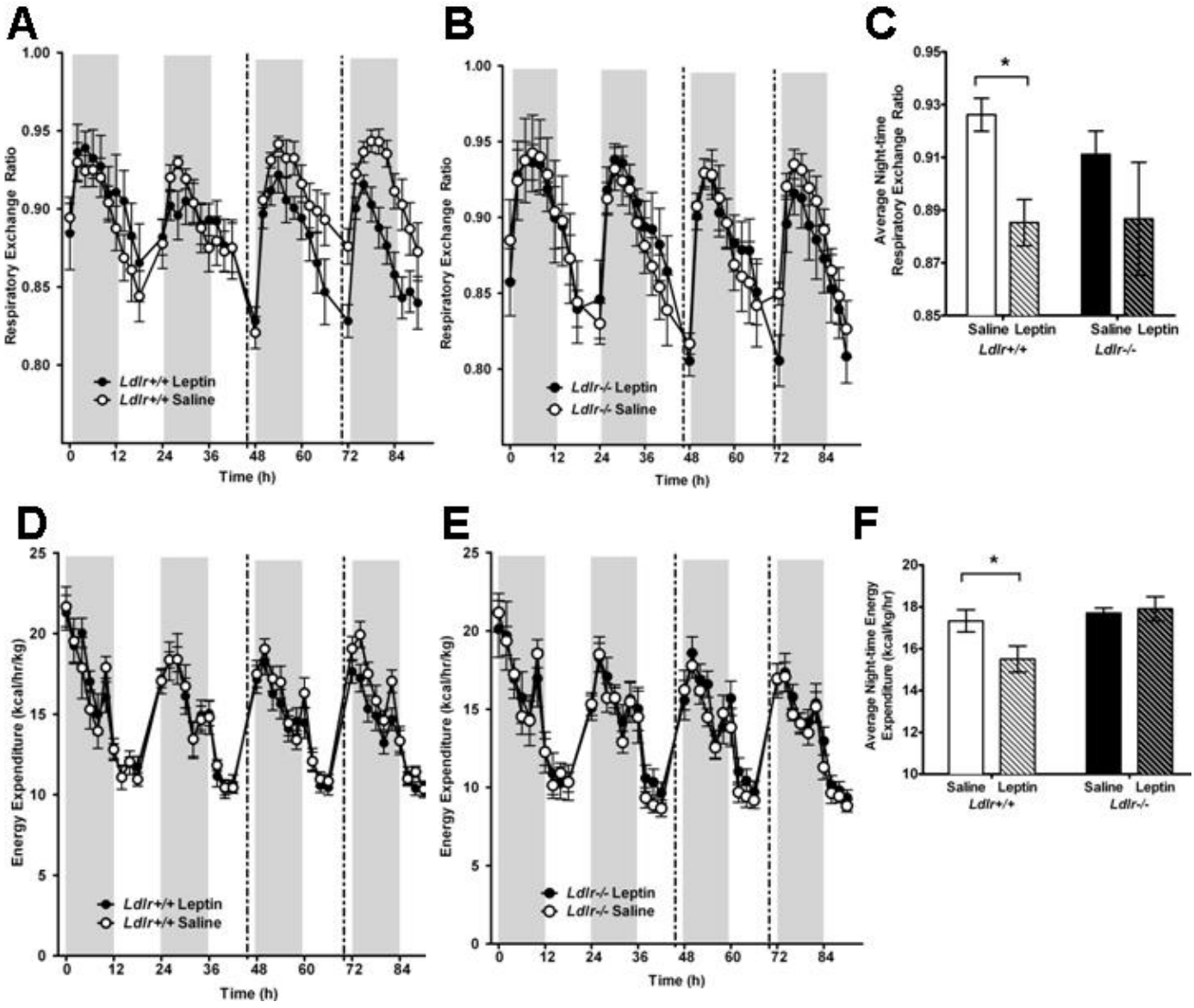

Figure 4.5: Energy expenditure after leptin administration. 26-week old male mice received intraperitoneal injections of leptin (black-dotted lines) for two consecutive days. In graphs **A, B, D, & E :** white circles represent saline-treated mice and black circles represent leptin-treated mice. EE was decreased after the second leptin injection in *Ldlr*+/+ mice **(A),** but was unchanged in *Ldlr*-/- mice **(B). C.** Average EE in dark phase in response to two leptin injections. RER was also decreased in *Ldlr*+/+ mice following leptin injections **(D),** but remained the same in *Ldlr*-/- mice **(E). F.** Average EE in the dark phase in response to two leptin treatments. n=8 for *Ldlr*+/+ mice, n=7 for *Ldlr*-/- mice. *p<0.05, **p<0.01. Data represent mean ± SEM.

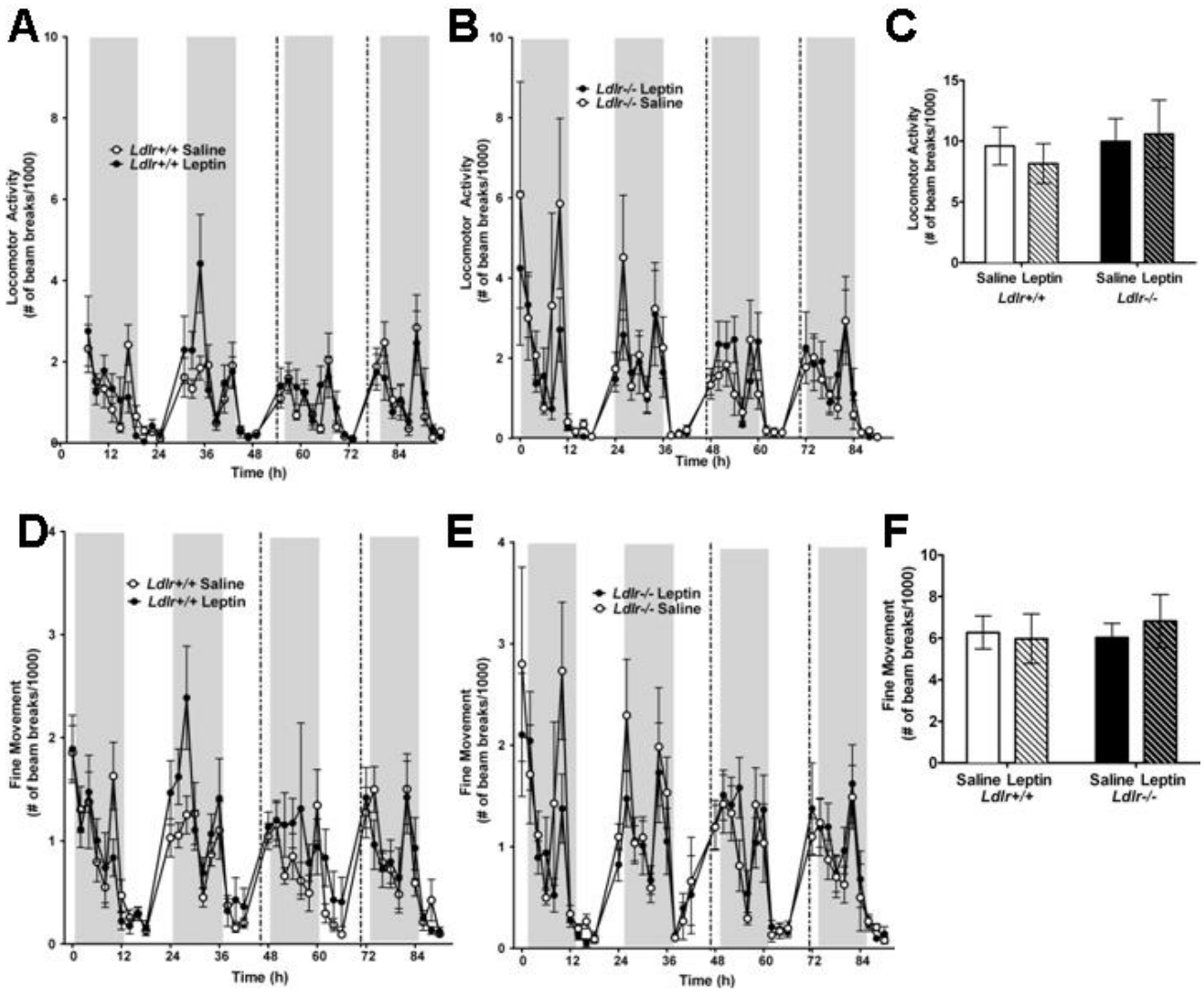

Figure 4.6: Activity levels after leptin administration. 26-week old male mice received intraperitoneal injections of leptin (black-dotted lines) for two consecutive days. Grey bars represent the dark phase. Locomotor activity was not affected by leptin injections in *Ldlr*+/+ mice **(A)** or in *Ldlr*-/- mice **(B). C.** Average locomotor activity in dark phase in response to two leptin injections. Fine movememt was also unchanged in *Ldlr*+/+ mice **(D)** and *Ldlr*-/- mice **(E)** following leptin injections**. F.** Average fine movement in the dark phase after two leptin treatments. n=8 for *Ldlr*+/+ mice, n=7 for *Ldlr*-/- mice. Data represent mean ± SEM.

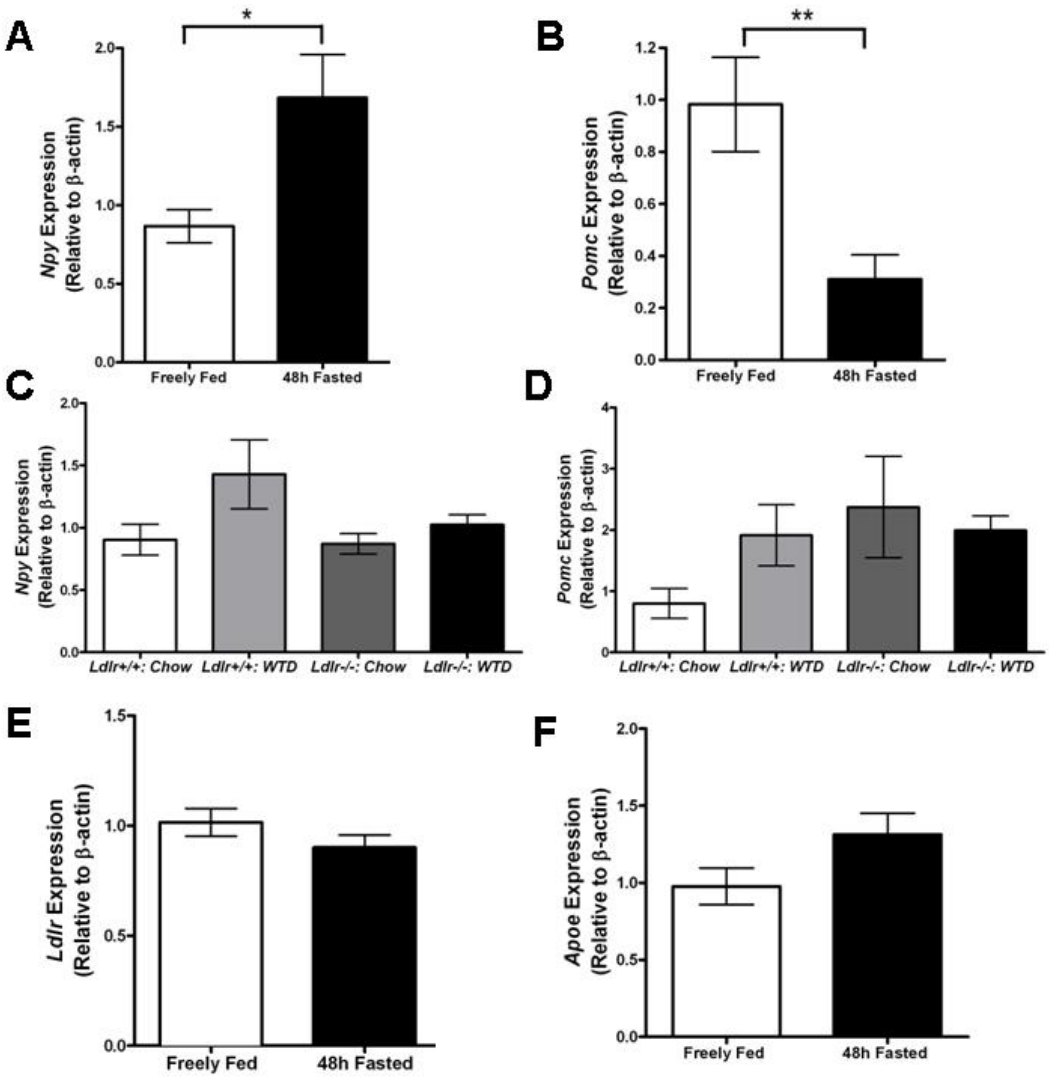

Figure 4.7: Hypothalamic gene expression of leptin-responsive neuropeptides. **A.** Orexigenic *Npy* expression was significantly increased in mice fasted 48 hours. **B.** Anorectic *Pomc* expression was significantly decreased in mice fasted 48 hours. **C.** *Npy* expression was not significantly different between *Ldlr*+/+ and *Ldlr*-/- mice on the chow or WTD. **D.** *Pomc* expression was also not significantly different between *Ldlr*+/+ and *Ldlr*-/- mice on the chow or WTD. **E.** *Ldlr* expression was not altered with fasting in wildtype animals. **F.** *Apoe* expression was also not altered with fasting in wildtype animals. n=4-13. Data represent mean ± SEM. *p<0.05, **p<0.01.

Data in Figure 4.7E & F was obtained with the assistance of W. Quong.

CHAPTER 5: General Discussion

5.1 Reliability of Methods

5.1.1 Energy Expenditure

Indirect calorimetry is a method to assess the energy consumed by an animal through measurement of respiratory exchanges involving oxygen consumption and carbon dioxide production[110,122]. These gaseous exchanges are associated with the oxidation of macronutrients (carbohydrates, protein, fat and occasionally ethanol) as energetic substrates. Therefore, indirect calorimetry is a useful method to assess energy expenditure of an organism[122]. In addition to indirect calorimetry, the use of infrared beam-breaks to measure activity levels and temperature telemetry transmitters to measure heat production allow assessment of specific subcomponents of energy expenditure.

5.1.2 Body Composition

Methods for *in vivo* analysis of rodent body composition have been developed to provide an alternative to chemical carcass analysis. Though carcass analysis is the gold standard, it is expensive, time-consuming and requires sacrifice of the animal, precluding longitudinal studies. QMR technology to study animal body composition *in vivo* has been used as an inexpensive yet highly reliable method[115,123-126]. Other technologies such as DEXA have also been used to study rodent body composition.[127-130] Studies have shown the reliability and comparability of results from both the QMR and DEXA systems with more traditional methods of rodent body composition, including whole carcass chemical analytical methods[131]. We validated the QMR system used in these studies by measuring the correlation between scale weights and QMR readings for mixtures of lean tissue and

fat (see **Appendix B**). Based on these data I believe that the QMR body composition method provides accurate non-invasive analysis of whole body composition in live animals.

5.1.3 Fecal Energy Content

To examine mouse fecal energy content, direct bomb calorimetry was used. While bomb calorimetry allowed quantitation of total energy content of fecal matter, analysis of lipid composition in mouse feces using mass spectrometry[132] may also provide a greater level of resolution of the absorptive phenotype of *Ldlr-/-* mice. A previous report examined lipid absorption of *Ldlr-/-* mice on a calorie dense-diet by administering a radiolabeled retinol gavage and analyzing the appearance of radioactivity in the plasma. This study did not find differences in fat absorption between *Ldlr-/-* mice and *Ldlr+/+* mice [108].

5.1.4 Glucose Sensitivity

To study glucose clearance and insulin sensitivity, IPGTTs and IPITTs were used. While IPGTTs did detect a difference between *Ldlr-/-* mice and *Ldlr+/+* mice on the WTD, IPITTs did not demonstrate a difference between the two genotypes in insulin sensitivity. IPITTs examine the physiological response of the entire organism, and do not provide information on the response of specific organs to insulin. Hyperinsulinemic euglycemic clamps[133,134] are the gold standard method for assessing insulin sensitivity in living animals, though this technique was not used in my studies due to the difficulty of the technique and the highly specialized training required.

5.1.5 Quantitative Reverse-Transcriptase Polymerase Chain Reaction

qRT-PCR is a widely used method to analyze gene expression[119]. *Npy* and *Pomc* are only expressed within specific nuclei of the hypothalamus[46]. In the studies presented here, qRT-PCR was used to examine gene expression in whole hypothalamic blocks, without specific microdissection of nuclei. Even with the specificity of expression, I believe that the assaying *Npy* and *Pomc* expression across all nuclei contained in the hypothalamic blocks would not obscure real changes in gene expression. Nevertheless, microdissection of specific nuclei prior to RNA isolation would be one way to improve the sensitivity and specificity of my qRT-PCR studies. RNA *in situ* hybridization is another technique that is used to detect changes in gene expression caused by alterations in energy balance (alterations that may be more sensitive to changes within specific populations of neurons in the brain). Visualization through *in situ* hybridization of leptin responsive transcripts like, *Npy* and *Pomc, Ldlr,* and *Apoe*, in specific neuronal populations may yield higher resolution answers than qRT-PCR. Because differences in gene expression were not detected using qRT-PCR, RNA *in situ* hybridization would be another means to confirm these results.

5.1.6 Leptin Administration

In my experiments, I administered acute injections of leptin over two days. Other studies have used methods that deliver leptin more slowly and over longer periods. These methods appear to be more potent in eliciting leptin's anorectic effects[26]. For example, when leptin is delivered to rodents through implanted mini-osmotic pumps slowly over

several weeks, the anorectic effects are greater relative to bolus injections[26,34,135]. Thus, while the studies described in this thesis found that *Ldlr*-/- mice were resistant to acute leptin injections, *Ldlr*-/- mice may be in fact sensitive to the effects of chronic leptin administration. Additionally, I administered leptin peripherally via an intraperitoneal injection. Leptin has been shown to elicit a more potent physiological response when delivered centrally[136,137]. When a cannula is implanted into the third ventricle of the brain, leptin may be targeted toward the arcuate nucleus[136]. Testing of central leptin sensitivity in *Ldlr*-/- mice would be a means to address whether the leptin resistance I observed in *Ldlr*-/- mice specifically included a component of central leptin resistance.

5.2 The Energy Balance Phenotype in *Ldlr*-/- Mice

5.2.1 Phenotype of *Ldlr*-/- Mice on Chow

The Ldlr is best known for its significant role in lipid clearance and in the pathogenesis of atherosclerosis. Thus, the *Ldlr*-/- mouse[92] has been studied extensively as a model for atherosclerotic lesion formation. In the work described here, I investigated the role of the Ldlr in modulating parameters of energy balance, including EE, activity levels, and response to a WTD. Other molecules in the lipoprotein system have also been implicated in energy balance. Centrally, apolipoproteins Apoe and ApoaIV have anorectic effects in the brain[81,82]. Peripherally, the low density lipoprotein receptor-related protein 1 (Lrp1) receptor in adipocytes appears important in maintaining body weight[87].

My experiments suggest that whole-body knockout of *Ldlr* in mice results in decreased food intake, decreased energy expenditure, decreased respiratory exchange

ratio, and increased activity levels when mice are fed a standard rodent diet. Interestingly, these changes in various aspects of EE were not accompanied by differences in body weight or body composition between *Ldlr-/-* mice and *Ldlr+/+* mice on a standard chow diet. Prior to my studies, *Ldlr-/-* mice had been reported to show increased locomotor activity during an open field test[111]. My findings complement these results using alternative methods to assay mouse activity. The observed global differences in energy balance between *Ldlr-/-* mice and *Ldlr+/+* mice suggest an important role for *Ldlr* in maintaining energy homeostasis.

5.2.3 Phenotype of *Ldlr-/-* Mice on WTD

Transgenic animals with perturbations in lipid transport have demonstrated interesting energy balance phenotypes when exposed to energy dense high-fat diets. In particular, *Apoe-/-* mice are less susceptible to diet-induced obesity when compared with *Apoe+/+* mice[84,85]. In my studies, I did not detect differences in body weight or body composition between *Ldlr+/+* and *Ldlr-/-* mice fed standard rodent chow. However, when *Ldlr-/-* mice were given a WTD, differences emerged in body weight and body composition, with *Ldlr-/-* mice accumulating significantly less fat than wildtype mice. In previous studies, *Ldlr-/-* mice have been reported to have increased weight gain on a diabetogenic diet[108] and decreased weight gain on a less calorie dense WTD[85]. My studies showed that *Ldlr-/-* mice gain less weight than *Ldlr+/+* mice after 8 weeks of consuming a WTD. The data on weight gain in *Ldlr-/-* mice I generated was obtained prior to the publication of the article by Karagiannides *et al.*[85], reporting decreased weight gain in *Ldlr-/-* mice fed a WTD compared to *Ldlr+/+* mice fed the same diet. Coincidentally, the

WTD I used was identical to the WTD used by Karagiannides *et al.*[85], with identical results obtained from both studies. My analysis of body composition and dissection of adipose depots found that *Ldlr-/-* mice failed to expand their fat mass. The differences in weight gain between *Ldlr-/-* and *Ldlr+/+* mice fed different high-energy diets suggest that *Ldlr* gene knockout alters body weight and energy balance, but in a manner that depends on the energy density and macronutrient content of the diet. Additionally, I found that WTD-fed *Ldlr-/-* mice had improved glucose homeostasis relative to WTD-fed *Ldlr+/+* mice, which I believe is due to the decreased weight gain of *Ldlr-/-* mice fed the WTD. However, molecular mechanisms specific to the pancreas are also plausible and were not investigated in these experiments.

Ldlr-/- mice consumed the same amount of energy as *Ldlr+/+* mice when fed the WTD, but showed diminished weight gain. The lower weight gain could not be attributed to impaired absorption, since fecal energy excretion was not different between *Ldlr+/+* mice and *Ldlr-/-* mice. A previous report had also shown no differences in fat absorption between *Ldlr-/-* mice and *Ldlr+/+* mice[108]. Collectively, the available data indicate that fat malabsorption does not explain the lower body weight gain in WTD fed *Ldlr-/-* mice. This suggests physiological differences in energy metabolism are the most likely reason for the altered response observed in *Ldlr-/-* mice fed the WTD.

In both chow-fed and WTD-fed mice, *Ldlr-/-* animals consistently had lower EE, despite gaining less fat mass relative to wildtype animals on the WTD. Interestingly, a differential metabolic response to the WTD was observed between *Ldlr-/-* mice and wildtype mice. *Ldlr-/-* mice fed the WTD had 35.2% higher EE when compared with *Ldlr-/-* mice fed chow, whereas WTD feeding did not elicit a significant increase in EE in

wildtype animals. This differential response to the WTD may decrease the sensitivity of *Ldlr-/-* mice to diet induced obesity, and thereby explain the decreased weight-gain phenotype observed in *Ldlr-/-* mice.

My experiments showed increased body temperature in *Ldlr-/-* mice on the WTD at ambient temperatures (24ºC – 25ºC), indicating the Ldlr may be involved in regulating thermogenesis. However, the absence of Ldlr mediated lipid transport in multiple tissues may activate compensatory pathways that do not necessarily rely on Ldlr. The overall phenotype observed in the *Ldlr-/-* mouse is a result of the complex interplay between these pathways as the organism attempts to achieve homeostasis. In addition, the major tissue site at which compensatory pathways act may not be identical to the tissue most greatly affected by the genetic defect. An example of this concept can be found in the Lrp1 pathway, wherein the deletion of *Lrp1* specifically from adipocytes activated compensatory pathways in muscle[87]. In my experiments, *Ldlr-/-* mice on the chow diet had increased brown adipose tissue weight compared to *Ldlr+/+* mice on the same diet, suggesting differences between *Ldlr-/-* mice and *Ldlr+/+* mice in the differentiation and maintenance of brown adipose tissue. Adaptive thermogenesis is a major contributor to an organism's overall energy expenditure[121]. Brown adipose tissue in rodents is known to regulate heat production through expression of *Ucp1*, a mitochondrial protein which acts to decouple the proton gradient generated by the electron transport chain from ATP synthesis[121]. This decoupling causes energy to be dissipated as heat[22,121]. *Ucp1* activity is regulated by the sympathetic nervous system, which activates β_3- adrenergic receptors in brown adipose tissue[22,121]. In addition to *Ucp1*, *Ucp2* and *Ucp3* are homologous proteins expressed in skeletal muscle[121]. Decoupling of the proton gradient from ATP synthesis in

muscle fibers by *Ucp2* and *Ucp3* activity is also thought to be a mechanism whereby adaptive thermogenesis is mediated[121]. In my experiments, *Ucp1* gene expression in brown adipose tissue of *Ldlr-/-* mice was unchanged relative to *Ldlr+/+* brown adipose tissue. While the means whereby the *Ldlr* may affect the function of brown adipose tissue were not elucidated, influences of the *Ldlr* on the sympathetic nervous system and skeletal muscle are attractive candidate mechanisms.

5.3 The Ldlr and Leptin

5.3.1 Leptin Levels in *Ldlr-/-* Mice

Leptin is an adipokine which plays a vital role in body weight regulation[46,135]. Due to the energy balance phenotype of *Ldlr*, I decided to examine whether loss of the *Ldlr* would affect leptin signaling or function. My experiments illustrate that *Ldlr-/-* mice have increased serum leptin levels per gram of fat mass. Under normal circumstances, leptin is secreted in proportion to adiposity levels, and leptin gene expression also increases in proportion to fat mass[38,39]. However, I detected that serum leptin levels are elevated in *Ldlr-/-* mice fed a WTD, despite no detectable increase in fat mass on the WTD. This suggests that serum leptin levels in *Ldlr-/-* mice on the WTD are not correlated with adiposity levels as they are in *Ldlr+/+* mice. To understand this further, leptin mRNA in visceral and subcutaneous adipose tissue was analyzed. However, leptin mRNA was not elevated in *Ldlr-/-* mice on chow or on WTD. These observations are in sharp contrast to what is seen in *Ldlr+/+* mice, in which circulating leptin levels and leptin gene expression are generally correlated. Therefore, while leptin levels are observed to be elevated in *Ldlr-/-* mice on the WTD, this is likely not due to changes in

leptin gene transcription. Instead, a reduction in leptin clearance may be responsible for the increased leptin levels in *Ldlr-/-* mice.

5.3.2 Leptin Responsiveness in *Ldlr-/-* Mice

The discovery and understanding of leptin biology has revealed the significance of these pathways mediating energy balance. I chose to examine leptin function in the context of the *Ldlr-/-* mouse. As leptin is a crucial regulator of energy balance, deregulation of energy homeostasis in *Ldlr-/-* mice might be expected to correlate with altered leptin signaling. Exogenous administration of leptin to *Ldlr-/-* mice demonstrated that whole-body gene ablation of the *Ldlr* blunts leptin's anorectic and weight-lowering effects. Interestingly, I also found that leptin administration to wildtype mice decreased RER and EE. While leptin has been shown to increase EE in leptin deficient *ob/ob* mice, reports of leptin's effects on EE in wildtype mice have suggested either an increase[138,139] or no change[140,141] in EE. In my experimental paradigm, two daily IP injections of leptin acutely lowered EE and RER in wildtype mice. Since leptin is known to increase EE in *ob/ob* mice, I hypothesize that decreased EE and RER in response to leptin administration is a secondary effect of decreased caloric consumption and weight loss elicited by leptin injections[142]. I did not observe these effects on EE and RER in *Ldlr-/-* mice, which I believe is due to their resistance to leptin's food- and body weight-lowering effects.

Experiments indicating decreased leptin responsiveness in *Apoe*-/- mice were also reported recently[83]. These studies showed that *Apoe* expression in the hypothalamus was decreased when leptin was administered via ICV injections[83]. ICV injections of leptin, when targeted at the third ventricle, allow delivery directly to the arcuate nucleus. These

results suggest that *Apoe*-/- mice show central leptin resistance. My studies did not directly address central leptin sensitivity in *Ldlr-/-* mice, as I used a peripheral method of leptin administration. Regardless, there is concordance of evidence between *Apoe*-/- and *Ldlr*-/- mice with respect to decreased leptin sensitivity. Thus, Apoe signaling through Ldlr may regulate feeding behavior via leptin-mediated pathways.

5.3.3 Expression of Hypothalamic Neuropeptides

As leptin is a hormone that is critical for energy balance and body weight regulation, data suggesting that the Ldlr mediates leptin's signal serves as important evidence that lipid transport pathways are directly involved in energy homeostasis. Because altered leptin sensitivity was detected in *Ldlr-/-* mice, I examined leptin-responsive hypothalamic neuropeptides in *Ldlr-/-* mice. I hypothesized that, because leptin sensitivity is decreased in *Ldlr-/-* mice relative to *Ldlr*+/+ mice, differences might emerge in expression of leptin responsive neuropeptides. Before performing these studies, I first validated that the qRT-PCR assay was able to detect fasting-induced changes in *Npy* and *Pomc* mRNA. Ultimately, no differences in basal expression of *Npy* or *Pomc* were detected in ad-libitum fed *Ldlr-/-* mice. The qRT-PCR method I used may not have been sensitive enough to detect subtle differences in hypothalamic *Npy* and *Pomc* levels between *Ldlr-/-* mice and *Ldlr*+/+ mice in the fed state. Other methods may be more sensitive to subtle differences, as discussed earlier (Section 5.1.5). In addition, states of fasting may elicit differences in hypothalamic *Npy* and *Pomc* levels between *Ldlr*+/+ and *Ldlr-/-* mice that are more readily detectable by qRT-PCR.

To examine the potential interaction between Ldlr and Apoe in mediating the anorectic effects of Apoe previously reported[82,83], I studied *Ldlr* gene expression in the hypothalamus of fasted and freely fed wildtype mice. However, I did not find that fasting elicited changes in *Ldlr* expression in the hypothalamus. A previous paper had reported that hypothalamic *Apoe* levels increased after a 36-hour fast in rats[82], which suggests transcriptional regulation through energy status occurs at the level of the ligand, Apoe. Yet I was not able to replicate the decrease in *Apoe* gene expression by qRT-PCR in mice fasted 48 hours. These contrasting results of hypothalamic *Apoe* gene expression may be due to differences in length of fasting, or to differences between rats and mice in hypothalamic *Apoe* gene regulation.

5.4 Conclusion of Findings and Future Directions

Globally, obesity is becoming increasingly prominent and dangerous to population health. Studies of the regulation of body weight are necessary to understand the molecular pathways perturbed in states of energy imbalance. In this thesis, interactions between the Ldlr pathway and energy homeostasis were examined. This research has provided novel evidence suggesting the Ldlr is involved with maintaining energy balance. Taken together with previous reports, my data suggest that interactions between lipid transport molecules and energy balance pathways contribute to energy homoeostasis. **Figure 5.1** summarizes these findings in the context of other energy balance systems.

My studies showed that *Ldlr-/-* mice have altered energy expenditure and decreased body weight gain on a WTD relative to wildtype mice. The direct mechanism

whereby the Ldlr affects body weight, fat mass accumulation, and energy expenditure is yet to be determined. However, my experiments suggest that the Ldlr mediates energy expenditure by regulating thermogenesis. Further studies are required to identify the interaction between Ldlr and thermoregulation. Another important finding from my thesis includes leptin resistance in *Ldlr-/-* mice. This suggests that the Ldlr mediates energy balance partially through leptin signaling and that leptin's effects on energy homeostasis may partially depend on molecules involved with lipid transport. Leptin is a key mediator of energy balance secreted by adipocytes. The fact that leptin signaling may depend on the Ldlr suggests that signals of adiposity are also incorporated from systemic circulation by organisms, although how this occurs requires further investigation. Leptin's regulation of Apoe, a major ligand for the Ldlr, appears to be a likely mediator. Additional research is required to understand the mechanisms whereby these interactions take place.

In conclusion, the studies in my thesis support a direct connection between lipid transport and energy homeostasis. Understanding of the influences of dyslipidemia on energy balance is critical to revealing the fundamental properties of energy homeostasis as well as for the discovery of potential anti-obesity drug targets. Future studies on the interactions between dyslipidemia, obesity, and T2D are critical to enhance our understanding of these widespread diseases and for the development of therapies to manage the obesity epidemic.

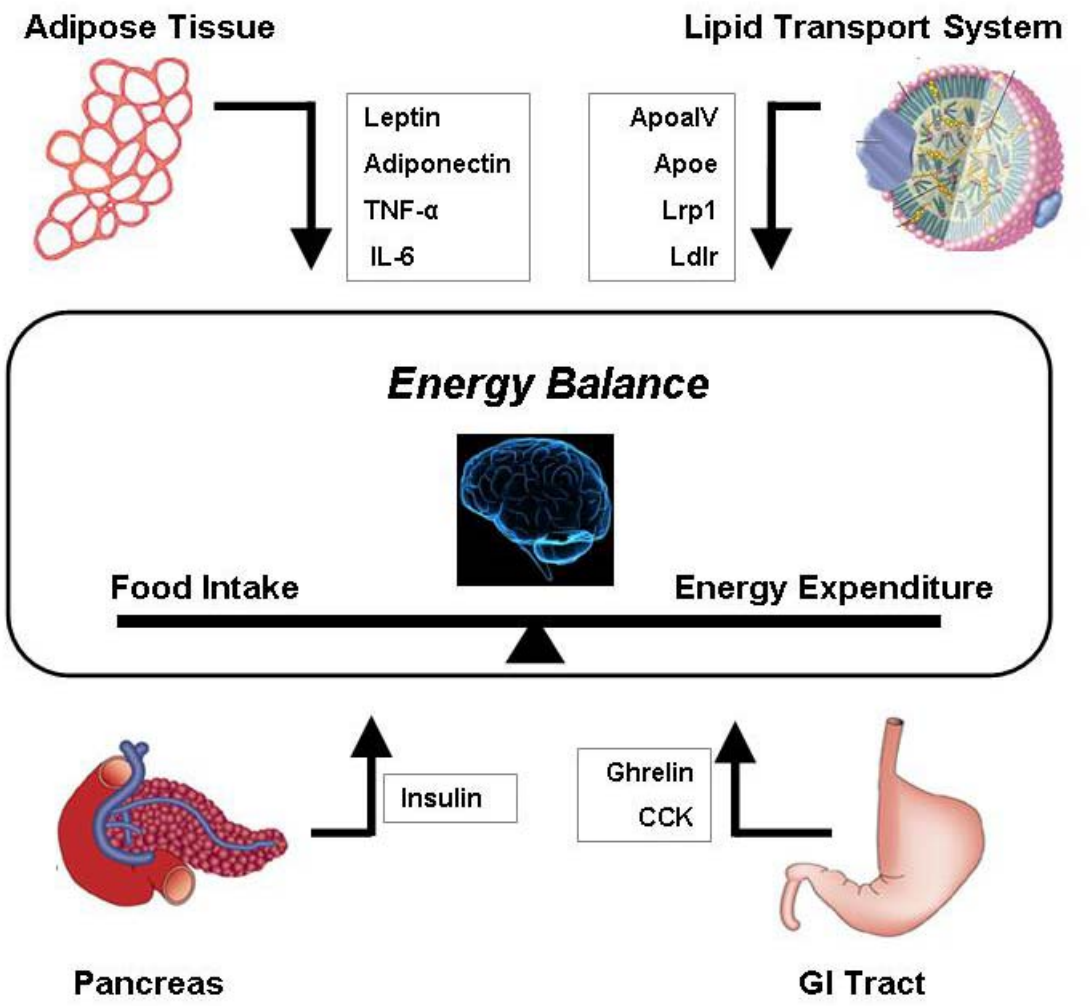

Figure 5.1. Regulators of energy balance. Same representation of the energy balance regulation as depicted in **Figure 1.2**, with the addition of the lipid transport system. Specifically, studies from the *Ldlr-/-* mouse in this thesis suggest that the Ldlr is a key regulator of the overall energy status of the organism.

References

1. Kopelman, P.G. Obesity as a medical problem. *Nature* **404**, 635-643 (2000).
2. Wang, Y. & Lobstein, T. Worldwide trends in childhood overweight and obesity. *International Journal of Pediatric Obesity* **1**, 11-25 (2006).
3. WHO. http://www.who.int/topics/obesity/en/. (Accessed January 12, 2010).
4. Hjartaker, A., Langseth, H. & Weiderpass, E. Obesity and diabetes epidemics: cancer repercussions. *Innovative Endocrinology of Cancer* **630**, 72-93 (2008).
5. Pradhan, A. Obesity, metalic syndrome, and type 2 diabetes: Inflammatory basis of glucose metabolic disorders. *Nutrition Reviews* **65**, S152-S156 (2007).
6. Sowers, J.R. Obesity as a cardiovascular risk factor. *American Journal of Medicine* **115**, 37-41 (2003).
7. Brown, C.D. et al. Body mass index and the prevalence of hypertension and dyslipidemia. *Obesity Research* **8**, 605-619 (2000).
8. Lear, S.A., Toma, M., Birmingham, C.L. & Frohlich, J.J. Modification of the relationship between simple anthropometric indices and risk factors by ethnic background. *Metabolism-Clinical and Experimental* **52**, 1295-1301 (2003).
9. Huxley, R. et al. Waist circumference thresholds provide an accurate and widely applicable method for the discrimination of diabetes. *Diabetes Care* **30**, 3116-3118 (2007).
10. Janssen, I., Katzmarzyk, P.T. & Ross, R. Body mass index, waist circumference, and health risk. *Archives of Internal Medicine* **162**, 2074-2079 (2002).
11. Luu, Y.K. et al. In vivo quantification of subcutaneous and visceral adiposity by micro-computed tomography in a small animal model. *Medical Engineering & Physics* **31**, 34-41 (2009).
12. Maurovich-Horvat, P. et al. Comparison of anthropometric, area- and volume-based assessment of abdominal subcutaneous and visceral adipose tissue volumes using multi-detector computed tomography. *International Journal of Obesity* **31**, 500-506 (2007).
13. Tremblay, M.S., Katzmarzyk, P.T. & Willms, J.D. Temporal trends in overweight and obesity in Canada, 1981-1996. *International Journal of Obesity* **26**, 538-543 (2002).
14. Tjepkema, M. Adult obesity in Canada: Measured height and weight. http://www.statcan.gc.ca/pub/82-620-m/2005001/article/adults-adultes/8060-eng.htm. (2008).
15. Nathan, B., Moran, A. Metabolic complications of obesity in childhood and adolescence: more than just diabetes. *Current Opinion in Endocrinology, Diabetes & Obesity* **15**, 9 (2008).
16. Ryan, J.G. Cost and Policy Implications From the Increasing Prevalence of Obesity and Diabetes Mellitus. *Gender Medicine* **6**, 86-108 (2009).
17. Colditz, G.A. et al. Weight as a Risk Factor for Clinical Diabetes in Women. *American Journal of Epidemiology* **132**, 501-513 (1990).
18. Reaven, G.M. Pathophysiology of Insulin-Resistance in Human-Disease. *Physiological Reviews* **75**, 473-486 (1995).
19. Kissebah, A.H. & Krakower, G.R. Regional Adiposity and Morbidity. *Physiological Reviews* **74**, 761-811 (1994).

20. Lane, J.T. et al. Comparison of CT and dual-energy DEXA using a modified trunk compartment in the measurement of abdominal fat. *Endocrine* **27**, 295-299 (2005).
21. Murphy, S., Martin, S. & Parton, R.G. Lipid droplet-organelle interactions; sharing the fats. *Biochimica Et Biophysica Acta-Molecular and Cell Biology of Lipids* **1791**, 441-447 (2009).
22. Redinger, R.N. Fat storage and the biology of energy expenditure. *Translational Research* **154**, 52-60 (2009).
23. Rosen, E.D. & Spiegelman, B.M. Adipocytes as regulators of energy balance and glucose homeostasis. *Nature* **444**, 847-853 (2006).
24. Flier, J.S. Obesity wars: Molecular progress confronts an expanding epidemic. *Cell* **116**, 337-350 (2004).
25. Rasouli, N. & Kern, P.A. Adipocytokines and the Metabolic Complications of Obesity. *Journal of Clinical Endocrinology & Metabolism* **93**, S64-S73 (2008).
26. Friedman, J.M. & Halaas, J.L. Leptin and the regulation of body weight in mammals. *Nature* **395**, 763-770 (1998).
27. Ahima, R.S. & Flier, J.S. Leptin. *Annual Review of Physiology* **62**, 413-437 (2000).
28. Ingalls, A.M., Dickie, M.M. & Snell, G.D. Obese, a New Mutation in the House Mouse. *Journal of Heredity* **41**, 317-318 (1950).
29. Chehab, F.E., Lim, M.E. & Lu, R.H. Correction of the sterility defect in homozygous obese female mice by treatment with the human recombinant leptin. *Nature Genetics* **12**, 318-320 (1996).
30. Jurgens, H.S. et al. Hyperphagia, lower body temperature, and reduced running wheel activity precede development of morbid obesity in New Zealand obese mice. *Physiological Genomics* **25**, 234-241 (2006).
31. Zhang, Y.Y. et al. Positional Cloning of the Mouse Obese Gene and Its Human Homolog. *Nature* **372**, 425-432 (1994).
32. Freeman, T.C., Dixon, A,K., Campbell, E.A., Tait, T.M., Richardson, P.J., Rice, K.M. Maslen, G.L., Metcalfe, A.D. Streuli, C.H., Bentley, D.R. . Expression Mapping of Mouse Genes in *MGI Direct Data Submission* (Mouse Genome Informatics, 1998).
33. Levin, N., Nelson, C., Gurney, A., Vandlen, R. & DeSauvage, F. Decreased food intake does not completely account for adiposity reduction after ob protein infusion. *Proceedings of the National Academy of Sciences of the United States of America* **93**, 1726-1730 (1996).
34. Pelleymounter, M.A. et al. Effects of the Obese Gene-Product on Body-Weight Regulation in Ob/Ob Mice. *Science* **269**, 540-543 (1995).
35. Gibson, W.T. et al. Congenital leptin deficiency due to homozygosity for the Delta 133G mutation: Report of another case and evaluation of response to four years of leptin therapy. *Journal of Clinical Endocrinology & Metabolism* **89**, 4821-4826 (2004).
36. Montague, C.T. et al. Congenital leptin deficiency is associated with severe early-onset obesity in humans. *Nature* **387**, 903-908 (1997).

37. Strobel, A., Issad, T., Camoin, L., Ozata, M. & Strosberg, A.D. A leptin missense mutation associated with hypogonadism and morbid obesity. *Nature Genetics* **18**, 213-215 (1998).
38. Considine, R.V. et al. Serum immunoreactive leptin concentrations in normal-weight and obese humans. *New England Journal of Medicine* **334**, 292-295 (1996).
39. Frederich, R.C. et al. Leptin Levels Reflect Body Lipid-Content in Mice - Evidence for Diet-Induced Resistance to Leptin Action. *Nature Medicine* **1**, 1311-1314 (1995).
40. Minocci, A. et al. Leptin plasma concentrations are dependent on body fat distribution in obese patients. *International Journal of Obesity* **24**, 1139-1144 (2000).
41. Maffei, M. et al. Leptin Levels in Human and Rodent - Measurement of Plasma Leptin and Ob Rna in Obese and Weight-Reduced Subjects. *Nature Medicine* **1**, 1155-1161 (1995).
42. Van Harmelen, V. et al. Leptin secretion from subcutaneous and visceral adipose tissue in women. *Diabetes* **47**, 913-917 (1998).
43. Balthasar, N. et al. Divergence of melanocortin pathways in the control of food intake and energy expenditure. *Cell* **123**, 493-505 (2005).
44. Fei, H. et al. Anatomic localization of alternatively spliced leptin receptors (Ob-R) in mouse brain and other tissues. *Proceedings of the National Academy of Sciences of the United States of America* **94**, 7001-7005 (1997).
45. McMinn, J.E. et al. Neuronal deletion of Lepr elicits diabesity in mice without affecting cold tolerance or fertility. *American Journal of Physiology-Endocrinology and Metabolism* **289**, E403-E411 (2005).
46. Schwartz, M.W., Woods, S.C., Porte, D., Seeley, R.J. & Baskin, D.G. Central nervous system control of food intake. *Nature* **404**, 661-671 (2000).
47. Caro, J.F. et al. Decreased cerebrospinal-fluid/serum leptin ratio in obesity: A possible mechanism for leptin resistance. *Lancet* **348**, 159-161 (1996).
48. Bjorbaek, C., Elmquist, J.K., Frantz, J.D., Shoelson, S.E. & Flier, J.S. Identification of SOCS-3 as a potential mediator of central leptin resistance. *Molecular Cell* **1**, 619-625 (1998).
49. Hetherington, A.W. & Ranson, S.W. Hypothalamic-Lesions and Adiposity in the Rat. *Nutrition Reviews* **41**, 124-127 (1983).
50. Barsh, G.S. & Schwartz, M.W. Genetic approaches to studying energy balance: Perception and integration. *Nature Reviews Genetics* **3**, 589-600 (2002).
51. Hahn, T.M., Breininger, J.F., Baskin, D.G. & Schwartz, M.W. Coexpression of Agrp and NPY in fasting-activated hypothalamic neurons. *Nature Neuroscience* **1**, 271-272 (1998).
52. Kristensen, P. et al. Hypothalamic CART is a new anorectic peptide regulated by leptin. *Nature* **393**, 72-76 (1998).
53. Schwartz, M.W. et al. Leptin increases hypothalamic pro-opiomelanocortin mRNA expression in the rostral arcuate nucleus. *Diabetes* **46**, 2119-2123 (1997).
54. Balthasar, N. Genetic dissection of neuronal pathways controlling energy homeostasis. *Obesity* **14**, 222-227 (2006).

55. Barsh, G.S., Farooqi, I.S. & O'Rahilly, S. Genetics of body-weight regulation. *Nature* **404**, 644-651 (2000).
56. Huszar, D. et al. Targeted disruption of the melanocortin-4 receptor results in obesity in mice. *Cell* **88**, 131-141 (1997).
57. Vaisse, C., Clement, K., Guy-Grand, B. & Froguel, P. A frameshift mutation in human MC4R is associated with a dominant form of obesity. *Nature Genetics* **20**, 113-114 (1998).
58. Yeo, G.S.H. et al. A frameshift mutation in MC4R associated with dominantly inherited human obesity. *Nature Genetics* **20**, 111-112 (1998).
59. Dridi, S. & Taouis, M. Adiponectin and energy homeostasis: consensus and controversy. *Journal of Nutritional Biochemistry* **20**, 831-839 (2009).
60. Kadowaki, T. & Yamauchi, T. Adiponectin and adiponectin receptors. *Endocrine Reviews* **26**, 439-451 (2005).
61. Kubota, N. et al. Disruption of adiponectin causes insulin resistance and neointimal formation. *Journal of Biological Chemistry* **277**, 25863-25866 (2002).
62. Ma, K. et al. Increased beta-oxidation but no insulin resistance or glucose intolerance in mice lacking adiponectin. *Journal of Biological Chemistry* **277**, 34658-34661 (2002).
63. Plomgaard, P. et al. Tumor necrosis factor-alpha induces skeletal muscle insulin resistance in healthy human subjects via inhibition of Akt substrate 160 phosphorylation. *Diabetes* **54**, 2939-2945 (2005).
64. Kern, P.A., Ranganathan, S., Li, C.L., Wood, L. & Ranganathan, G. Adipose tissue tumor necrosis factor and interleukin-6 expression in human obesity and insulin resistance. *American Journal of Physiology-Endocrinology and Metabolism* **280**, E745-E751 (2001).
65. Nogueiras, R., Novelle, M.G., Vazquez, M.J., Lopez, M., Dieguez, C. Resistin: Regulation of Food Intake, Glucose Homeostasis and Lipid Metabolism. *Endocr Dev* **17**, 10 (2010).
66. Ribalta, J., Vallve, J.C., Girona, J. & Masana, L. Apolipoprotein and apolipoprotein receptor genes, blood lipids and disease. *Current Opinion in Clinical Nutrition and Metabolic Care* **6**, 177-187 (2003).
67. Stryer, L. *Biochemistry*, (W. H. Freeman and Company, USA, 1988).
68. Marschang, P. & Herz, J. Mouse models as tools for dissecting disorders of lipoprotein metabolism. *Seminars in Cell & Developmental Biology* **14**, 25-35 (2003).
69. Stein, E.A. Managing dyslipidemia in the high-risk patient. *American Journal of Cardiology* **89**, 50c-57c (2002).
70. Brown, M.S. & Goldstein, J.L. The SREBP pathway: Regulation of cholesterol metabolism by proteolysis of a membrane-bound transcription factor. *Cell* **89**, 331-340 (1997).
71. Wouters, K., Shiri-Sverdlov, R., van Gorp, P.J., van Bilsen, M. & Hofker, M.H. Understanding hyperlipidemia and atherosclerosis: lessons from genetically modified apoe and ldlr mice. *Clinical Chemistry and Laboratory Medicine* **43**, 470-479 (2005).
72. Glass, C.K. & Witztum, J.L. Atherosclerosis: The road ahead. *Cell* **104**, 503-516 (2001).

73. Vance, J.E., Karten, B. & Hayashi, H. Lipid dynamics in neurons. *Biochemical Society Transactions* **34**, 399-403 (2006).
74. Goldstein, J.L. & Brown, M.S. Lipoprotein Receptors and the Control of Plasma Ldl Cholesterol Levels. *European Heart Journal* **13**, 34-36 (1992).
75. May, P., Herz, J. & Bock, H.H. Molecular mechanisms of lipoprotein receptor signalling. *Cellular and Molecular Life Sciences* **62**, 2325-2338 (2005).
76. Beffert, U., Stolt, P.C. & Herz, J. Functions of lipoprotein receptors in neurons. *Journal of Lipid Research* **45**, 403-409 (2004).
77. Herz, J. The LDL receptor gene family: (Un)expected signal transducers in the brain. *Neuron* **29**, 571-581 (2001).
78. Goldstein, J.L. & Brown, M.S. Regulation of the Mevalonate Pathway. *Nature* **343**, 425-430 (1990).
79. Rifkind, B.M. The Lipid Research Clinics Coronary Primary Prevention Trial Results .2. The Relationship of Reduction in Incidence of Coronary Heart-Disease to Cholesterol Lowering. *Jama-Journal of the American Medical Association* **251**, 365-374 (1984).
80. Shen, L. et al. Characterization of apolipoprotein A-IV in brain areas involved in energy homeostasis. *Physiology & Behavior* **95**, 161-167 (2008).
81. Gotoh, K. et al. Apolipoprotein A-IV interacts synergistically with melanocortins to reduce food intake. *American Journal of Physiology-Regulatory Integrative and Comparative Physiology* **290**, R202-R207 (2006).
82. Shen, L. et al. Brain apolipoprotein E: an important regulator of food intake in rats. *Diabetes* **57**, 2092-2098 (2008).
83. Shen, L. et al. Up-regulation of apolipoprotein E by leptin in the hypothalamus of mice and rats. *Physiology & Behavior* **98**, 223-228 (2009).
84. Hofmann, S.M. et al. Defective lipid delivery modulates glucose tolerance and metabolic response to diet in apolipoprotein E-deficient mice. *Diabetes* **57**, 5-12 (2008).
85. Karagiannides, I., Abdou, R., Tzortzopoulou, A., Voshol, P.J. & Kypreos, K.E. Apolipoprotein E predisposes to obesity and related metabolic dysfunctions in mice. *Febs Journal* **275**, 4796-4809 (2008).
86. Herz, J., Clouthier, D.E. & Hammer, R.E. Ldl Receptor-Related Protein Internalizes and Degrades Upa-Pai-1 Complexes and Is Essential for Embryo Implantation. *Cell* **71**, 411-421 (1992).
87. Hofmann, S.M. et al. Adipocyte LDL receptor-related protein-1 expression modulates postprandial lipid transport and glucose homeostasis in mice. *Journal of Clinical Investigation* **117**, 3271-3282 (2007).
88. Swanson, L., Simmons, D., Hofmann, S., Goldstein, J. & Brown, M. Localization of mRNA for low density lipoprotein receptor and a cholesterol synthetic enzyme in rabbit nervous system by *in situ* hybridization. *Proc. Natl. Acad. Sci. USA* **85**, 5 (1988).
89. Brown, M. & Gidlstein, J. The receptor model for transport of cholesterol plasma. *Ann N Y Acad Sci* **454**, 4 (1985).
90. Hobbs, H., Russell, D., Brown, M. & Gidlstein, J. The LDL receptor locus and familial hypercholesterolemia: mutational analysis of a membrane protein. *Annu Rev Genet* **24**, 38 (1990).

91. Kypreos, K.E. & Zannis, V.I. LDL receptor deficiency or apoE mutations prevent remnant clearance and induce hypertriglyceridemia in mice. *Journal of Lipid Research* **47**, 521-529 (2006).
92. Ishibashi, S. et al. Hypercholesterolemia in Low-Density-Lipoprotein Receptor Knockout Mice and Its Reversal by Adenovirus-Mediated Gene Delivery. *Journal of Clinical Investigation* **92**, 883-893 (1993).
93. Paigen, B., Morrow, A., Brandon, C., Mitchell, D. & Holmes, P. Variation in Susceptibility to Atherosclerosis among Inbred Strains of Mice. *Atherosclerosis* **57**, 65-73 (1985).
94. Silver, D.L., Wang, N. & Tall, A.R. Defective HDL particle uptake in ob/ob hepatocytes causes decreased recycling, degradation, and selective lipid uptake. *Journal of Clinical Investigation* **105**, 151-159 (2000).
95. Kennedy, D.J. et al. Dietary Cholesterol Plays a Role in CD36-Mediated Atherogenesis in LDLR-Knockout Mice. *Arteriosclerosis Thrombosis and Vascular Biology* **29**, 1481-U171 (2009).
96. Lewis, M.J. et al. Immunoglobulin M Is Required for Protection Against Atherosclerosis in Low-Density Lipoprotein Receptor-Deficient Mice. *Circulation* **120**, 417-U101 (2009).
97. Coenen, K.R., Gruen, M.L., Chait, A. & Hasty, A.H. Diet-induced increases in adiposity, but not plasma lipids, promote macrophage infiltration into white adipose tissue. *Diabetes* **56**, 564-573 (2007).
98. Hasty, A.H. et al. Severe hypercholesterolemia, hypertriglyceridemia, and atherosclerosis in mice lacking both leptin and the low density lipoprotein receptor. *Journal of Biological Chemistry* **276**, 37402-37408 (2001).
99. Verreth, W. et al. Weight loss-associated induction of peroxisome proliferator-activated receptor-alpha and peroxisome proliferator-activated receptor-gamma correlate with reduced atherosclerosis and improved cardiovascular function in obese insulin-resistant mice. *Circulation* **110**, 3259-3269 (2004).
100. Verreth, W. et al. Peroxisome proliferator-activated receptor-alpha,gamma-agonist improves insulin sensitivity and prevents loss of left ventricular function in obese dyslipidemic mice. *Arteriosclerosis Thrombosis and Vascular Biology* **26**, 922-928 (2006).
101. Nishina, P.M., Lowe, S., Wang, J.L. & Paigen, B. Characterization of Plasma-Lipids in Genetically-Obese Mice - the Mutants Obese, Diabetes, Fat, Tubby, and Lethal Yellow. *Metabolism-Clinical and Experimental* **43**, 549-553 (1994).
102. Nishina, P.M., Naggert, J.K., Verstuyft, J. & Paigen, B. Atherosclerosis in Genetically-Obese Mice - the Mutants Obese, Diabetes, Fat, Tubby, and Lethal Yellow. *Metabolism-Clinical and Experimental* **43**, 554-558 (1994).
103. Gruen, M.L. et al. Plasma insulin levels predict atherosclerotic lesion burden in obese hyperlipidemic mice. *Atherosclerosis* **186**, 54-64 (2006).
104. Merat, R., Raoul, H., Leste-Lasserre, T., Sonigo, P. & Pancino, G. Variable constraints on the principal immunodominant domain of the transmembrane glycoprotein of human immunodeficiency virus type 1. *Journal of Virology* **73**, 5698-5706 (1999).

105. Bernal-Mizrachi, C. et al. Dexamethasone induction of hypertension and diabetes is PPAR-alpha dependent in LDL receptor-null mice. *Nature Medicine* **9**, 1069-1075 (2003).
106. Schreyer, S.A., Lystig, T.C., Vick, C.M. & LeBoeuf, R.C. Mice deficient in apolipoprotein E but not LDL receptors are resistant to accelerated atherosclerosis associated with obesity. *Atherosclerosis* **171**, 49-55 (2003).
107. Towler, D.A., Bidder, M., Latifi, T., Coleman, T. & Semenkovich, C.F. Diet-induced diabetes activates an osteogenic gene regulatory program in the aortas of low density lipoprotein receptor-deficient mice. *Journal of Biological Chemistry* **273**, 30427-30434 (1998).
108. Schreyer, S.A., Vick, C., Lystig, T.C., Mystkowski, P. & LeBoeuf, R.C. LDL receptor but not apolipoprotein E deficiency increases diet-induced obesity and diabetes in mice. *American Journal of Physiology-Endocrinology and Metabolism* **282**, E207-E214 (2002).
109. Townsend, K.L., Lorenzi, M.M. & Widmaier, E.P. High-fat diet-induced changes in body mass and hypothalamic gene expression in wild-type and leptin-deficient mice. *Endocrine* **33**, 176-188 (2008).
110. DeLany, J.P.L., J.C. Energy Expenditure. in *Endocrinology and Metabolism Clinics of North America*, Vol. 25 831–846 (1996).
111. Elder, G.A. et al. Increased locomotor activity in mice lacking the low-density lipoprotein receptor. *Behavioural Brain Research* **191**, 256-265 (2008).
112. Bonfleur, M.L., Vanzela, E.C., Ribeiro, R.A., & Dorighello, G., Carvalho, C., Collares-Buzato, C.B., Carneiro, E.M., Boschero, A.C., Oliveira, H. Primary hypercholesterolaemia impairs glucose homeostasis and insulin secretion in low-density lipoprotein receptor knockout mice independently of high-fat diet and obesity. *Biochim. Biophys. Acta* (2009).
113. Kahn, B.B. & Flier, J.S. Obesity and insulin resistance. *Journal of Clinical Investigation* **106**, 473-481 (2000).
114. Foreyt, J.P. et al. Weight-reducing diets: Are there any differences? *Nutrition Reviews* **67**, S99-S101 (2009).
115. Tinsley, F.C., Taicher, G.Z. & Heiman, M.L. Evaluation of a quantitative magnetic resonance method for mouse whole body composition analysis. *Obesity Research* **12**, 150-160 (2004).
116. Ravussin, E., Lillioja, S., Anderson, T.E., Christin, L. & Bogardus, C. Determinants of 24-Hour Energy-Expenditure in Man - Methods and Results Using a Respiratory Chamber. *Journal of Clinical Investigation* **78**, 1568-1578 (1986).
117. Dupuis, L., Oudart, H., Rene, F., de Aguilar, J.L.G. & Loeffler, J.P. Evidence for defective energy homeostasis in amyotrophic lateral sclerosis: benefit of a high-energy diet in a transgenic mouse. *Proceedings of the National Academy of Sciences of the United States of America* **101**, 11159-11164 (2004).
118. Wideman, R.D. et al. Improving function and survival of pancreatic islets by endogenous production of glucagon-like peptide 1 (GLP-1). *Proceedings of the National Academy of Sciences of the United States of America* **103**, 13468-13473 (2006).

119. Livak, K.J. & Schmittgen, T.D. Analysis of relative gene expression data using real-time quantitative PCR and the 2(T)(-Delta Delta C) method. *Methods* **25**, 402-408 (2001).
120. Eisen, E.J. Results of Growth Curve Analyses in Mice and Rats. *Journal of Animal Science* **42**, 1008-1023 (1976).
121. Lowell, B.B. & Spiegelman, B.M. Towards a molecular understanding of adaptive thermogenesis. *Nature* **404**, 652-660 (2000).
122. Even, P.C., Mokhtarian, A. & Pele, A. Practical Aspects of Indirect Calorimetry in Laboratory-Animals. *Neuroscience and Biobehavioral Reviews* **18**, 435-447 (1994).
123. Gao, Z.G. et al. Inactivation of PKC theta leads to increased susceptibility to obesity and dietary insulin resistance in mice. *American Journal of Physiology-Endocrinology and Metabolism* **292**, E84-E91 (2007).
124. Isken, F. et al. Deficiency of glucose-dependent insulinotropic polypeptide receptor prevents ovariectomy-induced obesity in mice. *American Journal of Physiology-Endocrinology and Metabolism* **295**, E350-E355 (2008).
125. Isken, F. et al. Metabolic effects of diets differing in glycaemic index depend on age and endogenous glucose-dependent insulinotrophic polypeptide in mice. *Diabetologia* **52**, 2159-2168 (2009).
126. Nogueiras, R. et al. Direct Control of Peripheral Lipid Deposition by CNS GLP-1 Receptor Signaling Is Mediated by the Sympathetic Nervous System and Blunted in Diet-Induced Obesity. *Journal of Neuroscience* **29**, 5916-5925 (2009).
127. Chen, A.S. et al. Inactivation of the mouse melanocortin-3 receptor results in increased fat mass and reduced lean body mass. *Nature Genetics* **26**, 97-102 (2000).
128. Iida-Klein, A. et al. Precision, accuracy, and reproducibility of dual X-ray absorptiometry measurements in mice in vivo. *Journal of Clinical Densitometry* **6**, 25-33 (2003).
129. Masinde, G.L. et al. Quantitative trait loci for bone density in mice: The genes determining total skeletal density and femur density show little overlap in F-2 mice. *Calcified Tissue International* **71**, 421-428 (2002).
130. Nagy, T.R. & Clair, A.L. Precision and accuracy of dual-energy X-ray absorptiometry for determining in vivo body composition of mice. *Obesity Research* **8**, 392-398 (2000).
131. Taicher, G. Quantitative magnetic resonance (QMR) for whole body composition analysis of mice, rats and infants. *Obesity Research* **11**, A48-A48 (2003).
132. Setchell, K.D.R., Lawson, A.M., Tanida, N. & Sjovall, J. General-Methods for the Analysis of Metabolic Profiles of Bile-Acids and Related-Compounds in Feces. *Journal of Lipid Research* **24**, 1085-1100 (1983).
133. Kim, H.J. et al. Differential effects of interleukin-6 and-10 on skeletal muscle and liver insulin action in vivo. *Diabetes* **53**, 1060-1067 (2004).
134. Kim, J.K. et al. Redistribution of substrates to adipose tissue promotes obesity in mice with selective insulin resistance in muscle. *Journal of Clinical Investigation* **105**, 1791-1797 (2000).
135. Halaas, J.L. et al. Weight-Reducing Effects of the Plasma-Protein Encoded by the Obese Gene. *Science* **269**, 543-546 (1995).

136. Bowen, H., Mitchell, T.D. & Harris, R.B.S. Method of leptin dosing, strain, and group housing influence leptin sensitivity in high-fat-fed weanling mice. *American Journal of Physiology-Regulatory Integrative and Comparative Physiology* **284**, R87-R100 (2003).
137. Gullicksen, P.S., Flatt, W.P., Dean, R.G., Hartzell, D.L. & Baile, C.A. Energy metabolism and expression of uncoupling proteins 1, 2, and 3 after 21 days of recovery from intracerebroventricular mouse leptin in rats. *Physiology & Behavior* **75**, 473-482 (2002).
138. Scarpace, P.J., Matheny, M., Pollock, B.H. & Tumer, N. Leptin increases uncoupling protein expression and energy expenditure. *American Journal of Physiology-Endocrinology and Metabolism* **36**, E226-E230 (1997).
139. Rosenbaum, M., Murphy, E.M., Heymsfield, S.B., Matthews, D.E. & Leibel, R.L. Low dose leptin administration reverses effects of sustained weight-reduction on energy expenditure and circulating concentrations of thyroid hormones. *Journal of Clinical Endocrinology & Metabolism* **87**, 2391-2394 (2002).
140. Halaas, J.L. et al. Physiological response to long-term peripheral and central leptin infusion in lean and obese mice. *Proceedings of the National Academy of Sciences of the United States of America* **94**, 8878-8883 (1997).
141. Hwa, J.J. et al. Leptin increases energy expenditure and selectively promotes fat metabolism in ob/ob mice. *American Journal of Physiology-Regulatory Integrative and Comparative Physiology* **41**, R1204-R1209 (1997).
142. Leibel, R.L., Rosenbaum, M. & Hirsch, J. Changes in Energy-Expenditure Resulting from Altered Body-Weight. *New England Journal of Medicine* **332**, 621-628 (1995).

Appendix A: Ethical Approval of Animal Studies

THE UNIVERSITY OF BRITISH COLUMBIA

Ying Fai Ngai

has successfully completed the online training requirements of the Canadian Council on Animal Care (CCAC) / National Institutional Animal User Training (NIAUT) Program

Chair, Animal Care Committee

Veterinarian

Certificate #: 2794 - 08

Date Issued: March 13, 2008

THE UNIVERSITY OF BRITISH COLUMBIA

UBC

Certificate of Completion

This is to certify that

Ying Fai Tiffany Ngai

Was enrolled in and successfully completed the

Animal Care Centre

Anesthesia of Rodents Works

In 2009

[redacted]

Director of Animal Care

Certificate # RA-344-09

THE UNIVERSITY OF BRITISH COLUMBIA

ANIMAL CARE CERTIFICATE

Application Number: A07-0631

Investigator or Course Director: William T. Gibson

Department: Medical Genetics

Animals:

Mice C57Bl/6J 20
Mice Mice B6.LDLR -/- 20

Start Date: **May 1, 2008** **Approval Date:** **June 25, 2008**

Funding Sources:

Funding Agency:	Canadian Institutes of Health Research (CIHR)
Funding Title:	Regulation of body weight: Hypothalamic mediators and their peripheral targets
Unfunded title:	N/A

The Animal Care Committee has examined and approved the use of animals for the above experimental project.

This certificate is valid for one year from the above start or approval date (whichever is later) provided there is no change in the experimental procedures. Annual review is required by the CCAC and some granting agencies.

A copy of this certificate must be displayed in your animal facility.

Office of Research Services and Administration
102, 6190 Agronomy Road, Vancouver, BC V6T 1Z3
Phone: 604-827-5111 Fax: 604-822-5093

Appendix B: Validation of Methods

Example of QRTPCR Primer Validation with Standard Curve

Data for *leptin* primers from ABI3500 Fast Machine:

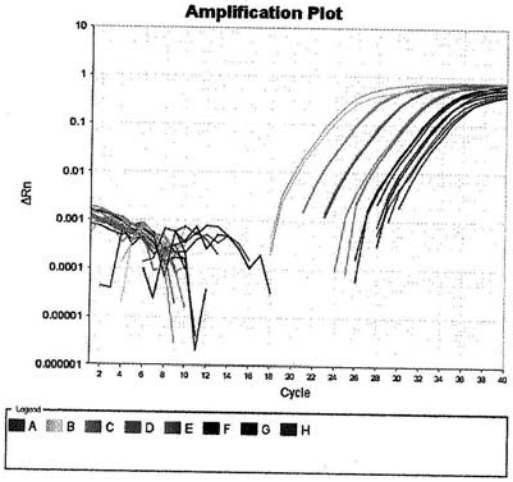

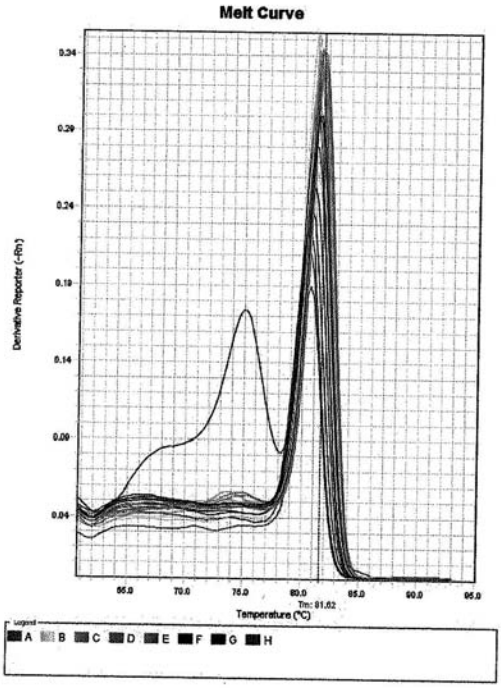

Sample	cDNA Conc (ng/ul)	Log (cDNA Con)	Gene		Ct (rep1)	Ct (rep2)	Ct (rep3)	Average Ct
NTC	*0*		*Leptin*		*34.3*	*33.7*	*33.9*	*34.0*
Undiluted Standard	*1254.7*	*3.099*	*Leptin*		*22.7*	*23.1*	*22.7*	*22.9*
1/5 dilution	*259.9*	*2.415*	*Leptin*		*25.5*	*25.5*	*25.4*	*25.5*
1/25 dilution	*52.8*	*1.723*	*Leptin*		*27.8*	*27.8*	*27.7*	*27.8*
1/125 dilution	*10.7*	*1.029*	*Leptin*		*30.1*	*30.1*	*29.9*	*30.0*
1/625 dilution	*2.5*	*0.398*	*Leptin*		*31.8*	*32.2*	*31.8*	*31.9*
1/3125 dilution	*0.7*	*-0.155*	*Leptin*		*32.8*	*33.0*	—	*32.9*
						%Efficiency:		**99.17**

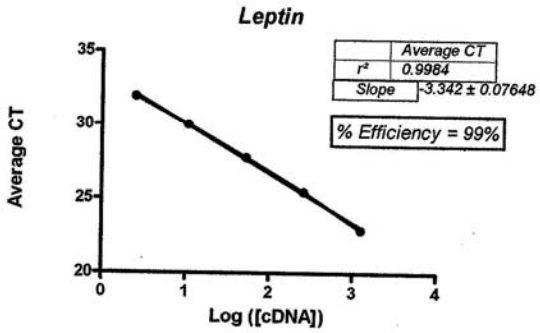

Primer efficiencies of 90-100% was accepted.

Slopes of standard curve within 0.1 of endogenous control was accepted.

(β-actin standard curve slope =-3.42)

List of QRTPCR Primer Efficiencies and Standard Curve Slopes

Gene	Standard Curve Efficiency (%)	Standard Curve Slope
β-actin	92.6	-3.42
Leptin	99.2	-3.34
Ucp1	99.9	-3.32
Npy	92.8	-3.51
Pomc	100.0	-3.41
Ldlr	98.1	-3.37
Apoe	92.6	-3.51

Example of Fecal Energy Content Data from Bomb Calorimetry:

Time (mins)	Degrees (C)		
		a: time of Firing:	6
1	20.88	b: time when temperature reaches 60% of total rise:	
2	20.87	c: time when temperature is constant	
3	20.87	t_a: temperature at firing:	20.88
4	20.87	t_c: temperature at time c:	22.6
5	20.88	r_1: rate at which temperature was rising in 5 mins before firing:	
6	20.88	r_2: rate at which temperature was rising in 5 mins after time C:	
6.75	21.20	c_1: millilitres of standard alkali solution used in acid titration:	6.6
7	21.45	c_2: percentage of sulfur in sample	0
7.25	21.70	c_3: centimeters of fuse wire consumed	5.4
7.5	21.88	W: energy equivalent of the calorimeter (Standardization):	2485.5
7.75	22.01	m1: Mass of sample in grams:	0.14
8	22.12	m2: Mass of accelerant in grams:	0.48
9	22.38	*m#: number of poops*	10
10	22.50	t: corrected temperature rise:	1.72
11	22.55	tW	4275.06
12	22.58	e3:	12.42
13	22.59	Hg: gross heat of combustion:	4256.04
14	22.60	Hg: gross heat of combustion - Butanol Component	471.24
15	22.60	Heat of combustion per g fecal matter	3366
16	22.60		

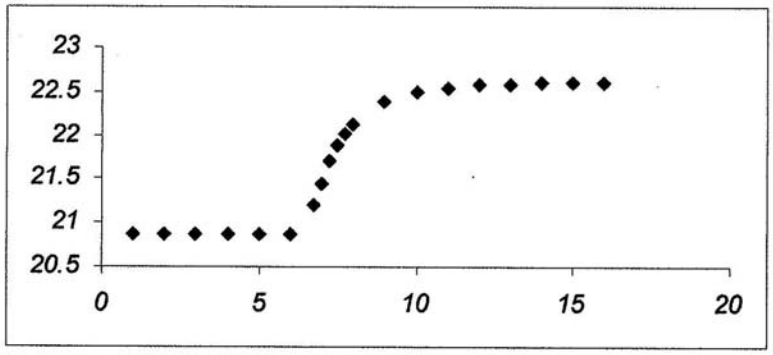

X-label: Time (min); Y-label = Temperature (°C)

Validation of QMR-body composition by Gibson Lab